Contribution of Cyclin G2 to the Cell Cycle Inhibitory Effects of Cancer Therapeutics

Dissertation

presented to the Department of Chemistry
University of Bielefeld

in partial fulfillment of the requirements for the degree of
Doctor rerum naturalium (Dr. rer. nat.)

Submitted by

Maike Zimmermann

Bielefeld 2012

Frist reviewer: Prof. Dr. Gabriele Fischer von Mollard, Biochemistry III,

Department of Chemistry, University of Bielefeld, Germany

Second reviewer: Prof. Dr. Mary Horne, Department of Pharmacology,

University of California, Davis, USA

Table of Contents

Table of Contents

Table of Contents

1. Introduction

Cancer is the second most common cause of death in the US (Society, 2012) and can be categorized as a group of diseases with diverse genetic and phenotypic appearances. Excessive cell proliferation induced by irregular entry into the cell cycle as well as cancer cell evasion from growth suppressors are two of the hallmarks of cancer (Hanahan and Weinberg, 2011).

Cancer is caused by both external (such as chemicals and radiation) and internal factors (including inherited mutations and metabolism by-products). Today's treatment options include surgery, radiation, chemotherapy and molecular targeted therapy. The major drawbacks of current therapies are the lack of initial response of tumors and occurring resistance toward therapeutic intervention (Society, 2012). Many gene expression signatures have been described in the past to influence treatment choice and predict relapse probability (Lord and Ashworth, 2012). These studies largely identify the high expression of proliferation-related genes and the loss of control or safeguard gene expression in patients with poor prognosis (Beroukhim et al., 2010).

This thesis focuses on the negative cell cycle control protein cyclin G2 (CycG2), expression of which is downregulated in several human cancers (Ito et al., 2003; Kim et al., 2004; Le et al., 2007). In contrast to regular proliferation promoting cyclins, CycG2 is implicated in growth restriction (Figure 1-3) following differentiation (Sepulveda et al., 2008; Zhou et al., 2009), inhibition of mitotic signaling (Le et al., 2007; Stossi et al., 2006) and stress induced cell cycle arrest (Bates et al., 1996; Murray et al., 2004).

1.1 Cell Cycle

Mammalian somatic cells reproduce by duplicating all of their molecules and organelles (including DNA, proteins and mitochondria) before dividing into two genetically identical daughter cells. This cell division cycle (cell cycle) is a complex process, which needs to be precisely controlled on multiple levels to ensure both the correct time for duplication and the accurate distribution of components between daughter cells. Proliferation of mammalian cells is initiated by growth factors and driven by cyclin depended kinases (CDKs) and their regulatory activators the cyclins

(Koepp et al., 1999; Morgan, 1997). CDKs are constitutively expressed in cells, whereas cyclins are synthesized at specific stages of the cell cycle, and are degraded at others, in response to various molecular signals. As cells go through the four phases (G_1, S, G_2 and M) of the cell cycle, four major proliferation-related cyclins (D, E, A, and B) are sequentially expressed to regulate CDK activity (Figure 1-1) (Satyanarayana and Kaldis, 2009).
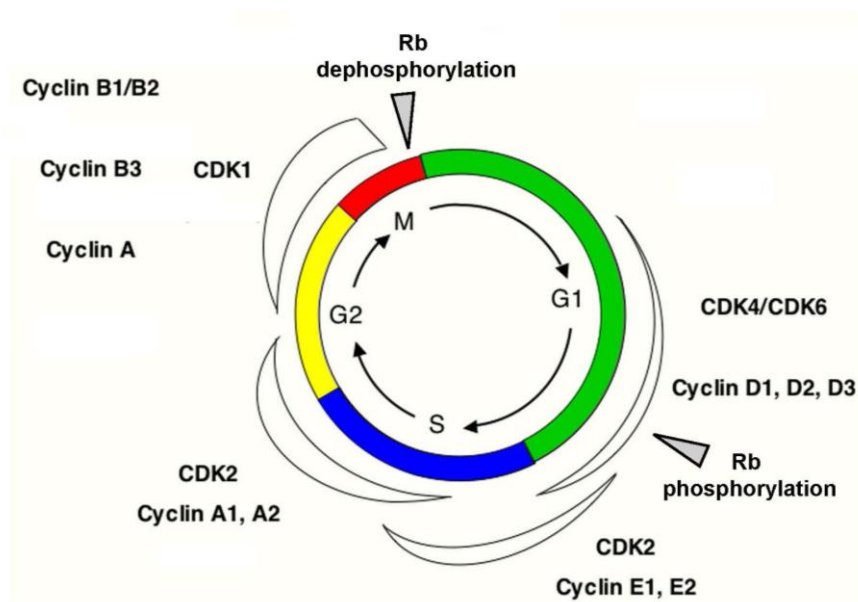
Figure 1-1: Schematic of the somatic cell cycle regulation. Typical somatic cell cycle can be divided into four phases (G_1, S, G_2 and M). Progression is triggered by sequential activation of cyclin dependent kinase (CDK) complexes with their regulatory partners the cyclins. Shapes outside the cycle indicate the increase and reduction of corresponding cyclin/CDK activity. Grey segment specifies Rb phosphorylation (restriction point) and dephosphorylation events (adapted from (van den Heuvel, 2005)).

1.1.1 G_1-phase

The majority of cells *in vivo* and *in vitro* exhibit a G_1-phase DNA content (2N). Cells that have exit the cell cycle (such as quiescent and senescent cells) are classified as being in G_0-phase, but display the same DNA content as G_1-phase cells. Mitogenic stimuli, such as growth factors, induce the expression of D-type cyclins (D1, D2, and D3), which bind and activate CDK4 and CDK6. Together, these CycD/CDK complexes drive the cell through G_1-phase by phosphorylation of the retinoblastoma (Rb) family (p105, p107 and p130) of proteins (Sherr and Roberts, 1999). Phosphorylated Rb can no longer bind to E2F transcriptions factors (TFs). Release of

E2F from Rb induced inhibition leads to the expression of proliferation-related genes, such as CycE and CycA (Harbour and Dean, 2000). Together with its regulatory subunit, CycD1, CDK4 is considered an oncogene, and both are frequently amplified in a diverse set of human cancers driving cellular proliferation (Beroukhim et al., 2010).

In the next step of cell cycle progression, CycE/CDK2 complexes further phosphorylate Rb, to mediate E2F-dependent transcription of genes involved in nucleotide metabolism and DNA synthesis. Once cells have passed through the restriction point they are committed to completing the cell cycle even when mitotic stimuli are withdrawn (Dulic et al., 1992; Zwang et al., 2011).

1.1.2 S-phase

After the E2F transcriptional program is initiated, cells no longer rely on persistent mitogenic signals to maintain Rb phosphorylation. Initiation of DNA synthesis is started at replication origins, that are activated only once during S-phase through phosphorylation by CycA/CDK2 complexes (Krude et al., 1997; Petersen et al., 1999). In early S-phase CycE is no longer needed and phosphorylation by GSKβ and CDK2 targets CycE for proteasomal degradation in the Skp1/Cul1/F-box protein (SCF) pathway (see 1.1.5 Ubiquitin Proteasome Pathway) (Clurman et al., 1996).

1.1.3 G_2-phase

The G_2-phase CycB/CDK1 kinase complexes prevent the re-replication of the DNA and initiate the G_2/M transition. Transcription of CycB starts in S-phase and peaks in late G_2-phase. The majority of the inactive complexes localize at the centrosomes (Hagting et al., 1998). The kinases Wee1 and Myt1 keep the formed CycB/CDK1 complexes inactive through phosphorylation of residues T14/Y15 in CDK1 (also known as Cdc2). Activation of CDK1 is initiated in late S- and early G_2-phase through phosphorylation of T161 by the CDK-activating kinase (CAK), and through dephosphorylation of T14/Y15 by Cdc25 phosphatases (O'Farrell, 2001). If cells enter mitosis prematurely, when CycB/CDK1 activity is low, the reduced phosphorylation of mitotic entry network components could lead to failure of normal execution of mitosis and thereafter cell death (Lindqvist et al., 2007).

1.1.4   Mitosis

Inactive CycB/CDK1 complexes are continuously exported from the nucleus. At the beginning of mitosis, activated CDK1 phosphorylates CycB. This phosphorylation masks the nuclear export sequence (NES) thereby enabling the nuclear accumulation that is critical for CycB1/CDK1 function (Lindqvist et al., 2007). Within the nucleus CycB/CDK1 complexes phosphorylate Wee1 kinases leading to the proteasomal degradation of Wee1 through SCF pathway (Watanabe et al., 2004). Active CycB/CDK1 complexes drive mitosis by promoting the breakdown of the nuclear envelope through phosphorylation of the nuclear lamins (Dessev et al., 1991). At the end of mitosis CycB is ubiquitinated and degraded through the anaphase promoting complex/cyclosome (APC/C) proteasome pathway (van Leuken et al., 2008).

1.1.5   Ubiquitin Proteasome Pathway

The timely destruction of multiple cell cycle regulatory proteins is accomplished by the proteasomal pathway, which is triggered by poly-ubiquitylation of the substrates (Chau et al., 1989). Two major E3 ubiquitin ligase complexes, SCF and APC/C, are in control of the timely ubiquitylation of numerous cell cycle related proteins (such as CycE and p27) (Nakayama and Nakayama, 2006). From late G_1- to early M-phase, SCF is active and ubiquitylates substrates, whereas APC/C is active from mid-M phase (anaphase) to the end of G_1-phase. Regulation of SCF activity is achieved throughout the cell cycle by the phosphorylation status of its substrates. Its activity is reduced by APC mediated ubiquitylation of SCF components (Nakayama and Nakayama, 2006; Petroski and Deshaies, 2005). In contrast to SCF, APC substrates do not require phosphorylation for recognition. APC's activity is tightly controlled throughout the cell cycle to regulate target destruction. In G_1 and S-phase APC is inhibited by CycA/CDK2 complexes, while it is activated by CycB/CDK1 complexes during mitosis (Lindqvist et al., 2009; Mocciaro and Rape, 2012). The activation of APC is important to regulate the metaphase to anaphase transition (Merbl and Kirschner, 2009; Mocciaro and Rape, 2012).

1.1.6   CDK Inhibitors

Two families of genes encode CDK inhibitors (CKIs), the CDK interacting protein/kinase inhibitory protein (cip/kip) family and the inhibitor of kinase

4/alternative reading frame (INK4a/ARF) family. CKIs prevent cyclin/CDK activity in response to negative stimuli and, as a result, avert cell cycle progression. CKIs are also known as tumor suppressors, and are commonly misregulated in cancers (Chu et al., 2008; Pateras et al., 2009). The cip/kip family includes p21, p27 and p57. These proteins halt the cell cycle in G_1-phase by inhibiting CDK1 and CDK2 activity. p21 is transcriptionally stimulated by DNA damage activated p53 (Gartel and Radhakrishnan, 2005). p27 is primarily regulated at the post-transcriptional level through phosphorylation by CycK/CDK6 (Kuntz and O'Connell, 2009) and by subsequent proteasomal degradation (Sherr and Roberts, 1999). In addition to its inhibitory effect on CDK1 and CDK2, binding of p21 and p27 to CycD/CDK leads to stabilization of their complexes, but not to inhibition of kinase activity (Sherr and Roberts, 1999). The INK family includes p15, p16, p18, and p19. INK family members bind to CDK4 and CDK6, disrupting the interaction with CycD and arresting the cell cycle in G_1-phase (Pei and Xiong, 2005).

1.2 Cyclin G2

Not all cyclins and CDKs are involved in cell cycle progression (Satyanarayana and Kaldis, 2009). CycG2 is one example of an atypical cyclin. It is encoded by the gene *CCNG2* and belongs, together with CycG1 and CycI, to the G-type family of unconventional cyclins. In contrast to proliferation promoting cyclins, G-type cyclin mRNAs are low in proliferating cells, but elevated in cells undergoing cell cycle arrest (Bates et al., 1996; Horne et al., 1997; Horne et al., 1996; Okamoto and Beach, 1994).

Northern blot analysis of various tissue types and cell lines shows a high level of *CCNG2* transcript in spleen, prostate, thymus, and cerebellar tissues (Horne et al., 1996). CycG2 mRNA is moderately expressed in proliferating cells, peaking in late S/early G_2-phase. It is, however, significantly upregulated in differentiated tissue and in cells undergoing cell cycle arrest in response to DNA damage, endoplasmic reticulum stress (ERS) and oxidative stress (Bates et al., 1996; Hofstetter et al., 2012; Horne et al., 1996; Murray et al., 2004; Thomas et al., 2007). Contrastingly, the transcription of *CCNG2* is inhibited by mitogenic signaling through the nuclear estrogen receptor (ER) and surface membrane growth factor receptors (such as HER2) (Le et al., 2007; Stossi et al., 2006).

1.2.1 CycG2 Protein

CCNG2 encodes a 344 amino acid protein that exhibits high sequence similarity with the prototypical cyclins such as CycA that drive cell cycle progression (Horne et al., 1996). In contrast to these proliferation promoting cyclins, overexpression of CycG2 in several cell lines leads to a G_1-phase cell cycle arrest (Arachchige Don et al., 2006; Bennin et al., 2002; Chen et al., 2006; Kim et al., 2004; Le et al., 2007; Xu et al., 2008). This arrest is largely mediated through its C-terminus (Bennin et al., 2002) and is dependent on the presence of p53 and Chk2 checkpoint proteins (Arachchige Don et al., 2006; Zimmermann et al., 2012).

Alignment of CycG2 and CycA amino acid sequences indicates that these two proteins form similar tertiary structures (Horne et al., 1997; Horne et al., 1996). Comparable to other cyclins, CycG2 possesses a conserved amino acid region called cyclin box that is required for binding and activation of CDKs. An additional sequence motif that is present in cell cycle promoting cyclins, required for interaction with the CKIs, p21 and p27, however, is not conserved in CycG2 (Horne et al., 1997). Through overexpression studies it was determined that CycG2 can bind to CDK5 but these complexes were not enzymatically active (Bennin and Horne, unpublished data). Interestingly, CycG2 directly interacts with catalytically active protein phosphatase 2A (PP2A) complexes (Arachchige Don et al., 2006; Bennin et al., 2002). The serine/threonine phosphatase PP2A plays major roles in growth control, development, cytoskeletal dynamics, DNA damage response, apoptosis, and regulation of signal transduction cascades such as the mitogen activated protein kinase (MAPK) pathway (Chowdhury et al., 2005; Dozier et al., 2004; Janssens and Goris, 2001). The heterotrimeric PP2A holoenzyme is composed of one catalytic (C), a structural scaffold (A) and a regulatory (B) subunit. Substrate specificity, selectivity and subcellular localization of PP2A are mediated by the various regulatory subunits (B55/PR55, B'/B56/PR56 and B''/PR72) that are able to bind to the A/C core (Janssens and Goris, 2001; McCright et al., 1996). CycG2 can form active complexes with the C and B'/B56 subunits, but does not interact with the scaffolding subunit. CycG2/PP2AC/B' complexes co-localize at centrosomes and in the cytoplasm as detergent-insoluble cytoskeletal-associated complexes. Some distinct CycG2/B' containing complexes also co-localize within nuclei. The C-terminus of CycG2 is both necessary and sufficient for the association with PP2A (Bennin et al., 2002).

Formation of the CycG2/PP2A complex may further modulate PP2A activity, and as a result, could influence a variety of cellular functions associated with PP2A (Arachchige Don et al., 2006; Bennin et al., 2002).

Similar to CycB1, CycG2 is a centrosome associated nucleocytoplasmic shuttling protein (Arachchige Don et al., 2006; Lindqvist et al., 2007). CycG2 does not contain a nuclear localization sequence (NLS), but contains several possible NES (Horne et al., 1996; Kutay and Guttinger, 2005, Arachchige Don, unpublished data). Nuclear accumulation of CycG2 is observed after inhibition of the nuclear export protein CRM1 with leptomycin B (Arachchige Don et al., 2006) and may occur after binding to proteins that contain a NLS (Bennin et al., 2002; Zhao et al., 2003).

Degradation of CycG2 can be prevented by proteasome inhibitors, an indication of the involvement of the ubiquitin proteasome system (UPS) in CycG2 stability. Moreover, CycG2 is a target of lysine 48-linked ubiquitylation (Cowan and Horne, unpublished data). The SCF complex (see 1.1.5 Ubiquitin Proteasome Pathway) is responsible for ubiquitylation of multiple inhibitors of the G_1/S transition (Nakayama et al., 2004; Xu et al., 2008). Consistent with the previous observations, the stability of CycG2 was shown to be regulated in part through a PEST sequence within its C-terminus (Xu et al., 2008). The PEST region of CycG2, promotes binding to Skp1 and 2, two components of the SCF complex (Xu et al., 2008). This interaction is one mechanism by which CycG2 degradation through the UPS is mediated. In addition, it was recently shown that CycG2 is a substrate of APC (Merbl and Kirschner, 2009).

1.2.2   CycG2 Gene Expression

Transcription of *CCNG2* is modulated by several TFs depending on the signaling pathways that are engaged (Figure 1-3) (Adorno et al., 2009; Ahmed et al., 2012; Jayapal et al., 2010; Martinez-Gac et al., 2004; Stossi et al., 2006). In contrast to the CycG1 gene, *CCNG1*, the promoter region of *CCNG2* does not contain binding sites for the tumor suppressor p53. However, *CCNG2* expression is positively regulated by the p53 homolog, p63. Inhibition of the p63-mediated stimulation of *CCNG2* expression promotes tumor cell invasion and metastasis (Adorno et al., 2009).

The forkhead box O (FOXO) family of TFs that promote cell cycle arrest and apoptosis were the first identified transcriptional activators of *CCNG2* (Martinez-Gac et al., 2004). FOXO TFs bind to FOXO response elements (FRE) within the *CCNG2*

promoter region and potently activate *CCNG2* transcription in response to inhibition of the phosphatidylinositol 3-kinase (PI3K) (Martinez-Gac et al., 2004). In addition, binding of FOXO and δEF1 to the insulin response sequences (IRS) within the *CCNG2* promoter has been demonstrated to stimulate *CCNG2* expression (Chen et al., 2006; Fu and Peng, 2011).

The tumor suppressor BRCA1 regulates multiple processes including gene transcription, DNA repair and cell cycle checkpoint control (Venkitaraman, 2002). Though the TFs involved have not been defined, induction of ectopic BRCA1 has been shown to increase *CCNG2* expression coincident with the reduction of the oncogene Myc (Bae et al., 2004; Welcsh et al., 2002).

Repression of *CCNG2* expression follows the activation of growth factor signaling and mitogenic stimuli (Frasor et al., 2003; Le et al., 2007; Oliver et al., 2003; Stossi et al., 2006). It was previously shown that elevated expression of the oncoprotein Myc in neuroblastoma and pancreatic cancer cells leads to increased expression of histone deacetylase (HDAC) 2, and a consequent reduction in *CCNG2* expression. Myc protein recruits HDAC2 to the promoter region of *CCNG2* and induces histone hypo-acetylation, leading to transcriptional repression. Consistently, downregulation of Myc expression or treatment with HDAC inhibitors leads to upregulation of *CCNG2* expression (Cellai et al., 2011; Jayapal et al., 2010; Marshall et al., 2010; Truffinet et al., 2007). Notably, Myc expression has been linked to endocrine therapy resistance in breast cancers (BCs) (Miller et al., 2011b).

The promoter region of *CCNG2* contains one half-estrogen response element (ERE) as well as a GC-rich region important for the estrogen receptor α (ERα) binding to DNA. Interestingly, treatment of estrogen (E2) responsive cells with E2 leads to ERα mediated transcriptional repression of *CCNG2* expression (Figure 1-2) (Frasor et al., 2003; Stossi et al., 2006; Stossi et al., 2009). Estrogen bound ERα binds with Sp1 to the ERE within the *CCNG2* promoter region and recruits the co-repressor complex N-CoR and HDAC, leading to histone deacetylation and release of the basal transcription machinery (Stossi et al., 2006). E2-mediated ER-activity drives proliferation (see 1.4 Breast Cancer) and is the target of various BC therapeutics (Lange and Yee, 2011).
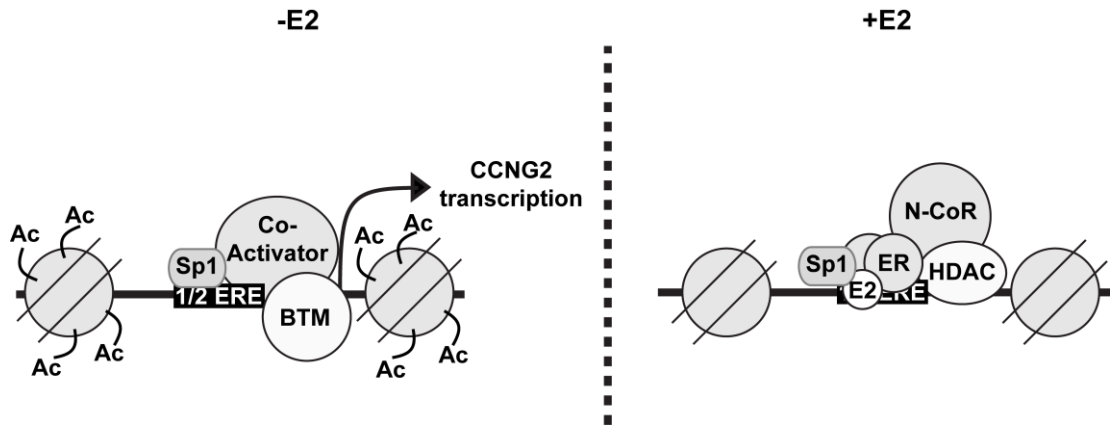
Figure 1-2: Proposed model for ERα-mediated repression of the CycG2 gene expression. In the absence of E2 (left), *CCNG2* basal transcription is regulated by Sp1 and other possible factors acting as transcriptional activators. Recruitment of co-activator complexes to the *CCNG2* promoter stabilizes the basal transcriptional machinery (BTM) and enables gene transcription by RNA polymerase II. Upon E2 treatment, Sp1 mediated ERα recruitment to the half-ERE, leads to displacement of RNA polymerase II and induces recruitment of a co-repressor complex containing N-CoR and histone deacetylases (HDAC). Formation of this complex leads to hypo-acetylation of histones, which causes stabilization of the nucleosome structure, limiting accessibility to the BTM and thus repressing CycG2 gene expression (adapted from (Stossi et al., 2006)).

CycG2 negatively regulates cell cycle progression and is itself negatively regulated by mitotic signaling (Figure 1-3) through growth factor receptors such as the human epidermal growth factor receptor 2 (HER2), the insulin receptor (IR), the insulin like growth factor (IGFR) as well as their downstream kinases PI3K and mammalian target of rapamycin (mTOR) (Casa et al., 2011; Jensen et al., 2008; Kasukabe et al., 2005; Le et al., 2007; Stossi et al., 2006). *CCNG2* expression is repressed following the inactivation of FOXO activity by growth factor mediated activation of the PI3K signaling pathway (Frasor et al., 2003; Martinez-Gac et al., 2004). Activation of the transmembrane receptors HER2 and IGFR is implicated in stimulation of cancer growth and resistance to endocrine therapy through activation of PI3K/mTOR and MAPK signaling (Zhang et al., 2011). mTOR activity is regulated (Figure 1-7) downstream of growth factor signaling, simultaneously sensing the status of energy, nutrients and stress (Zoncu et al., 2011). Recently is was shown that inhibition of mTOR activity in human embryonic stem cells (hESC) by rapamycin induces CycG2 expression, leading to reduced self-renewal capabilities and endoderm/mesoderm differentiation (Zhou et al., 2009). This indicates a role for CycG2 in regulating cell growth in hESC following induction of differentiation (Castro et al., 2011; Houldsworth et al., 2002; Sepulveda et al., 2008).

CycG2 mRNA expression is repressed in a variety of human cancers, including

thyroid (Ito et al., 2003), oral (Kim et al., 2004) and breast carcinomas (Adorno et al., 2009; Hu et al., 2006; van de Vijver et al., 2002). Analysis of publicly available cDNA microarray data indicates that low *CCNG2* expression correlates with more aggressive, poor-prognosis breast cancer subtypes (Adorno et al., 2009; Hu et al., 2006; van de Vijver et al., 2002). In contrast, higher levels of CycG2 mRNA can be found in normally differentiated breast and hormone responsive tumor cells treated with anti-estrogens (Dudek and Picard, 2008; Frasor et al., 2004). CycG2 mRNA levels are significantly upregulated in response to a variety of stresses such as DNA damage, hypoxia, heat shock, ERS and oxidative stress (Figure 1-3) (Akli et al., 2004; Bates et al., 1996; Hofstetter et al., 2012; Ito et al., 2004; Murray et al., 2004; Thomas et al., 2007).
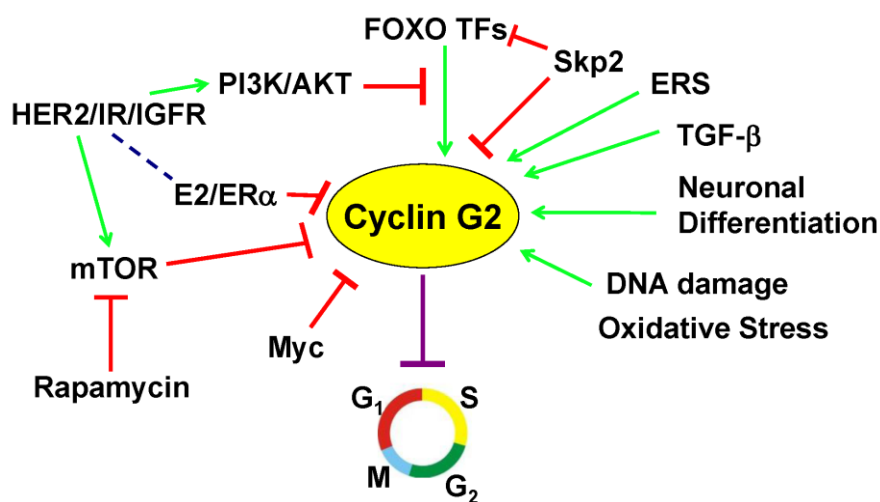
Figure 1-3: Model of the regulation of CycG2 expression. CycG2 expression is upregulated in response to growth inhibitory signals (for example: DNA damage, ERS, and differentiation) and suppressed by growth stimulatory signals (including growth factors). Ectopic expression of CycG2 inhibits cell cycle progression in G_1-phase. This arrest is p53 and Chk2 dependent. CycG2 gene expression is activated by FOXO3a and 1 TFs. FOXO activity is negatively regulated by PI3K/Akt pathway. CycG2 is degraded through the ubiquitin proteasome pathway by the E3 ligase SCF involving Skp2, which also targets FOXO TFs.

1.3 DNA Damage

Genomic instability is considered a hallmark of cancer. Maintaining genomic integrity is important to prevent cell death and cancer development (Hanahan and Weinberg, 2011). Damage of DNA can be triggered by various exogenous (UV light, ionizing radiation, chemicals) or endogenous factors (DNA replication, metabolic

products). Therefore, cells have developed multiple DNA repair mechanisms to protect cells from such perilous damage (Lord and Ashworth, 2012). The first cellular reaction to DNA damage is the induction of DNA damage response (DDR) to halt the cell cycle progression. Inducing a cell cycle arrest gives the cell time for DNA repair. If the damage is too substantial, apoptosis is induced (Oberle and Blattner, 2010).

1.3.1 DNA Damage Checkpoints

Cellular response to DNA damage is mediated through the activation of cell cycle checkpoints. These checkpoints (G_1/S, intra-S and the G_2/M) are used by the cell to monitor and regulate the progress of the cell cycle and to ensure the integrity of the genome (Houtgraaf et al., 2006; Rainey et al., 2006). The G_1/S checkpoint is frequently compromised in human cancers, due to loss of p53 or Rb tumor suppressor functions (Kastan et al., 1991; Sherr and McCormick, 2002). The intra-S checkpoint can slow the rate at which damaged DNA is replicated, in part by diminishing the rate of replication origin firing (Bartek et al., 2004). The G_2/M checkpoint helps prevent cells with damaged genomes from committing to mitosis by suppressing CycB/CDK1 activity and to allow time for DNA damage repair (O'Connell et al., 2000). A functional G_2/M checkpoint is retained in virtually all tumor cell lines (Kuntz and O'Connell, 2009).

Inducing DNA damage by radiation or chemotherapy is a widely used method in cancer therapy (Lord and Ashworth, 2012). Cancer cells are very sensitive to DNA damaging agents, due to loss of one or several checkpoints. Thus a combination of DNA damage induction and simultaneous inhibition of the DNA damage response (DDR) pathway holds promise for the enhancement of current therapeutics (Al-Ejeh et al., 2010).

1.3.2 DNA Damage Response

The DDR pathway (Figure 1-4) plays a crucial role in tumorgenesis and response to cancer therapy. It has evolved to maintain genomic integrity following DNA damage by inhibiting cellular replication and inducing DNA repair (Bohgaki et al., 2010; Houtgraaf et al., 2006). Information regarding DNA lesions is relayed within minutes through DDR signal-transduction pathways. The signaling cascade is composed of sensor, transducer, and effector proteins. The type of cellular response

(cell cycle arrest, DNA repair, and apoptosis) depends on the type and extent of the damage. DNA double strand breaks (DSBs) pose the most serious type of damage, and induce the activation of DNA DSB DDR pathway (Figure 1-4). Involved in DNA damage repair is the tumor suppressor BRCA1 (Welcsh et al., 2002).

Damage sensors initiate and coordinate activation of one of the PI3K-related kinases (PIKKs) that play central roles in maintenance of organismal longevity. Members of this family are ataxia telangiectasia mutated (ATM), ATM and Rad3-related (ATR) and DNA-dependent protein kinase (DNA-PK) (Jackson and Bartek, 2009; Lovejoy and Cortez, 2009). ATM is primarily activated by DNA DSBs incurred through γ-IR induced damage (Derheimer and Kastan, 2010), whereas ATR activation occurs mostly in response to singlestranded DNA (ssDNA) such as those presented in stalled replication intermediates or resected DSB ends (Shiotani and Zou, 2009a). DNA-PK is a critical participant in the non-homologous end-joining (NHEJ) pathway utilized for the repair of DSBs resulting from the normal process of V(D)J recombination, but it is also thought to serve a vital DNA repair function during DDRs to genotoxic stress (Hill and Lee, 2010). Growing evidence suggests, however, that extensive crosstalk between the DNA damage responsive PIKKs exists, the summation of which determines cell fate (Hill and Lee, 2010; Shiotani and Zou, 2009a).

ATM activation is critical for the initial response to DSBs (Derheimer and Kastan, 2010). The Mre11-Rad50-Nbs1 (MRN) sensor complex promotes ATM activation and recognition of DSBs (Lee and Paull, 2004). It facilitates trans-autophosphorylation of inactive ATM dimers on Ser1981 and ATM dissociation into catalytically active monomers (Derheimer and Kastan, 2010; Lee and Paull, 2004). Once activated, ATM interacts with and phosphorylates numerous proteins (including Nbs1, Chk2, Chk1 and p53) to amplify and propagate the signal. Later in the DSB response, the progressive resection of blunt end DSB junctions to ones with longer single strand ends triggers ATR activation (Derheimer and Kastan, 2010; Jazayeri et al., 2006; Shiotani and Zou, 2009b). ATM and ATR have overlapping substrate specificity towards Chk2 and Chk1 (Shiotani and Zou, 2009a). Activated Chk1 and Chk2 phosphorylate and modulate the activity of downstream effectors (such as Cdc25 A, B and C; p53), halting the progression of cells through G_1/S and G_2/M-

phase checkpoints (Derheimer and Kastan, 2010; Lindqvist et al., 2009; Shiotani and Zou, 2009a; Stracker et al., 2009).
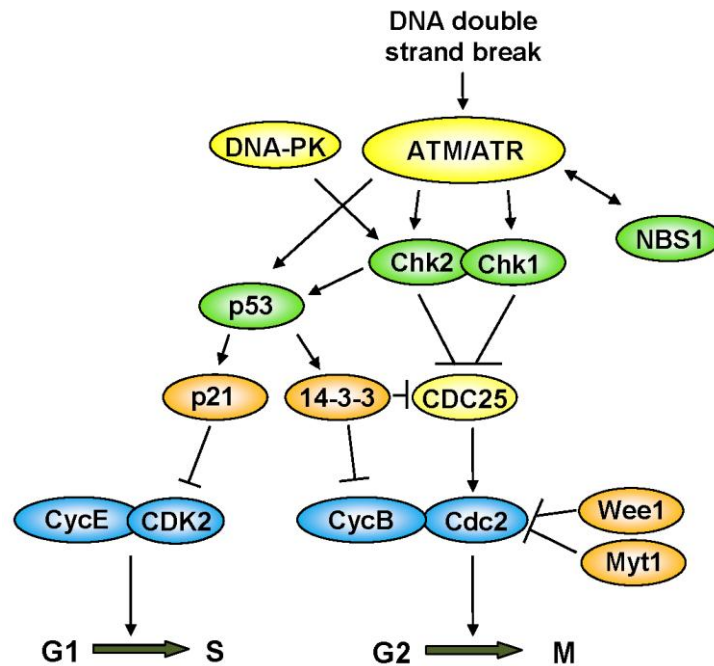
Figure 1-4: Illustration of the activation of the G_1/S and G_2/M checkpoints after DNA damage. In response to DNA damage, the ATM, ATR signaling pathway is activated, which leads to the phosphorylation and activation of Chk1 and Chk2 kinases. Chk1 and Chk2 phosphorylate CDC25, thereby triggering its sequestration into the cytoplasm by 14-3-3 proteins. CDC25 sequestration prevents activation of CycB/Cdc2 (CDK1), resulting in G_2-phase arrest. Activated ATM/ATR also activates p53-dependent signaling pathway. This contributes to the maintenance of G_2 arrest by upregulation of 14-3-3, which sequesters CDK1 in the cytoplasm. In addition, p53 induces transcription of p21, resulting in CycE/CDK2 complex inhibition and G_1/S-phase arrest (adapted from (Wang et al., 2009)).

1.4 Breast Cancer

Breast cancer (BC) is the most frequently diagnosed cancer (excluding cancers of the skin) in women. Increasing age is the most significant risk factor for BC. Additionally, factors such as obesity, usage of hormone replacement therapy, physical inactivity, alcohol consumption, never having children, and having one's first child after age 30 also contribute to a higher risk of developing BC (Society, 2012). Inherited mutations or deletion of breast cancer susceptibility genes (BRCA) 1 and 2 result in an increased risk for breast and ovarian cancer (Roy et al., 2012).

Cellular proliferation of BC is driven by signaling through activated ER, HER2 and mTOR pathways. Each of these signaling nodes is a target of adjuvant therapy

(Di Cosimo and Baselga, 2008), and activation of these pathways negatively regulate CycG2 expression (Kasukabe et al., 2008; Le et al., 2007; Stossi et al., 2006).

BC can be divided into at least five distinct subtypes in ascending order of unfavorable prognosis. First, the luminal A subtype is characterized by ER expression and low cellular proliferation. Second, the luminal B type is ER positive (some are also HER2 positive), and exhibits higher proliferation and poorer prognosis then luminal A. Third, the HER2-enriched class shows a more aggressive behavior. Fourth, the basal-like BC is triple negative for ER, progesterone receptor (PR) and HER2 and shows an aggressive behavior phenotype with high cellular proliferation, and very poor prognosis. Last, the normal-like type, which shows a gene expression pattern similar to adipose tissue (Alizart et al., 2012).

Approximately two-thirds of BCs demonstrate estrogen-dependent growth (Martin, 2006). Therefore, a common therapeutic approach is the targeting of ER and HER2 activity, but the majority of BC patients eventually develop resistance (*de novo* or acquired) (Lange and Yee, 2011; Zhang et al., 2011).

1.4.1   Estrogen Receptor

The estrogen receptor exists as two isoforms, ERα and ERβ, which are encoded by two different genes. Both are members of the nuclear receptor superfamily of TFs and mediate the proliferative actions of E2. ERα is expressed in the normal mammary gland and is critical for both, proper development and function of reproductive structures. It represents one of the most important molecular markers guiding therapy decisions in BC (DeNardo et al., 2007; O'Donnell et al., 2005; Pearce and Jordan, 2004). ERα is the main ER in the breast and its expression increases with the progression of BC, whereas the amount of ERβ decreases (Leygue et al., 1998). The biological relevance of ERβ in BC is not clear. Multiple studies show that ERβ is the primary ER expressed in the colon. Loss and change in localization of ERβ is associated with the progression of colon cancer (Pearce and Jordan, 2004).

ERα is expressed in about 70% of all BCs and is increased in both premalignant and malignant lesions (Fabris et al., 1987). Determination of ERα expression by immunohistochemistry or microarray is thus common practice to predict response to therapies directed against ER signaling (Viale, 2007).

1.4.2 Estrogen Receptor Signaling

E2 can freely diffuse into the cells and bind to the ER within the cytoplasm (Figure 1-5). Subsequently, the receptor undergoes conformational changes and forms homodimers. The dimers relocate into the nucleus where they initiate or inhibit gene expression by attracting co-activators or co-repressors to EREs within the promoters of target genes (Osborne and Schiff, 2011).
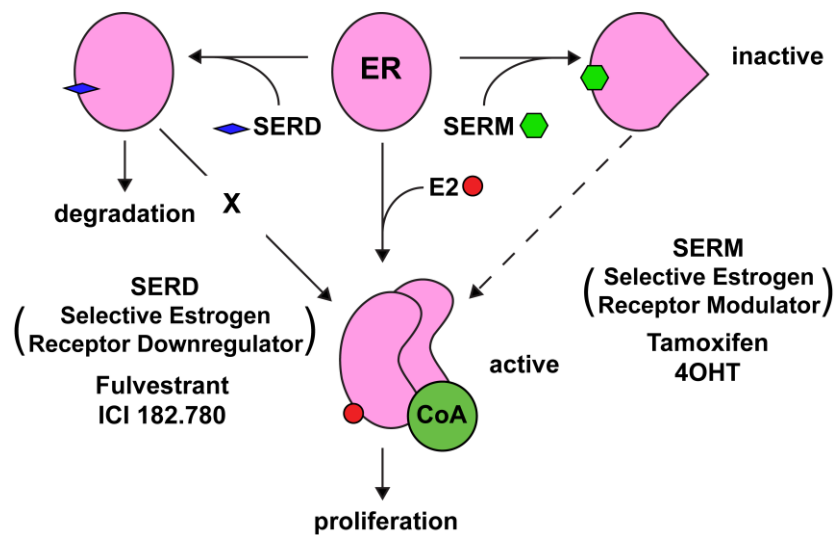
Figure 1-5: Schematic of estrogen receptor signaling and response to ER inhibitors. Binding of estrogen (E2) to the estrogen receptor (ER) leads to recruitment of co-regulator complexes and stimulation of cellular proliferation. Upon binding tamoxifen, ERα adopts a conformation (right) that is distinct from both the apo-ERα (top-middle) and that which occurs upon binding estradiol (bottom). This conformational change disrupts the primary co-regulator binding surface on ERα. Binding of fulvestrant (left) leads to ERα nuclear export and recognition by the UPS (adapted from (McDonnell and Wardell, 2010)).

E2 mediated ER activation stimulates the expression of genes positively influencing proliferation (such as CycD1 and CycA2) and downregulates transcriptional repressors, antiproliferative and proapoptotic genes (including, CycG2, p21, and FOXO3a) (Frasor et al., 2003). In addition, ER activity can regulate cellular function in a ligand independent manner (non-genomic effects) (Pearce and Jordan, 2004), which induces crosstalk to other signaling pathways like IGFR and MAPK (Kato, 2001; Lannigan, 2003; Zhang et al., 2002). This ligand independent activity is probably mediated by plasma membrane localized ER (Zhang et al., 2002), a consequence of both, a shift in localization from the nucleus to the plasma membrane and ER phosphorylation (Lannigan, 2003). Proliferation of ER positive BC tumors is

driven by activated ER signaling. Therefore, inhibition of ER signaling is common practice in BC therapy (Lange and Yee, 2011).

1.4.3 ER Targeted Therapeutics

The disruption of ER signaling can be achieved by various approaches. Selective estrogen receptor modulators (SERMs) such as tamoxifen (4OHT) are commonly used to treat ER positive BC. They compete with E2 for ER binding and can display agonist or antagonist behavior depending on the tissue and concentration (Jordan et al., 2001). Treatment of BC with selective estrogen receptor downregulators (SERDs) like fulvestrant (ICI 182,780), leads to the inhibition of E2 signaling and downregulation of the receptor itself by targeting ERα protein for degradation (Croxtall and McKeage, 2011; Dauvois et al., 1993). A third mechanism to prevent ER signaling is the use of aromatase inhibitors to hinder the production of E2 by blocking the conversion of precursor molecules to E2 (Pearce and Jordan, 2004).

Resistance to ER inhibition eventually develops in the majority of patients (Zhang et al., 2011), possibly through increased utilization of ligand independent signaling crosstalk with insulin-like or epidermal growth factor receptor (IGFR and EGFR, respectively) pathways (Song et al., 2010). This crosstalk leads to activation of the growth promoting MAPK and PI3K cascade pathways. Activation of IGFR signaling results in the phosphorylation of ER, leading to increased ER interaction with DNA and co-factor binding (Arpino et al., 2008). In addition, IGFR can form heterodimers with HER2 leading in the continued HER2 signaling presence of the HER2 inhibitor trastuzumab (Huang et al., 2010). In cell line models of endocrine resistant BC, CycD1 expression and Rb phosphorylation were maintained despite effective ER blockade (Thangavel et al., 2011). Simultaneously, inhibition of E2 signaling and ER crosstalk pathways may reverse resistance.

1.5 The Mitogen Activated Protein Kinase Cascade Pathway

Constitutive activation of the mitogen activated protein kinase (MAPK) pathway can be found in approximately 30% of all human cancers (Ohren et al., 2004). To date, four distinct MAPK cascades (ERK, JNK, p38, and ERK5) have been described (Abe et al., 2002). In general, the ERK-MAPK (Figure 1-6) pathway is activated by

growth factors, whereas the JNK, p38 and ERK5 pathways are activated by growth factors, and additionally by stress (Roberts and Der, 2007).
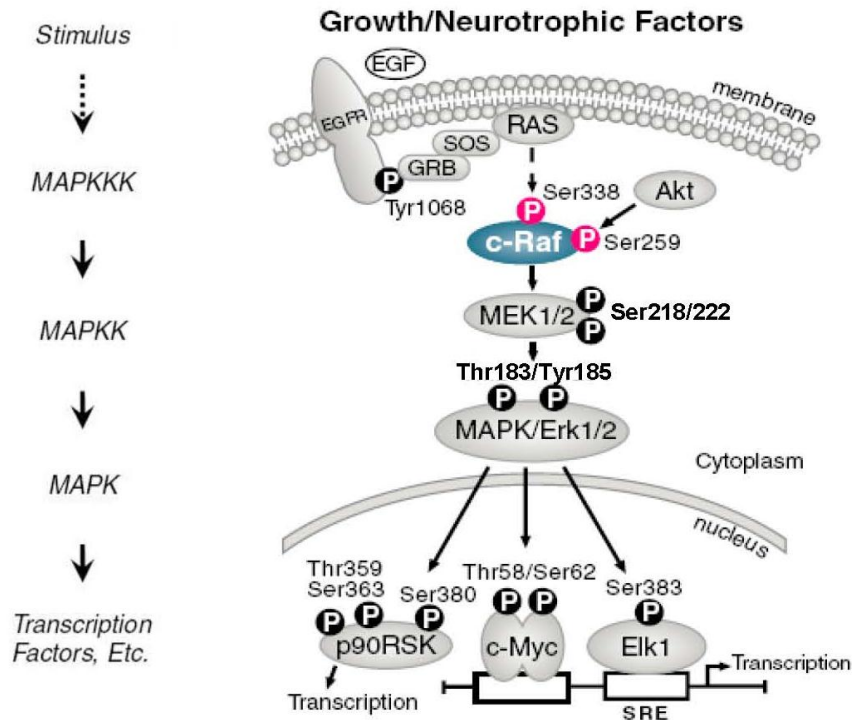
Figure 1-6: Schematic of the ERK-MAPK cascade activation. Activation of the receptor tyrosine kinase (RTK) EGFR by the growth factor EGF leads to activation of the MAPK cascade. Activated receptors recruit Ras guanine nucleotide-exchange factors, such as son of sevenless (SOS) through the adaptor protein growth-factor-receptor-bound-2 (Grb2), which generates GTP bound Ras. Ras facilitates the phosphorylation of MAPK and ERK kinase (MEK) by Raf, and enhances the generation of activated extracellular signal-regulated kinase (ERK). Activated ERKs translocate to the nucleus, where they phosphorylate and regulate various transcription factors leading to changes in gene expression (adapted from Cell Signaling phospho S259 cRaf datasheet, pdf downloaded 03-16-12).

1.5.1 ERK-MAPK Cascade

The extracellular signal-regulated kinase (ERK) cascade is stimulated by multiple extracellular signals, and, in turn, regulates various cellular processes, including proliferation, differentiation, survival and apoptosis (Shaul and Seger, 2007). Sensing and responding to extracellular signals is accomplished by binding of growth factors (such as EGF) to its specific surface membrane receptors (such as EGFR) and relaying the signal to downstream TFs (Figure 1-6). Following receptor activation, the signal is transmitted to the small G-protein Ras, that recruits the serine/threonine kinase Raf to the plasma membrane and mediates its activation (Wellbrock et al., 2004). The inhibitory Akt phosphorylation at residue S259 of Raf is removed by

PP2A (Abraham et al., 2000). Following phosphorylation of S338 by Pak (p21-activating protein), active Raf phosphorylates MAPK/ERK kinases (MEK) 1 and 2 at residues S218/222 and S222/226, respectively (King et al., 1998).

MEK activity is regulated through several phosphorylation sites, targeted either by upstream activators, downstream proteins (including ERK, PAK1), or by binding to scaffold proteins (such as Grb10) (Resing et al., 1995). Inactivation of MEK is achieved by dephosphorylation mainly through PP2A (Sontag et al., 1993). Additionally, N-terminal phosphorylation by PAK1 (T298), ERK (T292), and CDK5 (T286) contributes to MEK inhibition (Roskoski, 2012).

Active MEK1/2 activates its only substrates, ERK1 and ERK2, by phosphorylation at the regulatory residues T202/Y204 and T183/Y185, respectively (Seger et al., 1992). Dephosphorylation of either one or both of these regulatory sites by PP2A (S/Y specificity), PTP-SL (Y specificity), or MAPK phosphatase MKP (T/Y specificity) deactivates ERK (Alessi et al., 1995; Pulido et al., 1998; Sun et al., 1993). ERK activation triggers inhibitory phosphorylation of the upstream proteins SOS, Raf, and MEK. These negative feedback loops are important for the reduction of the mitogenic signal (Shaul and Seger, 2007). Activated ERK phosphorylates and activates a series of transcription factors such as Elk1, c-Fos, p53, Ets1/2 and c-Jun, which are implicated in the initiation and regulation of proliferation and oncogenic transformation.

1.6 PI3K/Akt Signaling Pathway

Many growth factors stimulate the activity of PI3K to phosphorylate phosphatidylinositol 4,5-bisphosphate (PIP$_2$) lipids to generate phosphatidylinositol 3,4,5-trisphosphate (PIP$_3$). This generates binding sites for Akt and PDK, recruiting them to the plasma membrane. Akt's activity and specificity is stimulated by PDK1 phosphorylating T308 (Calleja et al., 2007) and by mTOR phosphorylating S473 (Jacinto et al., 2006). Translocation of activated Akt into the nucleus influences downstream pathways such as metabolism, proliferation, cell survival and angiogenesis (Figure 1-7). Akt signaling is terminated by PTEN (PIP$_3$ dephosphorylation) and PP2A (Akt dephosphorylation) (Andjelkovic et al., 1996; Brognard et al., 2007). Inhibition of FOXO TFs, GSKβ and TSC2 by phosphorylation

through Akt (Figure 1-7), positively influences proliferation and cell survival (Manning and Cantley, 2007).
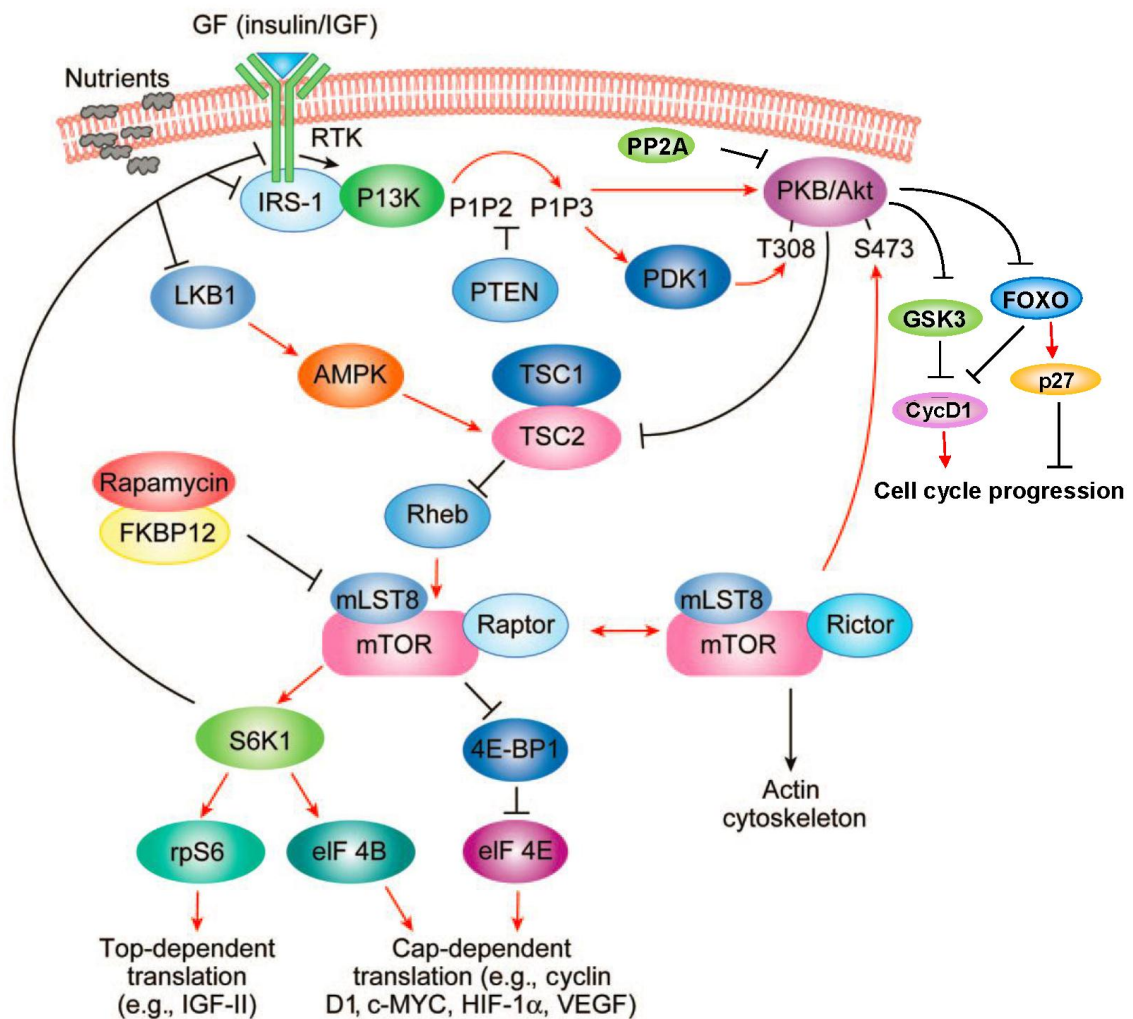
Figure 1-7: A model of PI3K/Akt/mTOR signaling cascade and its function. Mitogen signaling through RTK activates PI3K, which generates PIP3 to recruit Akt to the plasma membrane. Akt is activated by PDK1 through Thr308 phosphorylation and by mTORC2 (consisting of mTOR, mLST8 and Rictor) trough S473 phosphorylation. Activated Akt destabilizes the TSC1/TSC2 complex by phosphorylating TSC2 (T1462 or S939). TSC2 inhibits Rheb, which positively modulates mTORC1 (consisting of mTOR, mLST8, and raptor) function. Phosphorylated GSK3 leads to its translocation into the nucleus, where it mediates the phosphorylation dependent destruction of CycD and CycE. Phosphorylation of FOXO TFs by Akt leads to their nuclear export and degradation in the cytoplasm. Low energy level (ATP, amino acids) activates LKB1 (serine threonine kinase 11) and AMPK (AMP-activated kinase), which in turn activate TSC1/2, leading to mTORC1 inhibition. Active mTORC1 phosphorylates S6K1 and 4E-BP1 and leads to release of the inhibitory block of 4E-BP1 (eukaryotic initiation factor 4E binding protein-1) from elF-4E (eukaryotic initiation factor 4E). mTORC1 initiates a negative feedback loop to modulate Akt activity through S6K1 (protein S6 kinase 1) (adapted from (Wan and Helman, 2007)).

1.7 Forkhead Box O Transcription Factors

A key signaling molecule induced and activated in response to cellular stress is the highly conserved FOXO TF (Salih and Brunet, 2008). FOXO TFs are involved in the regulation of multiple cellular processes such as cell cycle arrest, cell death, and DNA damage repair. Inactivation of FOXO proteins is associated with BC, prostate cancer, and leukemia (Dong et al., 2006; Myatt and Lam, 2007; Yang et al., 2008). The activation of oncogenic pathways such as PI3K/Akt and ERK-MAPK triggers FOXO inactivation through phosphorylation at multiple sites, leading to its nuclear export and degradation within the cytosol (Brunet et al., 1999; Yang et al., 2008). Increasing FOXO activity by counteracting on its inhibitory pathways may provide an effective therapeutic cancer strategy.

1.8 Mammalian Target of Rapamycin

The protein kinase mTOR forms two distinct complexes (mTOR complex 1 and 2: TORC1/2) important for nutrient status recognition and growth factor signaling (Figure 1-7). Deregulation of mTOR signaling is implicated in cancer growth and survival (Wan and Helman, 2007). Two regulatory mechanisms regulate TORC1 activity. First, growth factor stimulation triggers the activation of the PI3K/Akt signaling pathway, which leads to the inhibition of the tuberous sclerosis complex (TSC) 2 (Inoki et al., 2002). Unphosphorylated TSC2 forms stable complexes with TSC1, consequently inhibiting the activity of the small GTPase Ras homologue expressed in brain (Rheb), which is required for mTOR activity (Hay and Sonenberg, 2004). Active Rheb promotes mTOR activation by preventing the binding of the endogenous mTOR inhibitor FKBP38 (Bai et al., 2007).

The second regulatory pathway senses the energy state of the cell through amino acid and ATP levels. Low energy levels activate AMP-activated kinase (AMPK), which in turn activates TSC2, leading to TORC1 inhibition (Inoki et al., 2003). TORC1 activation induces gene transcription via protein S6 kinase (S6K) and 4E-BP1 phosphorylation, promoting protein synthesis, cell growth and proliferation (Martin and Hall, 2005). A negative feedback loop is initiated by TORC1 through S6K1 to inhibit Akt activation (Figure 1-7) (Wan and Helman, 2007).

1.9   Aims of this Work

The goal of the present study was to define the role of the cell cycle regulatory protein CycG2 in the control of cell cycle progression following therapeutic treatment of cancer cells. We hypothesize that CycG2 mediates cell cycle restriction following induction of DSBs and ERS, and the inhibition of E2 and mTOR signaling. This hypothesis was investigated though the following three approaches:

1. To define the role of CycG2 in checkpoint control, the effects of ectopic CycG2 expression on cell cycle progression and DDR signaling in the absence of DNA damage was assessed. Next, shRNA mediated KD of endogenous CycG2 expression was used to investigate the involvement of CycG2 in chemotherapeutically induced DDR.

2. The contribution of CycG2 to therapeutically mediated growth restriction in BC cell proliferation was determined as was CycG2's implication in therapy resistance. To clarify the impact of CycG2 expression in BC therapy, the cellular response to therapeutic E2 and ER inhibition in combination with RNAi mediated knockdown of CycG2 expression was analyzed using both cell cycle distribution and the expression of proliferation-related proteins.

3. The possible contribution of CycG2 expression to growth control in TSC fibroblasts was addressed. To determine whether CycG2 upregulation during inhibition of mTOR activity or pharmacologically induced ERS modulates the proliferation of normal and TSC-deficient cells, biochemical and cell cycle analyses of CycG2 modulation were performed.

Together, these studies were intended to determine the degree to which CycG2 expression influences the growth-inhibitory effects on DDR inducing therapies, as well as inhibition of E2 and mTOR signaling.

2. Material und Methods

2.1 Material

2.1.1 Pharmacological Agents

All reagents not listed in table below were of standard quality from established suppliers.

Reagent	Vendor	Stock Solution	FC	Number
Aprotinin	Sigma-Aldich Corp., St. Louis, MO	20 mg/mL in H_2O	2 µg/mL	A1153
BrdU	Sigma-Aldich	10 mM in H_2O	10 µM	B5002
BSA	RPI Corp., Mount Prospect, IL	5% in TBS-T or 1% in PBS		A30075
Caffeine (Caff)	Sigma-Aldich	freshly dissolved in medium	3 mM	C0750
CGK 733	Tocris Bioscience, Ellisville, MO	20 mM in DMSO	2 µM	2639
Doxorubicin (Dox)	Sigma-Aldich	0.4 mg/mL in H_2O	0.2 µg/mL	D1515
Estradiol (E2)	Sigma-Aldich	50 mg/mL in ethanol	10 nM	E8875
Etoposide (ETP)	Sigma-Aldich	100 mM in DMSO	30 µM	E1383
Fulvestrant (ICI 182,780)	Tocris	5 mM in ethanol	100 nM	1047
Insulin	Sigma-Aldich	10 mg/mL in acidified H_2O	1 µg/mL	I1882
IPTG	Fisher Scientific, Pittsburgh, PA	1 M in H_2O	1 mM	367-93-1
KU 60019	Selleckchem, Houston, TX	50 mM in ethanol	1 µM	S1570
KU 55933	Calbiochem, Rockland, MA	100 mM in methanol	10 µM	118500
Leupeptin	Sigma-Aldich	10 mg/mL in H_2O	1 µg/mL	L2884
LY 294004 (LY)	Cell Signaling technology, Danvers, MA	50 mM in DMSO	25 µM	9901
Metformin (Met)	Sigma-Aldich	1 M in PBS	1 mM	D150959
Microcystin LR	Calbiochem	400 µM in DMSO	2 µM	475815
NaF	Sigma-Aldich	800 mM in H_2O	25 mM	201154
NaPPi	Sigma-Aldich	250 mM in H_2O	25 mM	S9515
Nocodazole (Noc)	Sigma-Aldich	10 mg/mL in DMSO	50 ng/mL	M1404
NU 7026	Cayman Chemical, Ann	10 mM in DMSO	5-10 µM	13308

Reagent	Vendor	Stock Solution	FC	Number
	Arbor, MI			
NU 7441	Selleckchem	50 mM in DMSO	1-2 μM	S2638
pepstatin A	Sigma-Aldich	1 mg/mL in methanol	1 μg/mL	77170
Polybrene	Sigma-Aldich	8 mg/mL in H_2O	4 μg/mL	H9268
PMSF	Sigma-Aldich	34 mg/mL in ethanol	34 μg/mL	P7626
pNPPi	Sigma-Aldich	1 M in DMSO	1 mM	N3254
Propidium Iodine (PI)	Sigma-Aldich	10 mg/mL in H_2O	0.5 mg/mL	P4170
Puromycin	Sigma-Aldich	5 mg/mL in H_2O	1.5 - 3 μg/mL	P8833
Rapamycin (rapa)	Cell Signaling	100 μM in methanol	10 nM	9904
Tamoxyfen (4OHT)	Sigma-Aldich	1 mM in ethanol	100 nM	H7904
Thapsigargin (Thap)	Invitrogen, Carlsbad, CA	1.5 mM in ethanol	200-500 nM	T7458
Tunicamycin (Tuni)	Santa CruzBiotechnology, Santa Cruz, CA	5 mM in DMSO	500 nM	sc-3506

2.1.2 Table of Kits for Chemiluminescence, DNA and RNA Preparation

Kits	Vendor	Cat. Number
BCA kit	Pierce Protein Research Products, Rockford, IL	23227
ECL detection reagent	GE Healthcare, Buckinghamshire, UK	RPN2106
ECL plus detection reagent	GE Healthcare	RPN2132
Lipofectamine 2000	Invitrogen, Carlsbad, CA	11668-019
Luminata Classico	Millipore, Billerica, MA	WBLUC0500
Nucleobond Xtra DNA maxiprep EF kit	E & K Scientific, Santa Clara, CA	740424.10
QIAprep spin DNA miniprep kit	Qiagen, Valencia, CA	27106
QIAquick Gel extraction kit	Qiagen	28704
QIAshredder kit	Qiagen	79654
RNasey kit	Qiagen	74104
RT^2 first strand kit	SABioscience, Frederick, MD	330131
SuperSignal West Femto	Pierce	34095

2.1.3 Enzymes and Markers

DNA Polymerases and restriction enzymes together with their respective reaction buffers were bought from New England Biolabs (Ipswich, MA). RNaseA (EN0531), GeneRuler 1kb Plus DNA Ladder (SM1333) and PageRuler Prestained Protein

Ladder (50-860-114) were purchased from Fermentas (Glen Burnie, MD). DNase (79254) was obtained from Qiagen.

2.2   Methods

2.2.1   Sterilization

Solutions, bacterial growth media and materials were sterilized by autoclaving for 45 min at 121ºC. Heat-labile solutions were sterilized by filtering through a sterile membrane filter with a pore size of 0.22 μm (Millipore or Corning).

2.2.2   Microbiological Methods

2.2.2.1 Culturing of Bacterial Strains

Bacterial strains used in this work are listed in the table below. The strains DH5α and NovaBlue were routinely used for molecular biology and protein expression. For storage and amplification of viral vectors Stbl3 was used. In general the bacteria were grown at 37ºC over night (ON) in LB medium (1 % (w/v) Tryptone (BD), 0.5 % (w/v) Yeast extract (BD), 171 mM NaCl, pH 7.4) containing the appropriate antibiotic (50 μg/mL for kanamycin or 10 μg/mL for ampicilin) whilst shaking at 250 rpm. LB plates contained 1.5 % (w/v) agar and were also incubated at 37ºC ON.

Strain	vendor	Genotype
DH5 alpha	Invitrogen 18265-017	F- φ80lacZΔM15 Δ(lacZYA-argF) U169 recA1 endA1 hsdR17(rk-, mk +) phoAsupE44 thi-1 gyrA96 relA1 λ-
NovaBlue	EMD 7018	endA1 hsdR17 (rK12- mK12+) supE44 thi-1 recA1 gyrA96 relA1 lac F′[proA+B+ lacIqZΔM15::Tn10] (TetR)
Stbl3	Gibco C737303	F– mcrB mrr hsdS20(rB–, mB–) recA13 supE44 ara-14 galK2 lacY1 proA2 rpsL20(StrR) xyl-5 λ– leu mtl-1

2.2.2.2 Expression Constructs

Backbone	Expression cassette	Source
pcDNA3	V5 tagged murine CycG2	Horne lab
pcDNA3	GFP tagged murine CycG2	Horne lab
pcDNA3	GFP tagged human CycG2	Horne lab
pcDNA3	Untagged human CycG2	Horne lab
pReceiver-Lv71	mCherry tagged human CycG2	GeneCopoeia
pcDNA3	GFP tagged murine CycG1	Horne lab
pcDNA3	GFP	Horne lab
pEGFP	GFP tagged murine CycG2 1-140	Horne lab
pEGFP	GFP tagged murine CycG2 1-160	Horne lab

Backbone	Expression cassette	Source
pEGFP	GFP tagged murine CycG2 1-187	Horne lab
pEGFP	GFP tagged murine CycG2 142-344	Horne lab
pReceiver-M08	HA tagged human CDK10	GeneCopoeia
pcDNA3	Myc tagged PP2AB'g	Horne lab
pSilencer1.0	RFP	Horne lab
pSilencer1.0	CycG2 shRNA 1-B, RFP	Horne lab
pSilencer1.0	shRNA NSC, RFP	Horne lab
pGeneClip hMGFP	CycG2 shRNA ID3, GFP	SABiosciences
pGeneClip hMGFP	Scrambled shRNA NC, GFP	SABiosciences
pSUPER.retro.puro	CycG2 shRNA 1-B	This study
pSUPER.retro.puro	shRNA NSC	This study
pSUPER.retro.puro	CycG2 shRNA ID3	This study
pVETL.gfp	CycG2 shRNA 1-B plus GFP	This study
pVETL.gfp	shRNA NSC plus GFP	This study
pVETL.gfp	CycG2 shRNA ID3 plus GFP	This study
pVETL.gfp	shRNA NC plus GFP	This study

2.2.2.3 Preparation of Plasmid DNA

DNA from fresh ON cultures was purified with QIAprep spin DNA miniprep kit or Nucleobond Xtra DNA maxiprep EF kit following the manufacturer's protocols. DNA concentration and purity was determined by measuring the optical density at 280 and 260 nm with a Take3 multi volume plate in a Synergy2 plate reader (BioTek) by using the analysis software Gen5. The purity of DNA was determined by the ratio of A260/280.

2.2.2.4 Enzymatic Modifications of DNA

Analytical restriction of plasmid DNA was prepared by digest with endonucleases. An aliquot of DNA was mixed with the enzyme to be used and the corresponding buffer according to the manufacturer's instructions and incubated at the recommended temperature for 3 h to ON. The volume of the digestion mixture was usually 20 μL for analytical and 50 μL for preparative restrictions. Generated fragments were separated by 0.8 to 1% agarose gel electrophoresis. Bands were stained by immersing the gel in TAE buffer (40 mM Tris-Acetate, 1 mM EDTA) containing 1:10000 SYBR gold (Invitrogen, S-11494) for 1 h to ON. For further experiments, reactions were purified from a preparative agarose gel via QIAquick Gel extraction kit following

manufacturer protocols. To ligate DNA-fragments, T4 DNA ligase from NEB was used according to manufacturer instructions. Ligation was carried out at 16ºC ON.

2.2.2.5 Transformation

DH5α and Stbl3 competent cells were transformed following manufacturers protocols. Briefly, E. coli cells were thawed on ice and DNA was added to the cell solution and incubated for 30 min on ice. Cells were subjected to a heat shock of 42ºC for 45 sec, and subsequently supplemented with 300 µL SOC (Invitrogen, 1544036) medium. After incubation for 1 h at 37ºC shaking, miscellaneous volumes of the culture were plated directly onto agar-selection plates and further incubated at 37ºC ON.

2.2.2.6 shRNA Expression Constructs Cloning into pSUPERretro.puro

shRNA target sites were chosen following the guidelines provided on Ambion's "siRNA Target Finder and Design Tool". The ID3 shRNA designed against a different target site and non-targeting NC control shRNA were purchased from SABiosciences (Frederick, MD). The oligonucleotide sequences were engineered to contain BglII and HindIII endonuclease restriction sites and the oligonucleotides were obtained from Integrated DNA Technologies (Coralville, IA). The DNA constructs for expression of shRNA targeting CycG2 and controls in pSUPER.retro.puro (OligoEngine, WA) were cloned as followed. Each shRNA insert (see oligo sequences in table below) was generated by annealing forward and reverse oligonucleotides and ligating them into BglII/HindIII digested pSuper.retro.puro vector. After transformation and initial screening for possible positive clones, via XhoI/EcoRI digest of purified mini-prep DNA, the constructs were verified by DNA sequencing.

Name	Sequence of forward and reverse oligonucleotides
1-B	5' GATCgctactactgccttaaact ttcaagaga agtttaaggcagtagtagctttttt 3' 5' AGCTaaaaagctactactgccttaaact tctcttgaa agtttaaggcagtagtagc 3'
ID3	5' GATCcccggagaatgataacacttt cttcctgtca aaagtgttatcattctccgggtttttt 3' 5' AGCTaaaaacccggagaatgataacacttt tgacaggaag aaagtgttatcattctccggg 3'
NSC	5' GATCgctcccaccaccttaaact ttcaagaga agtttaaggtggtgggagctttttt 3' 5' AGCTaaaaagctcccaccaccttaaact tctcttgaa agtttaaggtggtgggagc 3'
NC	5' GATCggaatctcattcgatgcatac cttcctgtca gtatgcatcgaatgagattcctttttt 3' 5' AGCTaaaaaggaatctcattcgatgcatac tgacaggaag gtatgcatcgaatgagattcc 3'

2.2.2.7 Cloning of shRNA Constructs into pVETL

For generating the pVETL.gfp (Davidson and Harper, 2005; Harper et al., 2006) shRNA containing expression constructs, the shRNA insert inclusive the H1 promoter from the previous generated pSUPERretro.puro vector was PCR amplified using primers listed below. Amplified and MfeI digested DNA was ligated into MfeI digested pVETL.gfp vector. All constructs were verified by DNA sequencing.

Name	Sequence
forward	5' ggcgccgCAATTGgatcgatctctcgaggtcgac 3'
reverse	5' cccggtaCAATTGgaacgctgacgtcatcaacccgc 3'
sequencing	5' ctaaggttggttatttgcg 3'

2.2.2.8 Gene Expression Analysis

Total RNA was isolated from cells using the QIAshredder and RNeasy kits (Qiagen). RT^2 first strand kit (SABiosciences) was used for reverse transcription of the RNA samples. Real-time-PCR (qRT-PCR) analysis was performed on an ABI 7900HT instrument (University of Iowa) with RT^2 Custom Profiler PCR Array (SABioscience) and SYBR Green qPCR master mix (SABioscience). Fold changes in gene expression were calculated via the Web-Based PCR Array Data Analysis program from SABioscience (http://pcrdataanalysis.sabiosciences.com/pcr/arrayanalysis.php).

2.2.3 Cell Culture

2.2.3.1 Cell Lines and Medium

U2OS and HCT116 (parental, p53-/-, p21-/-, and Chk2-/-, kind gift of Dr. B. Vogelstein) cell lines were cultured in high-glucose DMEM (Gibco), supplemented with 10% heat-inactivated fetal bovine serum (HI-FBS, Atlanta Biologicals), 100 units/mL penicillin, 100 µg/mL streptomycin sulfate (Gibco) and 1 mM sodium pyruvate (Sigma). NIH3T3 cells were grown in DMEM supplemented with 10% heat-inactivated calf-serum (Cellgro), 100 units/mL penicillin and 100 µg/mL streptomycin sulfate. MCF7 cells were cultured in EMEM (Gibco) supplemented with 10% HI-FBS, 2 mM L-glutamine (RPI), 1 mM sodium pyruvate, 100 units/mL penicillin and 100 µg/mL streptomycin sulfate, and 10 µg/mL bovine insulin (Sigma). Stable shRNA expressing MCF7 clones were selected in MCF7 medium containing 3 µg/mL puromycin and maintained in medium with 1.5 µg/mL puromycin. SV40 transformed

normal (GM00637), ATM deficient (GM05849), TSC (GM06121, GM06100, GM02332, GM04520) and normal untransformed (IMR90, WI-38) human primary fibroblast cells were purchased from Coriell Cell Repositories (Camden, NJ) and cultured in EMEM, 10-20% HI-FBS, 2 mM L-glutamine, with 2x concentration of essential and non-essential amino acids and vitamins (Gibco). B-cell lymphoma SU-DHL4, SU-DHL8 and SU-DHL16 cell lines (gift of Dr. Epstein) were grown in RPMI 1640 (Gibco) supplemented with 10% HI-FBS, 2 mM L-glutamine, 100 units/mL penicillin and 100 μg/mL streptomycin sulfate and 50 μM β-mercaptoethanol.

2.2.3.2 Subculturing of Adherent Cells

Cell monolayers were washed with 1x PBS (Gibco) to remove all traces of growth medium. Thereafter cells were detached from growth surface by incubation with 0.05% trypsin/EDTA (Gibco) solution until cells lifted from the surface. Trypsin was deactivated by re-addition of growth medium and pipetting multiple times up and down to break up cell clumps. All cultures were plated at 20-30% and maintained at 50-90% confluency in a humidified chamber at 37°C with 5% CO_2.

Treated cultures were harvested by detaching the cells with 0.05 % trypsin/EDTA and subsequent centrifugation of detached cells with the collected treatment medium. Cell counts were obtained by using trypan blue (Gibco) exclusion and a hemocytometer. Cells were washed twice with PBS before storage of the cell pellet at -80°C until further use.

2.2.3.3 Subculturing of Suspension Cells

Cells grown in suspension were subcultured by dilution of stock cultures. Cells were maintained at 0.3×10^6 to 2×10^6 cells per mL. For experiments cells were seeded at 0.2×10^6 per mL.

2.2.3.4 Freezing Human Cells

Generally, log phase cells where collected and cell number was determined. Cell pellet was resuspended in FBS containing 10% DMSO so that the cell concentration was 1×10^6 to 5×10^6 cells per mL. Aliquots were transferred into cryo tubes (Sarstedt) and placed in a crygenic freezing container (for gradual freezing, thus reducing the risk of ice crystal formation and cell damage). The container was placed into a -80°C freezer for 2 days before vials were moved into the LN_2.

2.2.3.5 Selection of Stable MCF7 CycG2 Knockdown Clones

For selection of stable MCF7 clones freshly established cultures were transfected with NdeI linearized vector using Lipofectamine 2000 (Invitrogen). One day later, cells were reseeded at different densities onto new dishes and plates. The following day selection for puromycin-resistant clones was started by an exchange of culture medium containing 3 µg/mL puromycin. Selected clonal populations were expanded and tested for their ability to suppress expression of exogenous and endogenous human CycG2 by immunoblot analysis.

2.2.3.6 Transfection

2.2.3.6.1 Lipofectamine

Cells were plated the day before transfection, to be 90-95% confluent at the day of transfection. The appropriate amounts of DNA and Lipofectamine 2000 (Invitrogen) were mixed separately in Opti-MEM (Gibco) and incubated at RT for 5 min. The two mixtures were then combined and further incubated for 20 min at RT. Half of the growth medium from cultures was aspirated and the DNA-Lipofectamine-OptiMEM mixture was added. The plates were gently rocked back and forth to ensure proper mixing of the components. Cultures were incubated at 37ºC for 4 h before the medium was changed.

2.2.3.6.2 Calcium Phosphate Transfection

Cells were plated the day before transfection, to be were ca. 50% confluent at the time of transfection. DNA was diluted with 250 mM $CaCl_2$ and the mix was added dropwise to the HeBS (50 mM Hepes, 280 mM NaCl, 1.5 mM Na_2HPO_4 -7 H_2O pH 7.11) buffer while aerating the buffer with a long sterile pasteur pipette. After incubation at RT for 10 min the mix was added dropwise to the cultures and mixed by moving the dishes back and forth. Cells were further incubated for 7 h to ON (depending on Ca^{2+} sensitivity of cells) at 37ºC before changing the media or re-plating cells.

2.2.3.6.3 Viral Infection

Cells were plated the day before infection, so that they were ca. 90% confluent at the time of infection. The appropriate amount of virus was diluted in low serum (2% FBS) medium containing 4 µg/mL polybrene. Growth medium was aspirated from

cells and virus containing solution was added to the cells. Following 4 to 6 h incubation at 37ºC, the medium was changed to regular growth medium. The infected cultures were incubated 24 to 72 h further to ensure gene expression or knockdown. Infection efficiency was verified by fluorescence microscopy.

2.2.3.7 Culture Treatments

2.2.3.7.1 DNA Damage Treatments

DNA damage was induced in the specified cultures by treatment with the chemotherapeutic agents doxorubicin hydrochloride (345 nM) or etoposide (30 µM) for the indicated time periods.

2.2.3.7.2 Hormone Treatments

For estrogen depletion experiments, plated cells were washed twice with 1x PBS and cultured for indicated periods of time in phenol red free MEM medium containing 10% heat inactivated charcoal/dextran (CD) treated FBS, 2 mM L-glutamine, 1 mM sodium pyruvate, 100 units/mL penicillin and 100 µg/mL streptomycin sulfate, 10 µg/mL bovine insulin and 10 mM HEPES (Gibco). For ICI and 4OHT treatments cells were seeded the day before treatment to be 70% confluent at the point of harvest. Culture medium was preplaced with ICI (100 nM) or 4OHT (100 nM) containing regular MCF7 (E2 and phenol red containing) medium for indicated periods of time.

2.2.3.8 Fixation of Cells

2.2.3.8.1 Fixation of Cells on Coverslips

After indicated treatments coverslips were rinsed with 1x PBS and immediately submerged with ice-cold MeOH and incubated at -20ºC for 5 min. Alternatively, coverslips were fixed with 4% PFA-PBS solution for 10 min at RT. In both instances, after additional PBS washings, the coverslips were stored in PBS containing 0.02% Na-Azide until further use.

2.2.3.8.2 Fixation of Cells for Flow Cytometry

For one parameter flow cytometry, cells were collected and washed with PBS before fixation with -20ºC 70% ethanol or 100% methanol. To preserve fluorescent signals, cells were 10 min prefixed with 0.5% PFA/10 mM EDTA in PBS, washed with PBS

and fixed with -20ºC 100% methanol. Fixed cells were stored at -20ºC in the alcohol solution until analysis.

2.2.3.9 Determination of Cell Viability by Trypan Blue Exclusion

A small sample of single cells in suspension, were stained with trypan blue solution for 2 min at RT and cells were counted in a hemocytometer. The ratio of viable (trypan blue negative) and non-viable (trypan blue positive) cells was determined.

2.2.4   Protein Biochemical Methods

2.2.4.1 GST Fusion Protein Expression and Antibody Column Preparation

GST and GST fusion proteins were expressed in *E. coli* (NovaBlue). Inoculated cultures were induced for protein expression for 4 h with 1 mM Isopropyl β-D-1-thiogalactopyranoside (IPTG). Cells were collected by centrifugation and stored at -80ºC until lysis. Cell pellet was resuspended in 50 mL TBS (150 mM NaCl, 15 mM Tris-Cl, pH 7.4) containing 0.1 mg/mL lysozyme and protease inhibitors (1 µg/mL pepstatin A, 1 µg/mL leupeptin, 2 µg/mL aprotinin, 200 nM PMSF). After 30 min incubation on ice, 15 mM dithiothreitol (DTT), 10 mM EDTA and 1.5% sarkosyl were added and further incubated for 15 min. Insoluble material was removed by centrifugation at 186 010 x g for 1 h (4°C, Ti-45 rotor). After addition of 2-3% Triton X-100 to the cleared lysate to neutralize the sarkosyl, 1 mL of prewashed glutathione-sepharose was added and incubated ON at 4°C. The resin was collected by centrifugation and transferred into Econo chromatography columns (BioRad, 737-1012). The resin was washed with TBS until $OD_{280} < 0.01$.

For cross linking the fusion proteins to the resin, the resign was washed with cross-link buffer (100 mM $NaHCO_3$/150 mM NaCl pH 8.3) and incubated in dimethyl pimelimidate (DMP) solution (7.75 mg/mL in cross-link buffer, pH 8.3) for 2 to 6 h at RT in the dark. The reaction was stopped with 100 mM Tris/150 mM NaCl pH 8.0 solution. Final cleaning of resin was achieved by extensive washings with 100 mM glycine pH 3.0 and TBS solutions. Columns were stored in TBS containing 0.02% sodium azide at 4ºC. The purity of all immobilized proteins was confirmed by SDS-PAGE and Coomassie staining.

2.2.4.2 Antibody Purification

Generation of rabbit anti-cyclin G2 antibodies was as previously described (Bennin et al., 2002). The antisera against CycG2 and CycG1 proteins were affinity purified with CycG2GST or CycG1GST glutathione-sepharose columns (described earlier). Thawed CycG2 sera (2.5 mL) were incubated consecutively with GST and Cyc1GST preclear columns for 1 h at RT to remove unspecific antibodies against GST moiety of the fusion protein or those cross-reactive against CycG1. Precleared sera were then incubated with the affinity column for at least 16 h at 4ºC. After rigorous washing steps with TBS 0.1% tween antibodies were eluted with 100 mM glycine pH 2.5, neutralized with 0.1 M (final concentration) Tris-Cl pH 8.0 and concentrated with Amicon Ultra centrifugal filter devices (Millipore, Bedford, MA).

2.2.4.3 Immunoblot Analysis

Collected cell pellets were lysed in RIPA buffer (10% glycerol, 1% Nonidet P-40, 0.4% deoxycholate, 0.05% SDS, 150 mM NaCl, 10 mM EDTA, 5 mM EGTA, 50 mM Tris, pH 7.4) containing protease inhibitors (1 μg/mL pepstatin A, 1 μg/mL leupeptin, 2 μg/mL aprotinin, and 200 nM PMSF) and phosphatase inhibitors (25 mM NaF, 25 mM NaPPi, 1 mM pNPPi, and 2 μM microcystin). To further break up cell structures and compartments, lysates were sonicated for 10 sec and further incubated on ice for 30 min. Cell lysates were centrifuged at 10,000 x g to remove insoluble material. Total protein concentration of each sample was determined with the BCA protein assay kit (Pierce, Rockford, IL). A total of 10 to 75 μg of protein was separated by 10% SDS-PAGE and transferred to poly vinylidene fluoride (PVDF) membranes (BIO-RAD, Hercules, CA) via the Mini protean III Trans-Blot (BIO-RAD) system. Blocking of membranes was performed using TBS-Tween-20 (0.1%) containing 5% nonfat milk powder at RT for 1 h. Membranes were incubated with primary antibodies (see table below) for 2 h at RT or for 16 h at 4ºC. After thorough washing with TBS-Tween-20, membranes were incubated for 1 h with peroxidase-conjugated secondary antibodies. Signals were detected by chemiluminescence (GE Healthcare, Millipore, Pierce) using Kodak BioMax light film (Carestream, Rochester, NY). Developed films were scanned and densitometric measurements were performed with Adobe Photoshop CS3.

Species	Antigene specificity	Source/Vendor	Catalog Number	Dilution used
Rabbit	Akt	Cell Signaling Technology, Danvers, MA	4691	1/1000
Rabbit	Akt phospho S473	Cell Signaling	4060	1/500
Rabbit	Akt phospho T308	Cell Signaling	2965	1/1000
Mouse	alpha Tubulin	Santa Cruz Biotechnology	sc-32293	1/20000
Rabbit	ATM	Cell Signaling	2873	1/500
Mouse	ATM phospho S1981	Cell Signaling	4526	1/500
Rabbit	beta Actin	Cell Signaling	4970	1/2000
Rabbit	BiP	Cell Signaling	3177	1/1000
Mouse	BrdU	Invitrogen	B35141	1/40
Rabbit	CDC2	Santa Cruz Biotechnology	sc-54	1/1000
Rabbit	CDC2 phospho Y15	Cell Signaling	9111	1/1000
Mouse	CDC25A	Santa Cruz Biotechnology	sc-7389	1/500
Rabbit	CDC25B	Cell Signaling	9525	1/1000
Rabbit	CDC25B	Santa Cruz Biotechnology	sc-326	1/1000
Rabbit	CDC25C	Cell Signaling	4688	1/1000
Rabbit	CDC25C phospho S216	Cell Signaling	4901	1/1000
Goat	CDK10 C19	Santa Cruz Biotechnology	sc-51266	1/100
Mouse	Chk1	Cell Signaling	2360	1/3000
Rabbit	Chk1 phospho S296	Cell Signaling	2349	1/1000
Mouse	Chk2 Ab5	Neomarkers, Fremont, CA	MS-1515	1/4000
Rabbit	Chk2 phospho T68	Cell Signaling	2661	1/1000
Mouse	Chop	Cell Signaling	2895	1/1000
Rabbit	cRaf	Cell Signaling	9422	1/500
Rabbit	cRaf	Millipore, Billerica, MA	04-412	1/4000
Rabbit	cRaf phospho S338	Cell Signaling	9427	1/1000
Rabbit	cRaf phospho S259	Cell Signaling	9421	1/1000
Rabbit	cyclin B1	Cell Signaling	4138	1/1000
Mouse	cyclin D1	Santa Cruz Biotechnology	sc-20044	1/6000
Rabbit	cyclin G1	Dr. Horne	1133	1/50
Rabbit	cyclin G1 C18	Santa Cruz Biotechnology	sc-320	1/100
Rabbit	cyclin G1 H46	Santa Cruz Biotechnology	sc-7865	1/100
Rabbit	cyclin G2	Dr. Horne	68232	1/500
Rabbit	cyclin G2	Dr. Horne	68964	1/500
Rabbit	cyclin G2	Dr. Horne	63622	1/200
Rabbit	cyclin G2	Dr. Horne	1263	1/250
Rabbit	cyclin G2	Dr. Horne	1264	1/250
Sheep	cyclin G2	Dr. Horne	422	1/50
Mouse	DsRed	BD pharmingen, San Diego, CA	51-8115GR	1/2000
Rabbit	ERK1/2	Cell Signaling	9102	1/2000
Rabbit	ERK1/2 phospho T202/Y204	Cell Signaling	9101	1/3000
Rabbit	FOXO1	Cell Signaling	2880	1/1000
Rabbit	FOXO1/3a phospho	Cell Signaling	9464	1/1000

Species	Antigene specificity	Source/Vendor	Catalog Number	Dilution used
	T24/T32			
Rabbit	FOXO3a	Cell Signaling	9467	1/1000
Mouse	GAPDH	Millipore	MAB374	1/200000
Mouse	GFP	NeuroMab Facility, Davis CA	N86/8	1/500
Bovine	Goat IgG (HRP labeled)	JacksonImmunoResearch, West Grove, PA	805-035-180	1/2000
Donkey	Goat IgG (HRP labeled)	JacksonImmunoResearch	705-035-147	1/2000
Mouse	HA	Covance, Emeryville, CA	MMS-101P	1/1000
Rabbit	MEK1/2	Cell Signaling	8727	1/1000
Rabbit	MEK1/2 phospho S217/221	Cell Signaling	9121	1/3000
Goat	mouse IgG (HRP labeled)	BioRad, Hercules, CA	170-6516	1/5000
Donkey	mouse IgG (alexa488)	Molecular Probes	A21202	1/1000
Donkey	mouse IgG (alexa594)	Molecular Probes	A21203	1/1000
Rabbit	mTOR	Cell Signaling	2983	1/1000
Rabbit	mTOR phospho S2448	Cell Signaling	2971	1/1000
Mouse	Myc	Dr. Horne	9E10	1/1000
Rabbit	Myt1	Cell Signaling	4282	1/1000
Rabbit	NBS1	Cell Signaling	3002	1/1000
Rabbit	NBS1 phospho S343	Novus Biologicals, Littleton, CO	NB100-92610	1/1000
Rabbit	p27	Cell Signaling	2552	1/3000
Mouse	p53	Neomarkers	MS-186	1/1000
Mouse	PP2A, C subunit	Millipore	05-421	1/1000
Mouse	rabbit IgG Fc (HRP)	JacksonImmunoResearch	211-032-171	1/5000
Goat	rabbit IgG (HRP labeled)	BioRad	170-6515	1/5000
Donkey	rabbit IgG (alexa488)	Molecular Probes	A21206	1/1000
Donkey	rabbit IgG (alexa647)	Molecular Probes	A31573	1/1000
Mouse	Rb	Cell Signaling	9309	1/2000
Rabbit	Rb phospho S780	Cell Signaling	9307	1/3000
Rabbit	S6K phospho S371	Cell Signaling	9208	1/1000
Rabbit	S6K phospho T389	Cell Signaling	9234	1/1000
Goat	Sheep IgG (HRP labeled)	JacksonImmunoResearch	713-035-147	1/2500
Donkey	Sheep IgG (alexa660)	Molecular Probes	A21101	1/1000
Rabbit	Wee1	Cell Signaling	4936	1/1000
Rabbit	Wee1 phospho	Cell Signaling	4910	1/1000

2.2.4.4 Immunoprecipitation

Cleared whole lysate protein (150 to 1000 µg) was precleared with 20 µL protein A agarose or protein G sepharose bead slurry including non-specific IgG and incubated

at 4ºC for 1 h, to remove non-specific binding to sepharose or agarose beads. Precleared supernatant was incubated with 20 µL bead slurry and 1 to 10 µg precipitation antibody for 16 h at 4ºC. Preclear and immunoprecipitation beads were extensively washed with lysis buffer and proteins were eluted by adding 20 µL 1.5x SDS loading buffer. After heating the samples for 5 min at 95ºC supernatant was separated by 10% SDS-PAGE and subjected to immunoblotting.

2.2.4.5 Immunofluorescence Microscopy
2.2.4.5.1 Preparation of Coverslips

Square shaped 22 mm #1 glass coverslips (Surgipath, Richmond, IL) were treated with 2 M NaOH solution for 2 h at RT, rinsed with H_2O and immersed in pure ethanol. Individual coverslips were flamed until dry, placed into an aluminum lined glass dish and autoclaved for 20 min. Sterilized coverslips were coated with 10 mg/mL collagen and 1 µg/mL poly-L-lysine (Sigma) and stored at 4ºC until use.

2.2.4.5.2 Immunostaining

Cells were seeded at 1.5×10^5 cells/35 mm well on glass coverslips 14-18 h before treatment. PFA fixed specimens were permeabilized with 0.4% Triton-X in PBS for 20 min at RT. After incubation for 2 h in blocking solution (2% Glycerol, 50 mM NH_4Cl, 5% FBS, 2% goat serum in PBS) cells were stained with indicated antibodies diluted in blocking solution ON at 4ºC. After extensive washings with PBS wash solution (PBS, 0.15% Tween-20, 0.15% NP40) cells were blocked with 2% Glycerol, 50 mM NH_4Cl, 5% FBS, 2% goat serum, 0.2% Tween-20 in TBS for 30 min. Secondary antibodies and Hoechst 33342 stain was diluted in TBS containing blocking solution and incubated with the cells for 2 h at RT. Coverslips were washed with TBS, 0.15% Tween-20, 0.15% NP40 before being mounted with ProLong Antifade from Molecular Probes on microscope slides. Images were collected by confocal microscopy.

2.2.5   Flow Cytometry
2.2.5.1 Cell Cycle Analysis via Propidium Iodide Staining

To perform DNA cell cycle analysis, fixed cells were washed twice with 1x PBS and stained in with 50 µg/mL propidium iodide (PI, Sigma) and 0.25 mg/mL RNaseA (Fermentas) in PBS for 30 min at RT. A minimum of 20,000 events were collected

using a FACScan (Becton Dickinson, San Jose, CA) flow cytometer. DNA content cell cycle profiles were determined using FlowJo 8.5 analysis software.

2.2.5.2 Cell Cycle Analysis via Hoechst

For analysis of DNA content in non-fixed populations, cells were stained with 1 μM TO-PRO3 and 10 μg/mL Hoechst 33342 in medium for 30 min at 36°C. Cell cycle analysis was performed on the TO-PRO negative (dead) and Hoechst positive population using a LSRII flow cytometer (Becton Dickinson).

2.2.5.3 BrdU Incorporation

To measure DNA synthesis the BrdU incorporation method was used. Cells were pulsed for 1 h prior methanol fixation with 10 μM BrdU and incubated at 37°C. MeOH fixed cells were washed with PBS prior to DNA denaturation with 2 M HCl for 45 min at RT. Neutralization of hydrochloric acid was archived by adding 0.1 M Sodium-Borate buffer pH 8.2. After additional washing with PBS containing 1% BSA, cells were blocked with PBS 1% BSA solution for 20 min at RT following incubation with anti BrdU primary antibody for 2 h at RT. After washing of cells with 1% BSA in PBS cell were incubated with Alexa488 (Molecular Probes) conjugated secondary antibodies for 1 h at RT. Subsequent, cells were washed and DNA was stained with PI.

2.2.5.4 Fluorescence Activated Cell Sorting

Cells were stained with 1 μM of the cell stain TO-PRO3 for 30 min to exclude dead cells from collection. TO-PRO3 negative HCT116 cells transfected with the GFP tagged CycG2 were sorted on the basis of GFP expression with the MoFlo cell sorter (Beckman Coulter). Collected cell pellets were subsequently lysed and subjected to immunoblot analysis.

2.2.6   Statistical Analysis

Means and SEMs were calculated from at least three experimental repeats and analyzed using Prism 5.01 statistical analysis software (GraphPad Software, Inc. www.graphpad.com) with one-way analysis of variance tests and the indicated post-tests.

3. Results

3.1 Contribution of CycG2 to DNA Damage Response

Induction of genotoxic DNA damage in tumor cells, via ionizing radiation or chemotherapy, is a central approach for the control of cancer growth. Existing data showed that the mRNA expression of CycG2 is induced by the DNA damaging agent actinomycin-D, however the function of CycG2 in DNA damage checkpoint remains unclear (Bates et al., 1996; Gajate et al., 2002). To begin to address these questions, the effect of ectopic CycG2 expression on cell cycle progression and DNA damage response (DDR) signaling in the absence of DNA damage was assessed.

To further investigate the involvement of CycG2 in therapeutic-induced DNA double strand break (DSB) DDR, alterations in expression pattern for CycG2 and DDR signaling proteins induced by doxorubicin (Dox) and etoposide (ETP) were evaluated alongside the cell cycle arrest response. RNAi mediated knockdown (KD) of CycG2 expression was carried out to assess its contribution to Dox-induced signaling and cell cycle checkpoint responses.

3.1.1 Ectopic Expression of CycG2 Induces G_1-Phase Cell Cycle Arrest

Cell lines used in this study were transiently transfected with GFP tagged CycG2 (mCycG2GFP) expression constructs for 32 to 48 h, before harvesting for cell cycle analysis (Figure 3-1). The DNA in harvested and fixed cells was stained with propidium iodide (PI) and cell cycle distribution was analyzed by flow cytometry. Histogram overlays of DNA content of mCycG2GFP expressing (red line) and non-expressing (grey area/black line) cells from the same transfected culture are shown in Figure 3-1. Compared to the non-expressing control, expression of CycG2 leads to an increase in the number of cells in G_1-phase and a simultaneous reduction in the S- and G_2/M-phases of the cell cycle (numbers in upper right corner of each histogram). These experiments confirmed previous observations (Arachchige Don et al., 2006; Bennin et al., 2002; Chen et al., 2006; Kim et al., 2004; Xu et al., 2008) that ectopic expression of CycG2 leads to G_1-phase cell cycle arrest in various cell lines.
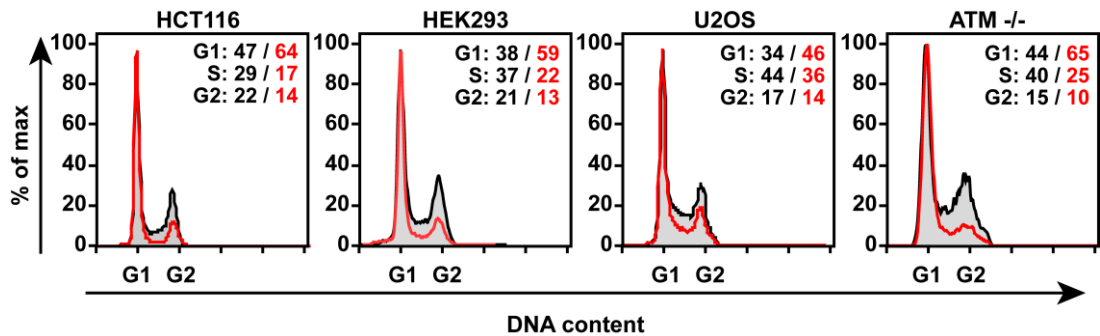
Figure 3-1: Overexpression of CycG2 leads to G$_1$-phase arrest in various cell lines. Representative flow cytometry cell cycle analysis of indicated cell lines transiently transfected with mCycG2GFP expression constructs. Histogram overlays of PI stained DNA of non-expressing (grey area) and mCycG2GFP expressing (red line) cells of the same transfected culture. Numbers of cells in respective phases of the cell cycle are indicated in the upper right corner of each overlay.

3.1.2 Activation of DDR Proteins after Ectopic CycG2 Expression

Previous results of Dr. Arachchige Don established that the CycG2 induced cell cycle arrest is dependent on the DDR pathway proteins p53 and Chk2 (Arachchige Don et al., 2006; Zimmermann et al., 2012). As the cell cycle inhibitory effects of CycG2 are dependent on these critical DDR signaling effectors, the status of DDR proteins after ectopic expression of CycG2 was analyzed. Based on preliminary results of ectopically expressed CycG2 compared to GFP expression, a more thorough investigation of the effect of CycG2 overexpression on DDR signaling was conducted. Therefore, transiently transfected HCT116 cultures were sorted for mCycG2GFP positive and negative populations (Figure 3-2). Lysates prepared from sorted HCT116 WT and p53-/- (Figure 3-2, A) or WT and Chk2-/- (Figure 3-2, B) cultures were analyzed for the expression of activated forms of several DDR pathway proteins; fold change in expression is indicated under each lane. Treatment for 8 h with the DNA DSB inducing agent Dox serves as a positive control for the activation of the DDR pathway. As expected, phosphorylation of NBS1, Chk2 and Chk1 increases following Dox treatment. In HCT116 WT cells ectopic CycG2 expression (+) also increases the presence of phospho-activated forms of Chk2 (54 to 64 fold increase) and NBS1 (6.8 to 12 fold increase) compared to non-expressing (-) cells. Activation of Chk2 and NBS1 was maintained in p53-/- cultures. As anticipated, no Chk2 immunosignals were detected in Chk2-/- cultures, but NBS1 activation was still present in CycG2 expressing cells. No change in Chk1 phosphorylation was observed

between the sorted CycG2 expressing and non-expressing samples in WT, p53-/- and Chk2-/- cell lines.
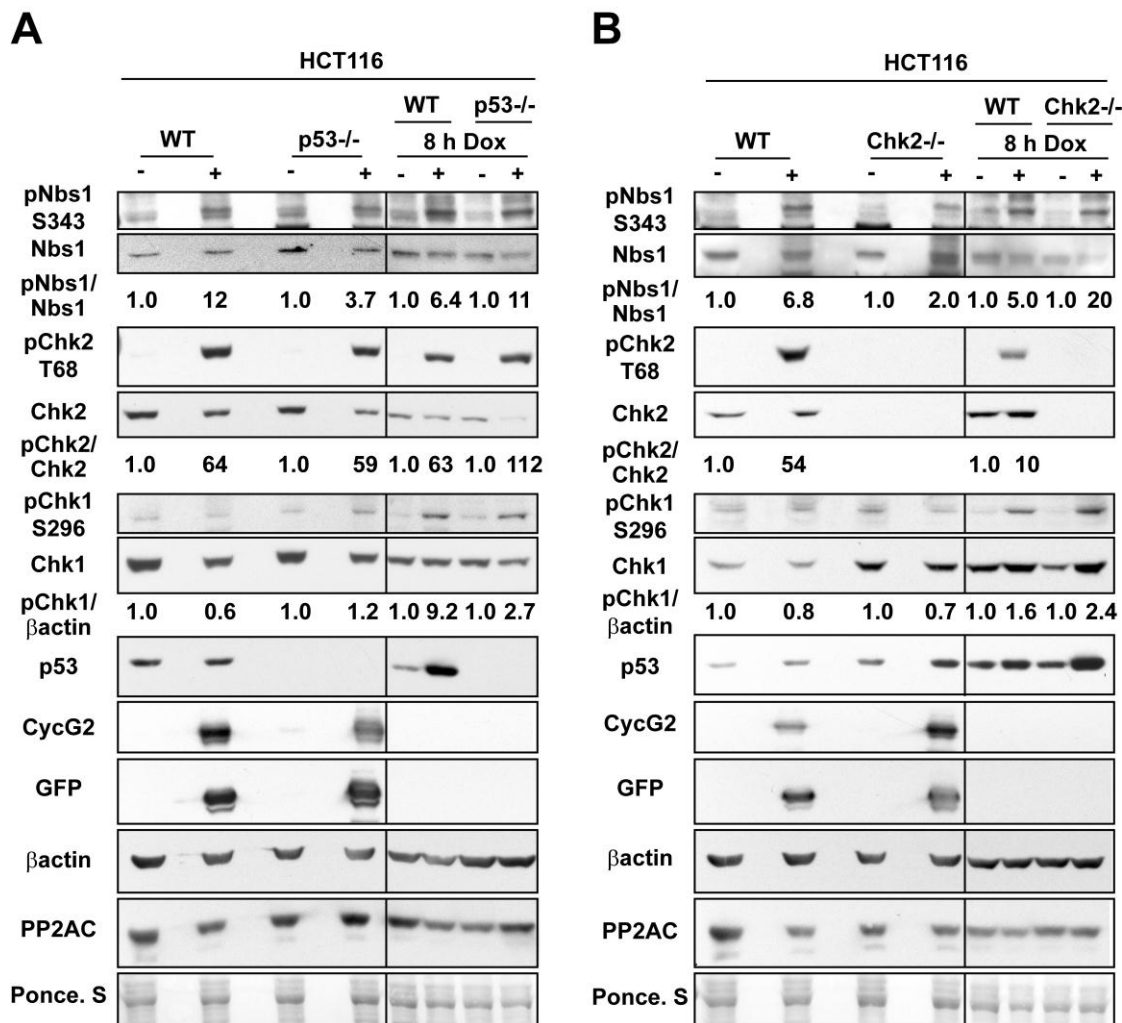
Figure 3-2: Ectopic expression of CycG2 induces the activation of DNA damage response proteins Chk2 and NBS1. A-B) Immunoblots of proteins in total lysates isolated from transiently transfected cultures probed with antibodies directed against the indicated proteins. Indicated cell lines were transfected for 44 h with mCycG2GFP constructs before sorting for GFP expressing (+) and non-expressing (-) populations. Culture treatment for 8 h with (+) doxorubicin (Dox) or vehicle (-) serves as a positive control. Fold increase of NBS1, Chk2 and Chk1 phosphorylation is indicated under total protein lanes (non-treated or non-expression controls are set to 1.0). Expression of phosphorylated Nbs1 (pNbs1 S343), Chk2 (pChk2 T68), Chk1 (pChk1 S296) compared to NBS1, Chk2, Chk1, p53, CycG2, GFP, βactin and PP2AC of HCT116 WT and p53-/- **A)** or WT and Chk2-/- cultures **B)**.

3.1.3 CycG2 Induced Cell Cycle Arrest is not ATM Dependent

The observations that ectopic CycG2 expression induces a Chk2 dependent cell cycle arrest and phosphorylation of Chk2 at the ATM target site T68, suggested that these effects could involve ATM. HCT116 WT cells were transfected with

mCycG2GFP in the presence of the specific ATM inhibitor KU55933 and the cell cycle distribution was assessed (Figure 3-3, A left).
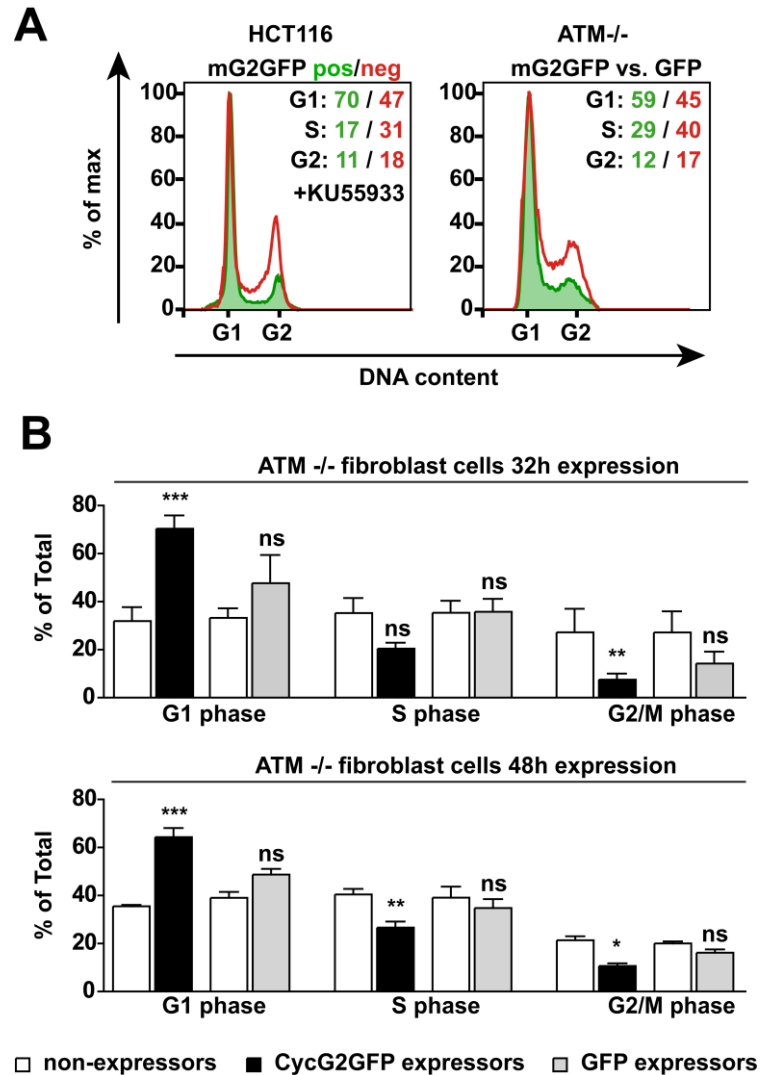
Figure 3-3: CycG2 induced cell cycle arrest is not ATM dependent. A) Representative flow cytometry analysis of DNA content in fixed HCT116 WT and ATM deficient (ATM-/-) fibroblast cell cultures. Numbers in the upper right of each histogram panel specify the percentage of cells in indicated cell cycle phases. Cell cycle analysis was performed 32 h (HCT116) or 48 h (ATM) after transfection. *Left)* HCT116 cells were transfected with mCycG2GFP and treated with ATM inhibitor KU55933. Presented are non-expressing (red line) and mCycG2GFP expressing (green area) histogram overlays of PI stained DNA in cells of the same transfected culture. *Right)* Histogram overlays of ATM -/- cells transfected with indicated constructs. Shown are the mCycG2GFP expressing (green area) and GFP expressing (red line) cell population. **B)** Statistical analysis (one way ANOVA with Bonferroni`s post-test) of cell cycle phase distribution ATM -/- cultures transfected for 32 h (top) or 48 h (bottom) (*** $p < 0.001$, ** $p < 0.01$, * $p < 0.05$, ns indicates no significant difference).

The presence of ectopic GFP tagged CycG2 (green area) compared to non-expressing cells (red line) of the same transfected culture leads to a strong increase of

the percentage of cells in G_1-phase of the cell cycle (70% compared to 47%). To validate these findings, the ATM deficient (ATM-/-) primary human fibroblast cell line (GM05849) was used in similar experiments. ATM-/- cultures were transfected with mCycG2GFP or GFP control constructs and the DNA distribution was analyzed (Figure 3-3, A right). The histogram overlay of CycG2 (green area) and GFP control (red line) expressing population in ATM-/- cells shows that CycG2 induces a G_1-phase cell cycle arrest (59% compared to 45%). Statistical analysis of the cell cycle distribution of ATM-/- cells transfected with CycG2, shows a significant increase ($p<0.001$) of cells in G_1-phase compared to non-expressing cells after 32 h (Figure 3-3, B top) and 48 h (Figure 3-3, B bottom) of expression. Simultaneously, the number of cells in S-phase is reduced at 32 h of transfection but is significantly diminished after 48 h. A significant decrease of cells in G_2/M-phase is also observed at both time points. In contrast to CycG2 expressing cultures, expression of GFP alone has no significant influence on the cell cycle profile of ATM deficient cells.

3.1.4   The DNA Damage Agent Doxorubicin Induces Cell Cycle Arrest

Previously published results show that Dox treatment leads to a robust G_2/M-phase arrest in various cell lines (Reinke et al., 1999; Schonn et al., 2011). In order to verify and better characterize the effect of Dox treatment on the cell cycle distribution in the cell lines used in this study, cultures were treated with Dox and the DNA content was determined by flow cytometry. Cell cycle analysis showed a robust increase of cells G_2/M-phase in response to the induction of DSBs (Figure 3-4). This G_2/M checkpoint arrest was apparent in many of the cell lines within 12 h of treatment (not shown) and clearly after 16 h of treatment. U2OS and ATM cells also exhibited an accumulation of cells in S-phase, indicating an intact S-phase checkpoint.
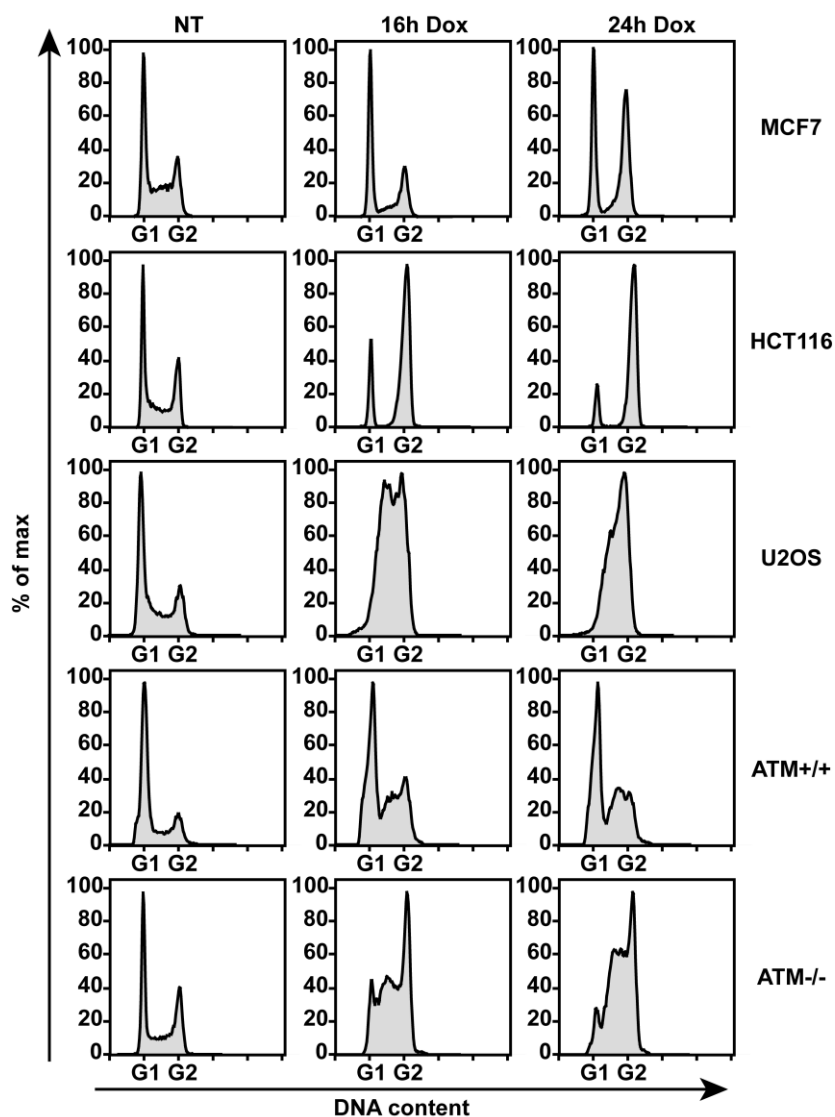
Figure 3-4: DNA damaging agent doxorubicin induces G$_2$-phase cell cycle arrest in multiple cell lines. Histograms of DNA content of indicated cell lines, cultured in the absence (left column) or presence of doxorubicin (Dox) for 16 h (middle column) or 24 h (right column). Note, U2OS and ATM cell lines show a distinct S-phase arrest, before G$_2$-phase arrest.

3.1.5 Upregulation of CycG2 Protein Following DNA Damage

The observation that a high level of CycG2 protein induces activation of DDR proteins motivated the decision to investigate CycG2 expression during DDR. Treatment of the BC cell line MCF7 with the genotoxic chemotherapeutics Dox and ETP (Figure 3-6) elevates CycG2 protein level in a time-dependent manner. CycG2 expression is significantly upregulated after 16 h (fold increase 3.0 ± 0.7, $p<0.05$) and 24 h (fold increase 3.8 ± 0.6, $p<0.01$) of Dox and ETP treatment.
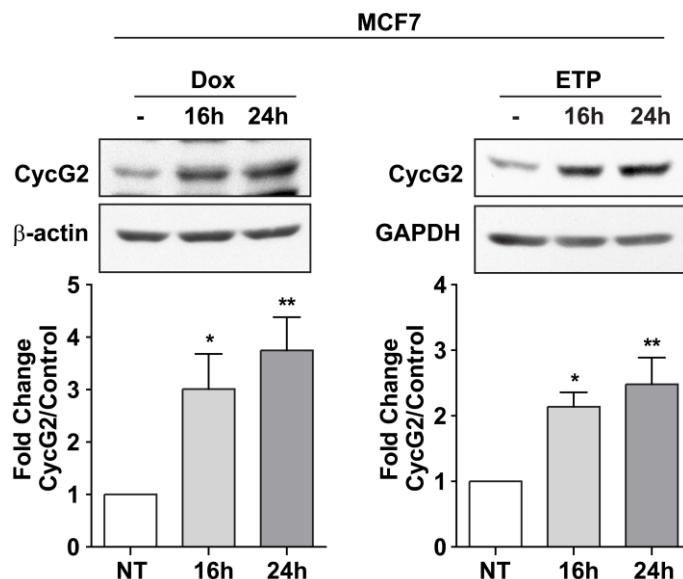
Figure 3-5: Treatment of MCF7 cells with doxorubicin and etoposide elevates CycG2 protein level. *Top)* Representative immunoblot analysis of CycG2 protein expression after indicated treatments. CycG2 level in non-treated controls (0) are set to 1.0. Statistical analysis of CycG2 expression in MCF7 cells treated with chemotherapeutics doxorubicin (Dox) or etoposide (ETP) for 16 or 24 h (* indicates $p<0.05$, ** indicates $p<0.01$). Analysis was performed using one way ANOVA with Tukey's post-test, shown are mean ± SEM.

To define CycG2's upregulation in relation to the activation of DDR proteins and cell cycle checkpoints, MCF7 cell cultures were treated over a time course with Dox or ETP (Figure 3-6). Immunoblot analyses of CycG2 expression and the phospho-activated forms of the DDR proteins are presented in Figure 3-6 top. Upregulation of CycG2 expression was clearly induced after 4 h of treatment and continued to increase during the 24 h response period. The activation of the early response DDR proteins ATM, Nbs1 and Chk2 could already be detected after 2 h of Dox exposure, 2 h before a prominent elevation of CycG2 was evident. The activation of the ATR target Chk1 was detected at later points, between 4 h and 8 h of Dox exposure. An obvious arrest of cells in G_2-phase did not occur before 16 h of exposure (Figure 3-6, bottom), thus CycG2 expression preceded the onset of cell cycle arrest but followed the activation of DDR proteins.
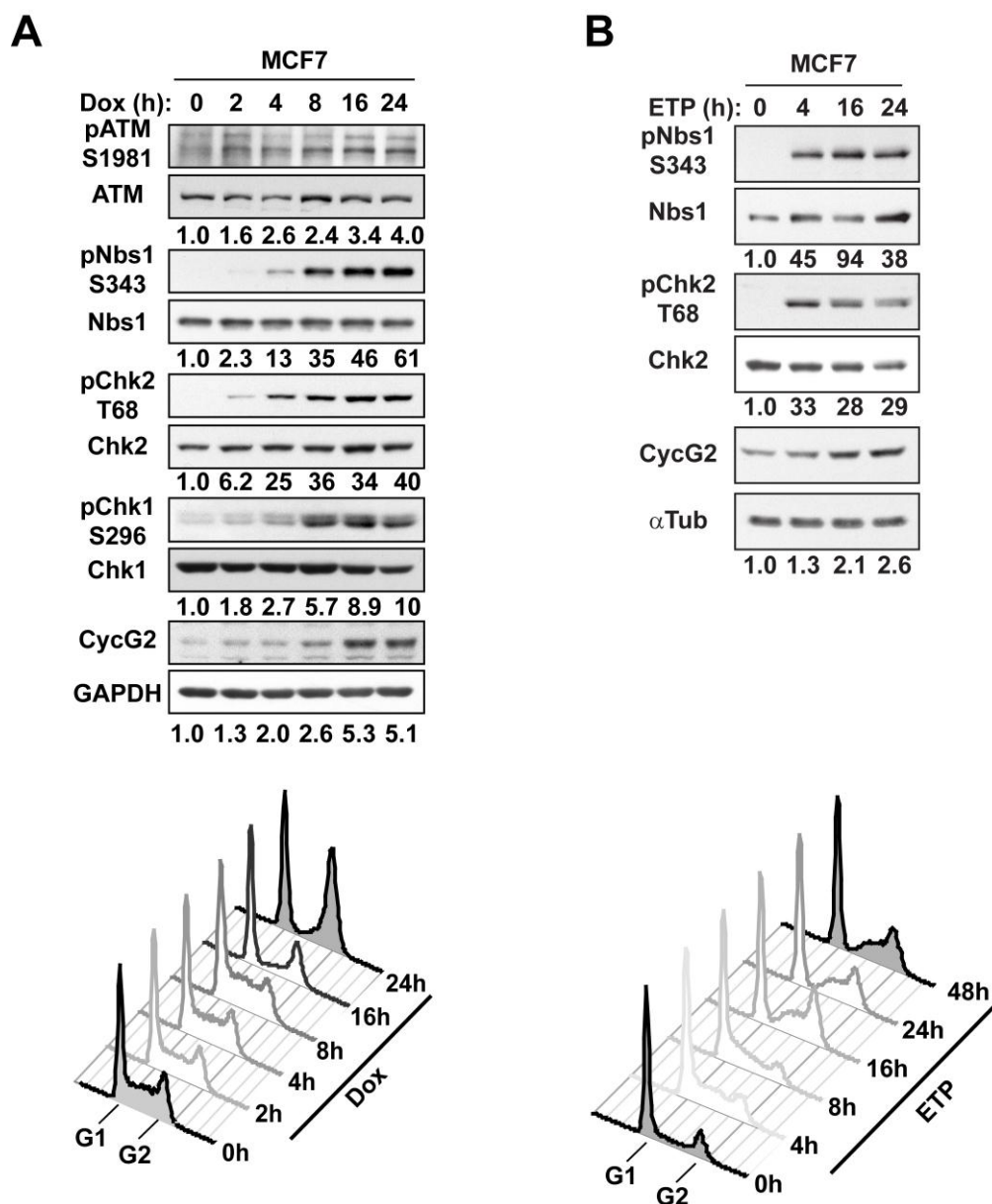
Figure 3-6: DNA damage induced upregulation of CycG2 expression follows activation of the ATM signaling pathway but precedes accumulation of cells at the G$_2$-phase checkpoint. Immunoblot analysis of CycG2 expression relative to the phospho-activated forms of DDR proteins during indicated time periods of Dox **A)** or ETP **B)** treatment. Protein expression of pATM S1981, ATM, pNbs1 S343, Nbs1, pChk2 T68, Chk2, pChk1 S296, Chk1, CycG2 and loading control (GAPDH or αTub) in indicated cultures. Quantification of fold upregulation of protein expression induced by indicated treatment relative to control for each time point in MCF7 is indicated below each lane. Protein levels in non-treated controls are set to 1.0. The corresponding cell cycle profile of the specified cell culture is shown at the bottom.

3.1.6   Testing of shRNA Constructs for CycG2 Knockdown

To assess the contribution of elevated CycG2 expression to DDR signaling and cell cycle checkpoint arrest, shRNA constructs were generated to target *CCNG2* gene

expression. The specific shRNA 1-B was designed to target human *CCNG2* mRNA whereas ID3 targets human and murine CycG2 transcripts (Figure 3-7, A). The control vector NC contains a scrambled sequence, whereas the non-silencing control NSC sequence overlaps with the 1-B sequence, but contains 3 to 4 point mutations in the murine or human *CCNG2* sequence, respectively. Validation of shRNA specificity and efficiency was performed by co-expression experiments and immunoblot analysis (Figure 3-7). The indicated murine (Figure 3-7, B) and human (Figure 3-7, C) CycG2 expression constructs were co-transfected with specific shRNA (1-B and ID3) or control (vec., NC and NSC) plasmids (ratio 1:4). Expression of ectopic mCycG2 was reduced in ID3 co-expressed samples compared to controls (NC and vec.). As expected, expression of NC had no effect on CycG2 expression compared to vector alone. Co-transfection of human CycG2 with shRNA 1-B and ID3 resulted in a blunted CycG2 expression. Specificity was determined by co-transfection of the indicated shRNA constructs with plasmids encoding for CycG2's closest homolog, CycG1. None of the tested shRNAs reduced the expression level of CycG1.
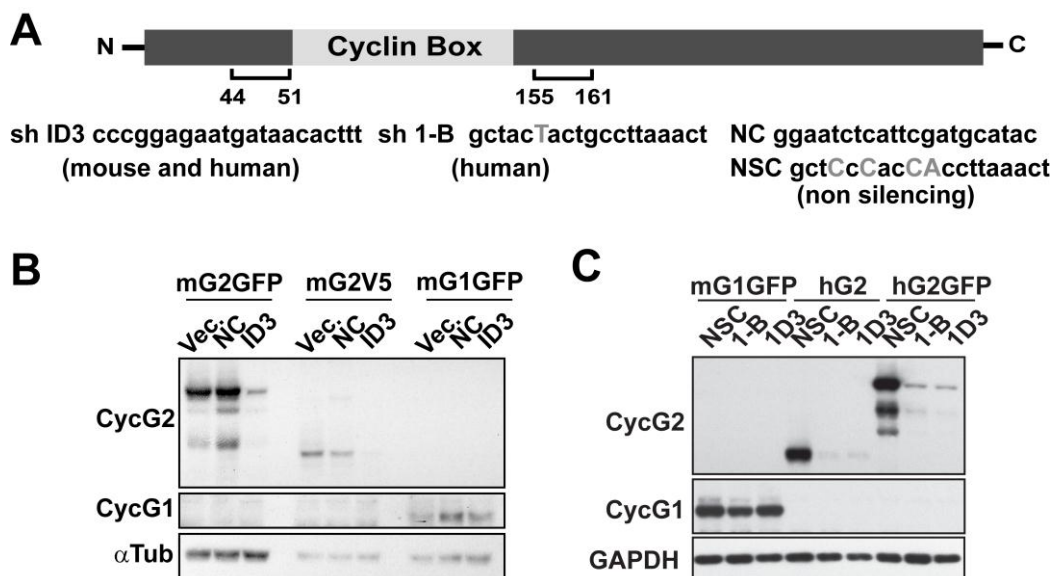
Figure 3-7: Design and testing of *CCNG2*-specific shRNAs. A) Schematic of the CycG2 protein. Black bars indicate amino acid region encoded in the mRNA target site of the indicated shRNAs. The nucleotides that differ between human and non-silencing control (NSC) shRNAs are indicated by capitalized font. **B-C)** Immunoblot analysis of ectopic expression of indicated constructs relative to loading control α-tubulin (αTub) to test effectiveness and specificity of shRNAs. **B)** Expression level of murine CycG2 and CycG1 in cells co-transfected with control (Vec., and NC) or CycG2-targeting (ID3) shRNA vectors (ratio 1:4). **C)** Expression level analysis of human CycG2 and murine CycG1 in cells co-transfected with indicated specific (1-B, ID3) or control (empty vector or NSC) shRNA plasmids (ratio 1:4).

3.1.7 Transient Knockdown of CycG2 Blunts Dox Induced Cell Cycle Arrest

The validated shRNAs constructs were subsequently used to knockdown CycG2 in transient transfection assays (Figure 3-8). To preclude off target site effects of the used shRNAs, initial results obtained with shRNA 1-B (Zimmermann et al., 2012) were confirmed with the second shRNA ID3. HCT116 WT cells were transfected with shRNA 1-B or ID3 alone, and in combination for 48 h before cultures were treated with Dox. After 24 h of exposure to Dox, the cultures were harvested for immediate analysis. The DNA of the unfixed cells was stained with Hoechst 33342 and cell cycle analysis was performed on the TO-PRO3 negative (live cell) populations.
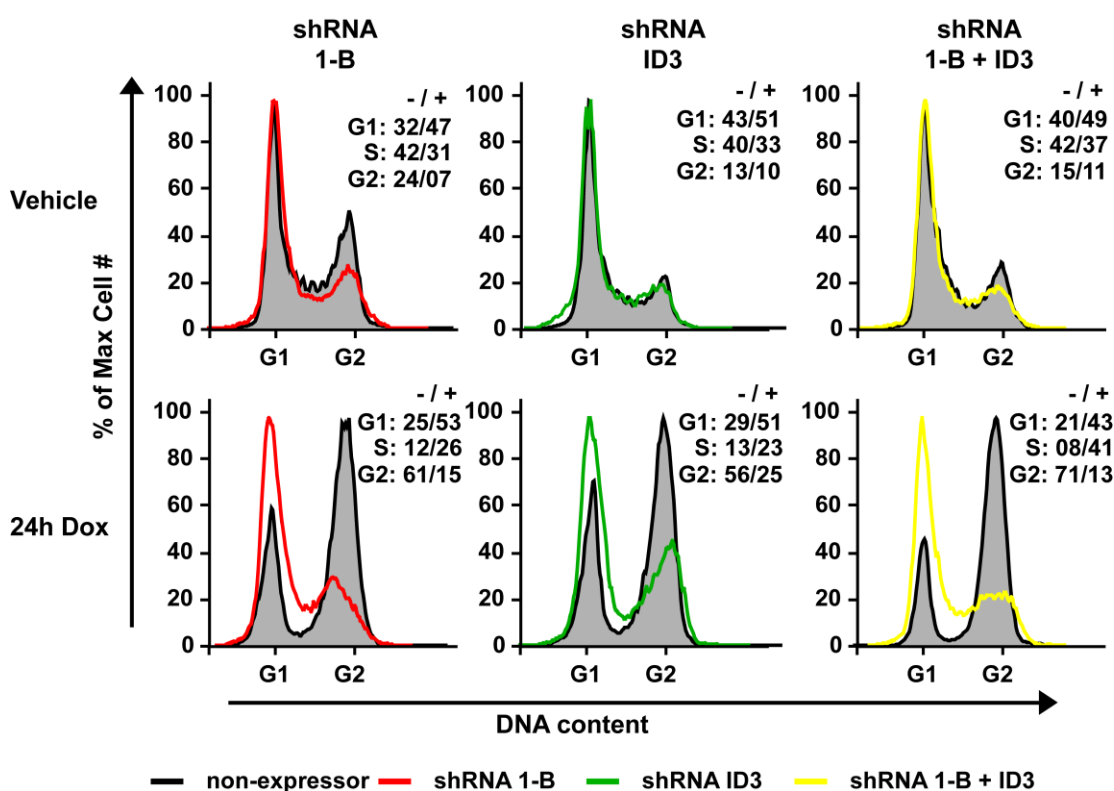
Figure 3-8: shRNA-mediated knockdown of CycG2 represses doxorubicin induced G$_2$-phase cell cycle arrest. Comparative cell cycle analysis of vehicle control (top row) or doxorubicin (bottom row) treated HCT116 WT cells transfected with indicated plasmids. Shown are histogram overlays of Hoechst 33342 stained DNA content from live cell cultures of non-expressing cells (grey area), and cells expressing the shRNA 1-B (red line), shRNA ID3 (green line) or both (yellow line). Percentage of cells in each phase of the cell cycle (determined by the Watson-Pragmatic cell cycle program) is shown at the right of each overlay (non-expressors (-) and shRNA-expressing (+) cells) of the respective histogram.

As expected, Dox treatment of the non-expressing (grey area/black line) cell population leads to a potent G$_2$/M-phase cell cycle arrest (G$_2$/M: 56 to 71%).

Histogram overlays of DNA content in Dox treated cultures show an abrogated G_2-phase arrest (G_2/M: 13 to 25%) in the shRNA expressing (colored lines) compared to non-expressing populations. The strongest effect is demonstrated in cells expressing both shRNAs (Figure 3-8, right). The percentage of G_2/M cells in Dox treated shRNA expressing populations (G_2/M: 13 to 25%) is comparable to that observed for mock-treated non-expressing populations (G_2/M: 13 to 24%). Expression of CycG2 specific shRNA constructs does not alter the cell cycle profile of mock treated cells (Figure 3-8, top).

3.1.8 Establishment of Stable shRNA Mediated CycG2 Knockdown Clones

To further analyze the contribution of CycG2 to Dox-induced DDR, cell lines were generated that stably incorporated the validated shRNA expression cassettes 1-B, ID3 and NSC (Figure 3-9). Selected clonal populations were screened by immunoblot analysis for their ability to limit the expression of ectopic CycG2 (Figure 3-9, A). Transient transfection experiments showed that numerous shRNA 1-B and ID3 containing clones showed the ability to repress the expression of ectopic CycG2 when compared to CycG2 expression levels in MCF7 WT and NSC2 control clones. The generated clones that exhibited the strongest knockdown of ectopic CycG2 expression were used for subsequent analysis of endogenous CycG2 expression (Figure 3-9, B and C). Dox induced CycG2 expression was diminished in KD clones compared to WT and NSC2 controls. Statistical analysis of immunoblot data showed a significant decrease of CycG2 expression in MCF7 harboring the specific shRNA 1-B and ID3 compared to controls (WT and NSC2).
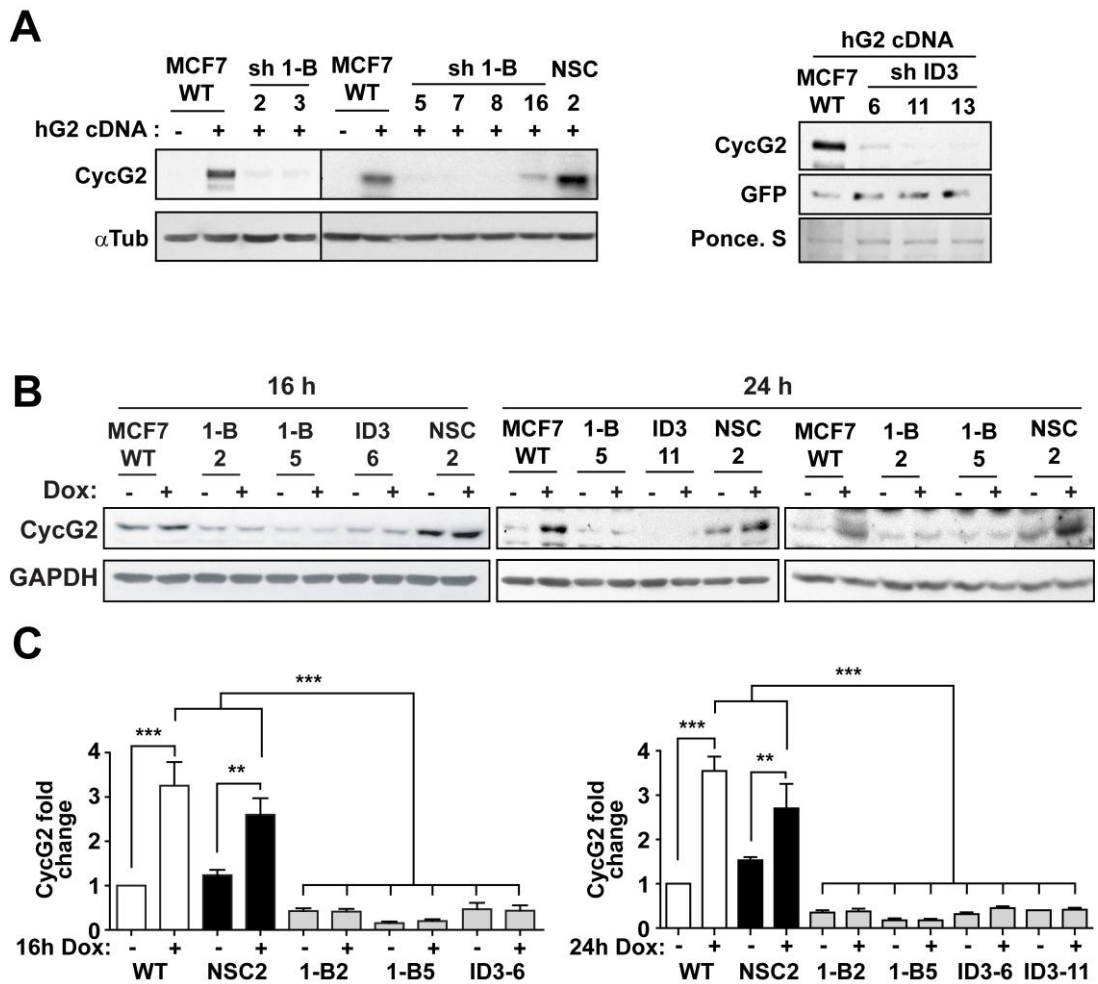
Figure 3-9: Establishment and testing of stable shRNA-mediated knockdown of CycG2 cell cultures. A) Immunoblot assessment of transiently transfected mCherry-tagged human CycG2 levels in the specified MCF7 stable clones and WT control populations relative to α-tubulin (αTub), GFP or total protein (Ponce. S) in cell lysates from indicated cultures. **B)** Expression of endogenous CycG2 in indicated KD or control MCF7 cultures, treated with Dox (+) or vehicle (-) for 16 h (left) or 24 h (right) compared to loading control GAPDH. **C)** Statistical analysis (one way ANOVA with Bonferroni's post-test) of fold increase in CycG2 expression levels in indicated cultures before (-) and after (+) Dox treatment for 16 h (left) or 24 h (right) compared to WT control.

3.1.9   Stable CycG2 KD Attenuates G_2-Phase Arrest Following DNA Damage

Several CycG2 KD clones were tested for their ability to induce G_2-phase cell cycle arrest after induction of DNA damage. Treatment with Dox induces a strong G_2-phase cell cycle arrest in MCF7 WT and NSC2 control cells (Figure 3-4 and Figure 3-10). Multiple CycG2 KD clones display a statistically significant (p <0.01 to 0.001) reduction in the percentage of cells in G_2/M-phase (Figure 3-10, C) compared to controls. In addition to the reduction of cells in G_2/M-phase, the KD clones exhibit an

increase in the percentage of the population in G_1- and S-phase, when compared to controls (Figure 3-10, B).
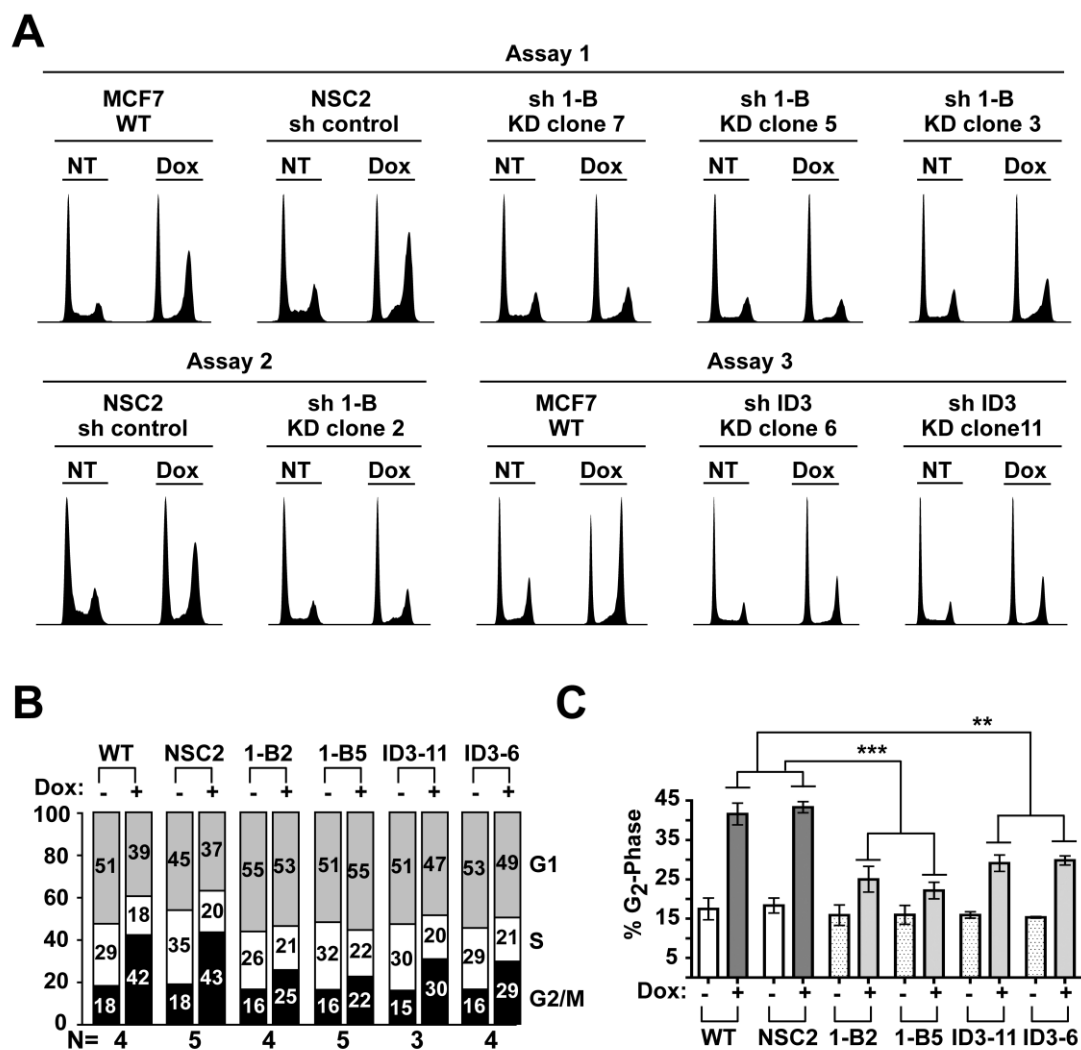
Figure 3-10: Stable shRNA-mediated knockdown of CycG2 represses doxorubicin-induced G_2-phase cell cycle arrest. A) Assays of DNA content of MCF7 WT, NCS control and stable KD clones after 24 h mock (NT) or Dox treatment. **B)** Bar graph of average percentage of cells in G_1, S and G_2/M-phase of indicated clones treated with vehicle (-) or with (+) Dox for 24 h. Numbers embedded in each bar represent the percentage of cells in the indicated cell cycle phase. Numbers below each bar graph pair denote the number of experimental repeats. **C)** Statistical analysis of average percentage of cells in G_2/M-phase of the indicated Dox treated (+) and vehicle treated (-) cultures (one way ANOVA with Tukey's post-test, *** $p<0.001$, ** $p<0.01$).

3.1.10 Maintained Induction of CycG1 Expression and Activation of Chk2 and Nbs1 Following DNA DSB Induction

The closest homolog of CycG2, CycG1, is a DNA damage response protein linked to the regulation of G_2/M transition (Kimura et al., 2001). Dox-induced DNA damage triggered upregulation of CycG1 in MCF7 WT and NSC2 cells and as well as in

CycG2 KD clones (Figure 3-11, A), verifying that *CCNG1* expression is not affected by *CCNG2*-targetting shRNA. These results indicate that CycG1 does not compensate for the loss of CycG2.
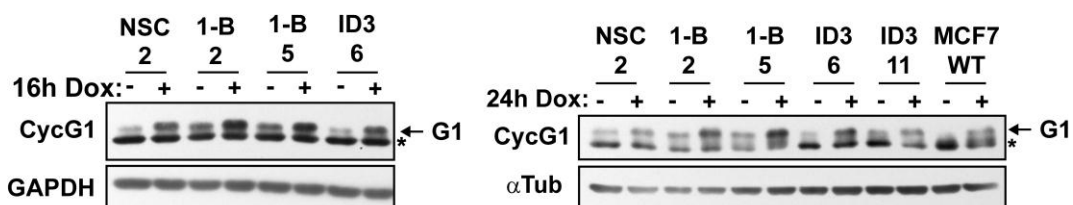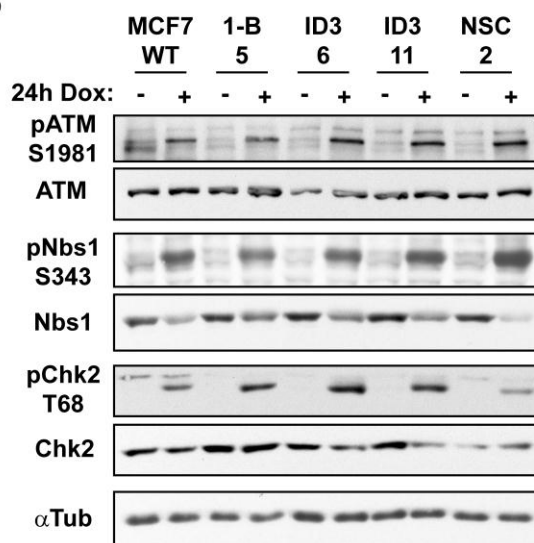
Figure 3-11: Doxorubicin induced expression of CycG1 and phospho-active forms of ATM, NBS1, Chk2, is maintained in CycG2 KD clones. A) Immunoblot analysis of expression of CycG1 in lysates from indicated cultures treated with Dox for 16 h **A)** or 24 h **B)**, compared to loading controls GAPDH or α-tubulin (αTub) (* denotes unspecific background band). **B)** Expression of phosphorylated ATM (pATM S1981), Nbs1 (pNbs1 S343) and Chk2 (pChk2 T68) compared to total ATM, Nbs1, Chk2 and loading control α-tubulin (αTub) in indicated vehicle (-) and Dox (+) treated cultures.

Given that ectopic CycG2-induced cell cycle arrest requires expression of Chk2 and p53 and promotes the phosphorylation of Chk2 and Nbs1, the effect of CycG2 KD on the expression of several activated forms of the DDR pathway was examined (Figure 3-11, B). Immunoblot results show that depletion of CycG2 did not affect the Dox dependent induction of pATM, pNbs1 or pChk2 compared to control cells (WT and NSC2).

3.1.11 Decreased Accumulation of Inactive CycB1/Cdc2 Complexes in Dox-Treated CycG2 KD Cells

Passage from G_2-phase into mitosis requires active CycB1/Cdc2 complexes, but once in mitosis CycB1 is targeted for proteasomal-mediated degradation (Lindqvist et al., 2009). DNA damage induces G_2-phase cell cycle arrest and causes the accumulation of CycB1 protein level. MCF7 WT and NSC2 control cells display a robust increase in CycB1 levels (5.5 to 5.6 fold increase) after Dox treatment (Figure 3-12, A). Compared to controls, accumulation of CycB1 was reduced (0.7 to 2.0 fold change) in the CycG2 KD clones, consistent with the relative reduction in the number of cells arrested at the G_2/M boundary (Figure 3-10, C).

DNA damage signaling is known to inhibit CycB1/Cdc2 activation through maintenance of the Wee1 and Myt1 mediated inhibitory phosphorylation of Cdc2 on T14 and Y15 (Lindqvist et al., 2009). Consistent with the findings above, immunoblot analysis (Figure 3-10, B) shows an obvious increase in Y15-phosphorylated Cdc2 (pCdc2 Y15) in the Dox-treated control cultures (2.4 to 3.4 fold increase), but the abundance of pCdc2 Y15 is decreased (0.9 to 1.5 fold change) in treated CycG2 KD clones.

Activation of CycB1/Cdc2 complexes is largely promoted through dephosphorylation of Cdc2's inhibitory sites (T14 and Y15) by the dual specificity phosphatases Cdc25B and Cdc25C (Lindqvist et al., 2009). A sharp reduction in Cdc25B level is necessary for an efficient G_2/M checkpoint response to DNA DSB (Bansal and Lazo, 2007; Lemaire et al., 2010; Miyata et al., 2001). Immunoblot analysis revealed a 50 to 80 % reduction in Cdc25B expression in Dox-treated, MCF7 WT and NSC2 cells relative to untreated controls (Figure 3-12, C). In contrast, Cdc25B expression in the Dox-treated CycG2 KD clones appeared to be similar to or even increased above the level of its respective non-treated controls. This suggests that loss of CycG2 abrogates the sharp reduction in Cdc25B that promotes G_2/M checkpoint arrest. The basal level of Cdc25B in CycG2 KD cultures seems to be lower than in unperturbed MCF7 WT and NSC2 populations. The fact that the lower basal level of Cdc25B in the untreated CycG2 KD cultures did not induce an increase in the percentage of cells with a G_2/M-phase DNA content (Figure 3-10) suggests that the CycG2 KD clones have adapted to lower Cdc25B levels.
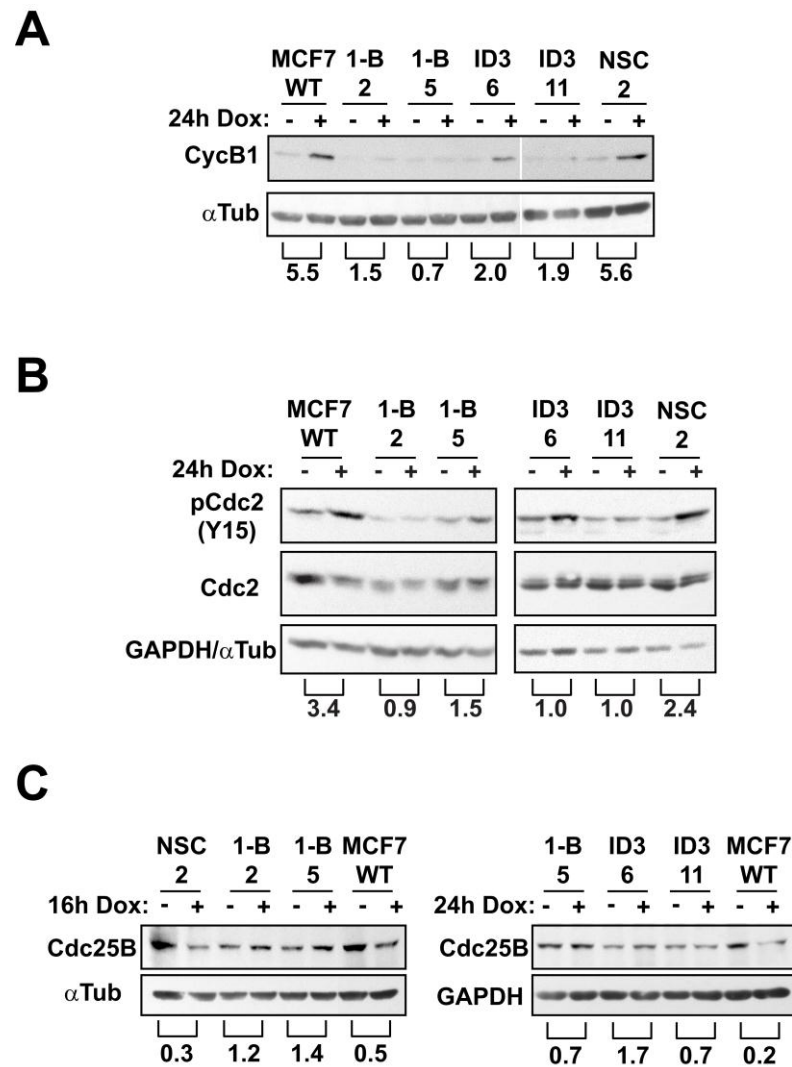
Figure 3-12: Inhibition of CycG2 expression represses doxorubicin-induced accumulation of phospho-inhibited CycB/Cdc2 complexes. (A-C) Immunoblot analysis of changes in protein expression induced by treatment of indicated MCF7 cultures with Dox. Fold change of protein expression compared to NT (-) controls, indicated under brackets. **A)** Expression level of CycB1 compared to loading control α-tubulin (αTub) in cultures treated for 24 h. **B)** Phosphorylated Cdc2 (pCdc2 Y15) expression relative to total Cdc2 and loading control GAPDH or αTub in indicated cell populations. **C)** Immunoblot detection of Cdc25B expression relative to GAPDH in designated cultures.

3.2 Contribution of CycG2 to Endocrine Therapy Response

Estrogen (E2) and the estrogen receptor (ER) are critical for both, proper development and function of reproductive organs and mammary tissue. ER signaling pathways regulate cell growth and survival, but also promote breast cancer (BC) progression. Therefore, the inhibition of E2 mediated ER signaling is the basis of endocrine therapies against BC (Pearce and Jordan, 2004). *CCNG2* expression is directly inhibited at the promoter level by E2-bound ER complexes (Stossi et al.,

2006). The contribution of CycG2 to the endocrine therapy response and resistance, however, is unknown. KD of CycG2 in the ER positive BC cell line MCF7 was used to study CycG2's contribution to endocrine therapy response. Immunoblot and cell cycle analyses were performed to compare the effects of E2 signaling blockade in CycG2 KD cells relative to control MCF7 cell populations.

3.2.1 Inhibition of E2 Signaling Leads to G_1-phase Cell Cycle Arrest

Initial studies were performed to examine the effect of E2 signaling inhibition on cell proliferation. Culturing of the E2-dependent cell line MCF7 in E2 and phenol red free medium, induces growth arrest (Figure 3-13, A).
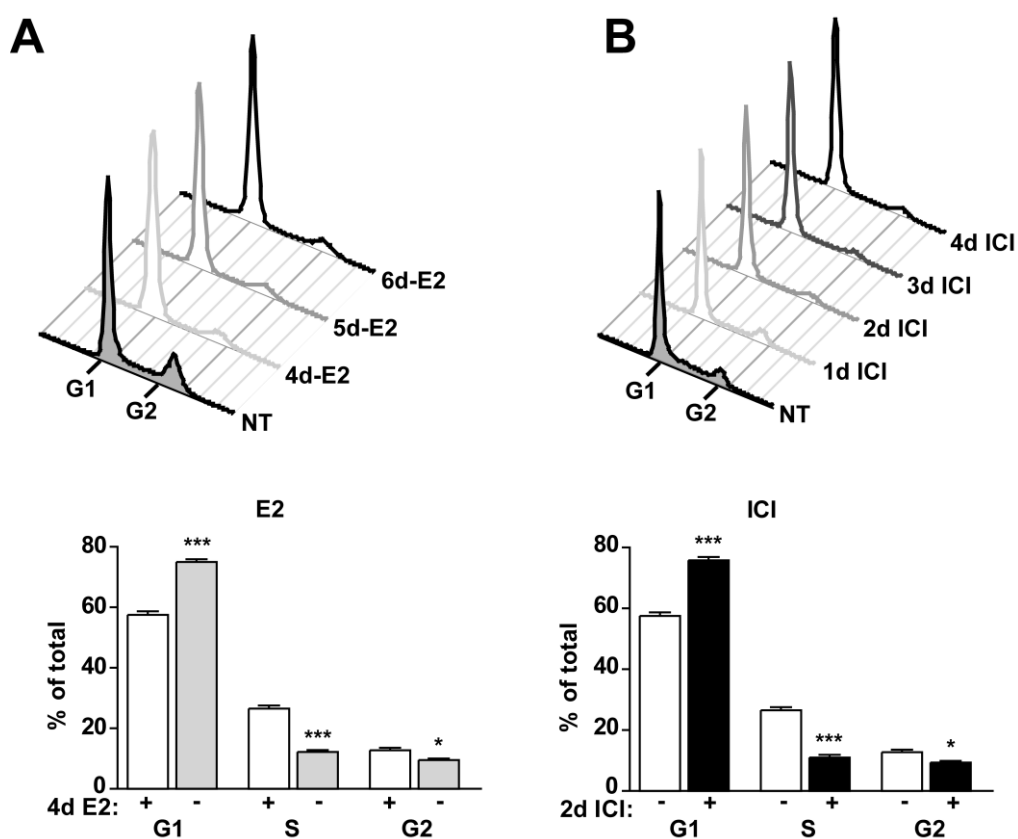
Figure 3-13: Inhibition of estrogen receptor signaling in MCF7 leads to G_1-phase cell cycle arrest. **A-B)** Shown are offset histogram overlays of MCF7 cell cultures depleted of E2 **A)** or treated with ICI **B)** for the indicated periods of time. **A)** Cell cycle analysis of MCF7 cells cultured in estrogen depleted medium (-E2) for up to 6 days. Statistical analysis (one way ANOVA with Bonferroni's post-test) of cell cycle distribution of MCF7 cells depleted from E2 for 4 days is shown below. **B)** Cell cycle profiles of MCF7 cell cultures treated with the ER downregulator fulvestrant (ICI) for up to 4 days. Statistical analysis (one way ANOVA with Bonferroni's post-test) of cell cycle distribution of MCF7 cells treated with ICI for 2 days (*** $p < 0.001$, * $p < 0.05$).

This arrest is marked by a significant increase of cells in G_1-phase ($p<0.001$), and by a decrease in the cell population in the S- and G_2/M-phases ($p<0.001$ and $p<0.05$, respectively) of the cell cycle. Similarly, inhibition of ER signaling by the selective estrogen receptor downregulator (SERD) fulvestrant (ICI) induces a significant G_1-phase ($p<0.001$) cell cycle arrest in treated MCF7 cell cultures (Figure 3-13, B), and reduced the percentage of the population in S- and G_2/M-phases ($p<0.001$ and $p<0.05$, respectively) within 2 days of treatment.

3.2.2   Upregulation of CycG2 Protein after Inhibition of E2 Signaling

Published mRNA data show that *CCNG2* expression is influenced by the presence or absence of E2 (Stossi et al., 2006). In agreement with these mRNA data, CycG2 protein levels are also influenced by E2 mediated ER signaling (Figure 3-14, A). Compared to cells grown in regular E2 and phenol red containing medium (RM), culturing of MCF7 cells in E2 depletion medium (DM) leads to a 1.7 fold increase of CycG2 protein level (lanes 1 and 2). Addition of E2 to DM (DM/E2, lane 3) repressed CycG2 expression. Furthermore, compared to E2 re-stimulation (DM/E2), inhibition of E2 induced ER activation by co-treatment with ICI (DM/E2/ICI) or tamoxifen (4OHT, DM/E2/4OHT) leads to the increase (8.1 and 6.1 fold, respectively) of CycG2 protein level in MCF7 cells (lanes 3, 4 and 5).

Cell cycle analysis revealed that the growth arrest induced by E2 depletion (Figure 3-13, A and Figure 3-14, B top-left), can be reversed by re-addition of E2 (Figure 3-14, B top-2nd left). Consistent with earlier results, treatment of cells grown in RM or DM/E2 with either ICI or 4OHT leads to G_1-phase arrest. The growth-stimulating effect of the re-addition of E2 to the depletion medium could be prevented by co-treatment with ICI and 4OHT (Figure 3-14, bottom).
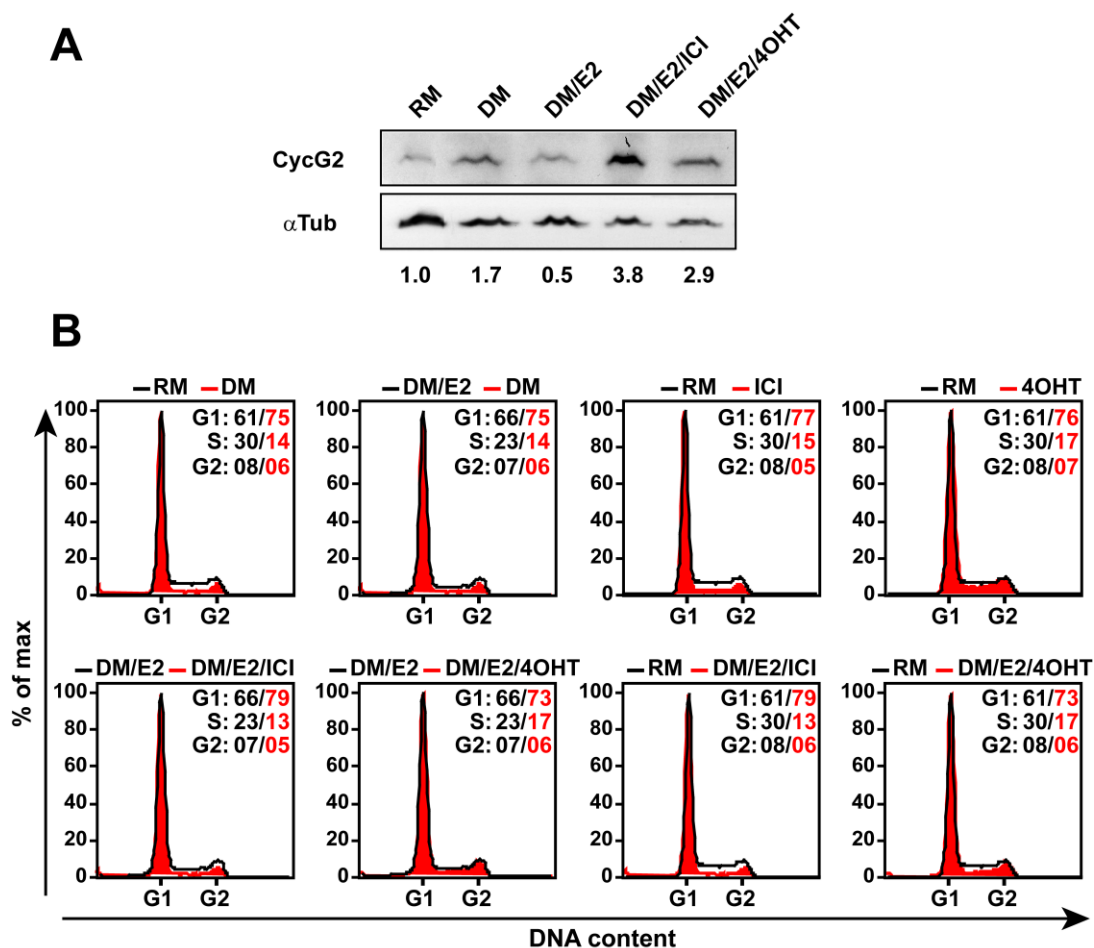
Figure 3-14: Inhibition of ER signaling leads to upregulation of CycG2 expression and G_1-phase cell cycle arrest. A) Expression level of CycG2 compared to loading control α-tubulin (αTub) from MCF7 cultures grown in regular medium (RM) or estrogen depleted medium (DM). After five days of depletion, cultures were treated with 10 nM estradiol (E2), 100 nM fulvestrant (ICI) or 100 nM 4-hydroxytamoxifen (4OHT) for two additional days before harvesting. Fold change of CycG2 expression is indicated below each lane. **B)** Cell cycle analysis of MCF7 cells grown in RM or DM for nine days. In addition, indicated cultures were depleted for six days followed by three subsequent days of indicated drug treatment in DM.

3.2.3 Upregulation of CycG2 after Inhibition of E2-mediated ER Signaling is Abolished in KD Clones

To examine the influence of CycG2 on the cell cycle effects of E2 signaling inhibition, the previously described and validated stable MCF7 CycG2 KD clones were tested for their ability to induce CycG2 expression (Figure 3-15) and to undergo cycle arrest (Figure 3-16, Figure 3-17, and Figure 3-18) following inhibition of E2 mediated ER signaling.

The indicated cell cultures were grown in the presence (+) or absence (-) of E2 and lysates were tested for CycG2 expression via immunoblotting (Figure 3-15, A).

Statistical analysis of CycG2 protein expression (Figure 3-15, A bottom) revealed that the treated KD clones (1-B and ID3) display a significant reduction (p<0.001) in CycG2 expression compared to controls (WT and NSC2). Control MCF7 cultures deprived of E2 exhibited significantly elevated levels of CycG2 expression (p<0.001), a response that is completely repressed in CycG2 KD clones.
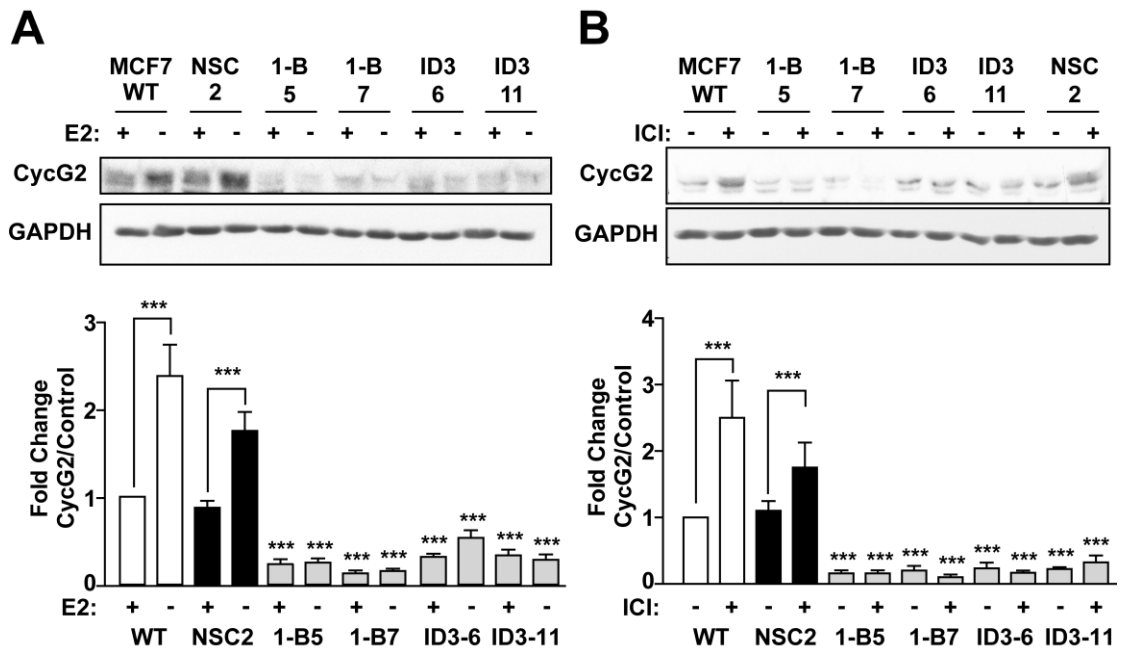
Figure 3-15: The upregulation of CycG2 expression upon inhibition of estrogen receptor signaling of MCF7 cultures is abolished in CycG2 KD clones. A) MCF7 cells were cultured in the presence (+) or absence (-) of E2 for four days prior to analysis. *Top)* Representative western blot analysis of CycG2 protein expression from whole lysate (WL) in control (WT, NSC2) and CycG2 KD (1-B, ID3) samples relative to loading control GAPDH. *Bottom)* Statistical analysis of fold change expression of CycG2 relative to loading control shown as mean +/- SEM with one-way ANOVA and the Bonferroni post-test. **B)** Top) Representative western blot analysis of CycG2 protein expression from whole lysate (WL) in control (WT, NSC2) and CycG2 KD (1-B, ID3) samples relative to loading control GAPDH treated with (+) or without (-) ICI for 2 days. Bottom) Statistical analysis of fold change expression of CycG2 relative to loading control shown as mean +/- SEM with one-way ANOVA and the Bonferroni post-test (*** p<0.001).

Likewise, 48 h treatment of control MCF7 cells (WT and NSC2) with ICI (+) leads to a significant (p<0.001) increase in CycG2 expression, compared to mock treated (-) samples (Figure 3-15, B). All tested CycG2 KD clones showed a significant (p<0.001) decrease in basal CycG2 expression and did not display a pronounced increase in CycG2 levels following exposure to ICI (Figure 3-15, B bottom).

3.2.4 CycG2 Knockdown Diminishes G_1-Phase Arrest Following the Inhibition of E2-mediatd ER Signaling

Next, CycG2 KD clones were tested for their ability to undergo the expected G_1-phase cell cycle arrest response following inhibition of E2 mediated ER signaling. First, MCF7 cells were cultured in E2-deprived medium for 4 days before analysis of DNA content by flow cytometry. Histogram overlays of PI stained DNA from cells grown in regular E2 containing (grey area with black line) or E2 deprived (green line) medium is shown in Figure 3-16, A. Cell cycle analysis revealed a clear inhibition of MCF7 WT and NSC2 cell proliferation in treated cultures; the percentage of the S-phase population was reduced (from 23% and 25% to 11% and 13%, respectively) and accompanied by a corresponding increase of cells in G_1-phase (from 58% and 55% to 78% and 71%, respectively). Compared to these control cell lines, CycG2 KD clones show an increased number of cells in S-phase (17 to 25 %) and a clear reduction in the percentage of the population accumulating in G_1-phase (59 to 64%). Similarly, in comparison to the potent response of MCF7 WT and NSC2 cultures to ICI (red line), CycG2 KD clone cultures did not display as robust a G_1-phase cell cycle arrest response to ICI treatment (Figure 3-16, B).

A

B
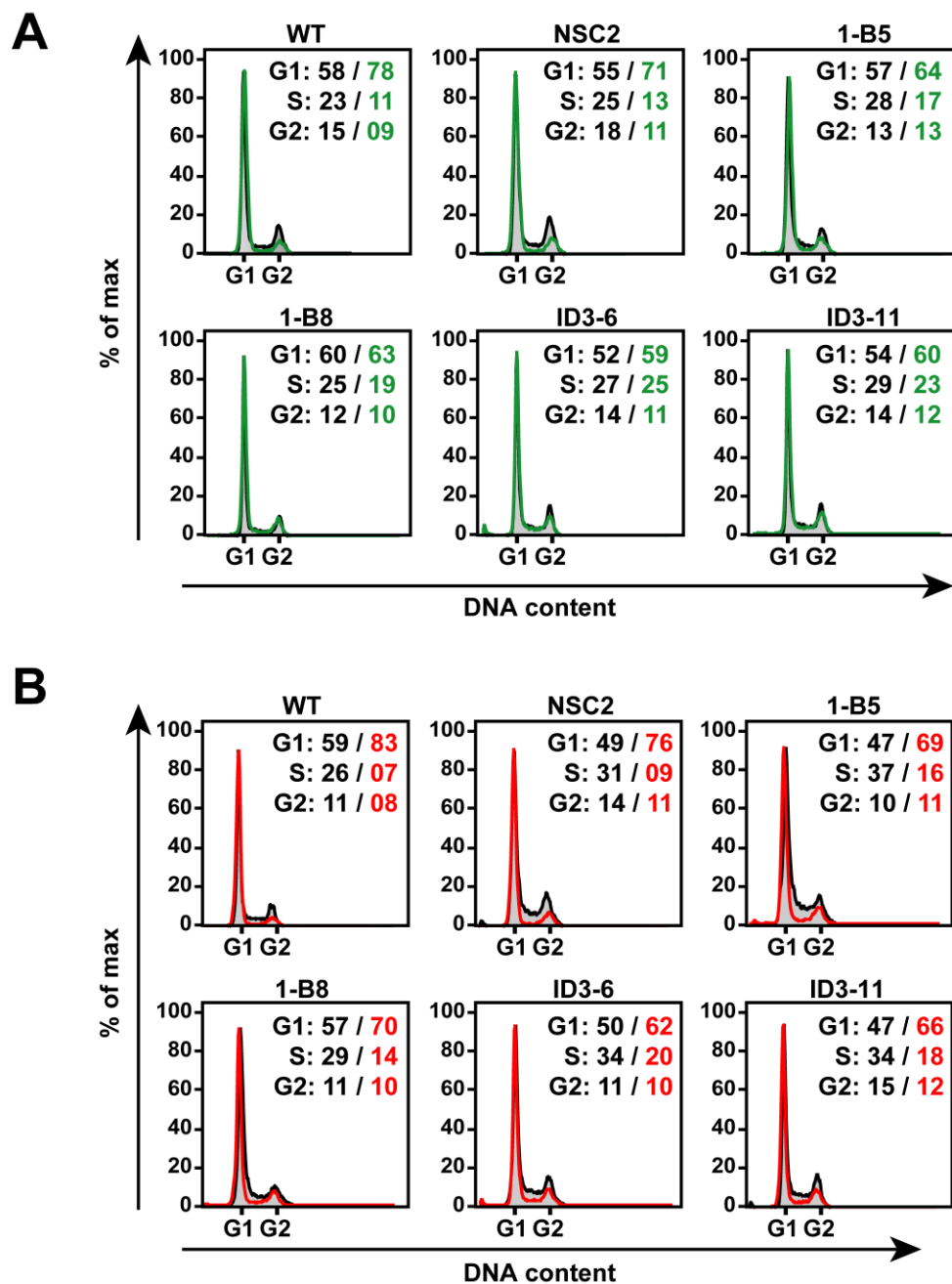
Figure 3-16: CycG2 knockdown diminishes G$_1$-phase cell cycle arrest after ER inhibition. A+B) Representative cell cycle analysis of indicated MCF7 cultures deprived of estrogen **A)** or treated with ER antagonist ICI **B)**. Treatment induced G$_1$-phase cell cycle arrest is reduced in CycG2 KD clones (1-B, ID3) compared to control (WT, NSC2) cultures.

Statistical analysis revealed a significant difference in the cell cycle distribution of CycG2 KD clone and MCF7 control cultures, responding to the inhibition of E2 signaling (Figure 3-17). Untreated MCF7 control and CycG2 KD cultures exhibit no significant difference in distribution of cells throughout the cell cycle (Figure 3-17, left column). Inhibition of E2/ER signaling through ICI treatment (middle column) or

deprivation of E2 (right column), induced a reduced G_1-phase arrest response in CycG2 KD clones when compared to MCF7 WT and NSC2 controls (Figure 3-17, top row, p<0.01 or 0.001, middle row, p<0.05 to 0.001).
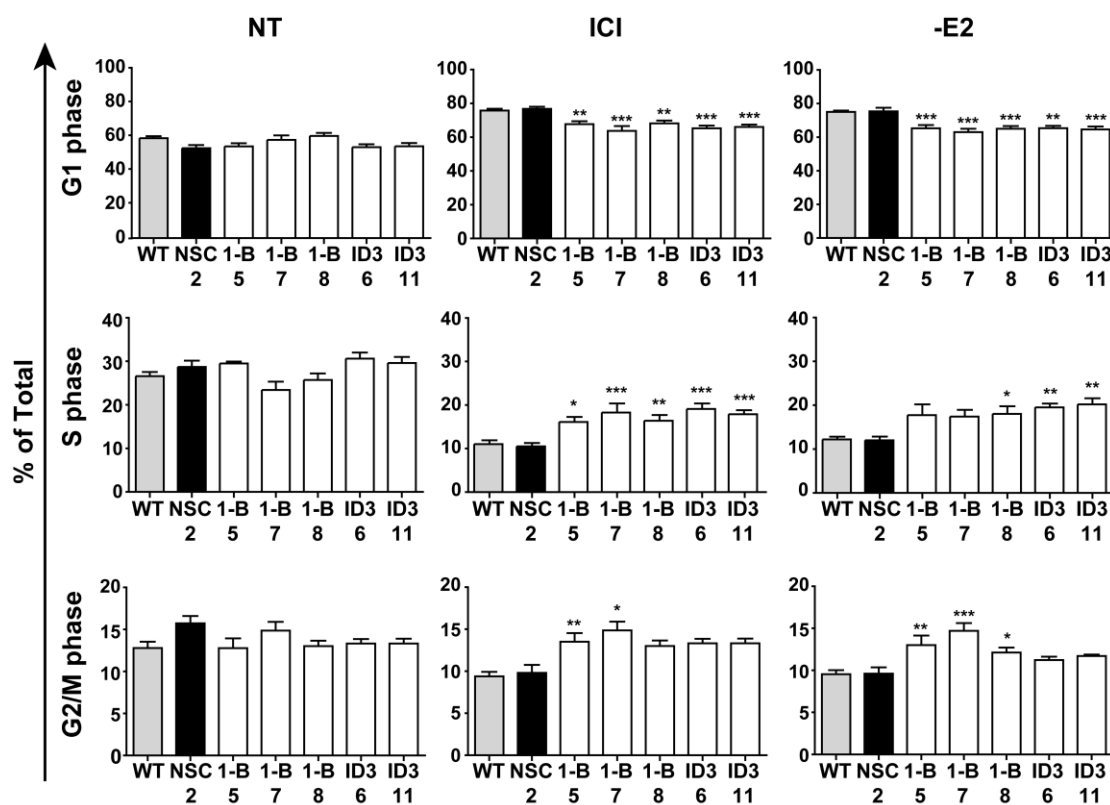
Figure 3-17: Decreased cell cycle arrest in CycG2 KD clones in response to ER inhibition. Shown are bar graphs of indicated cell cycle phases of specified cultures after treatment (left, mock treatment; middle, 48 h 100 nM ICI; right, 4 days of E2 depletion). KD clones display a significantly decreased G_1-phase arrest (top) and an increase of % of cells in S-phase (middle) compared to control cultures.

To test whether the blunted G_1-phase arrest response of CycG2 KD clones reflects an increase in the population of replicating cells undergoing DNA synthesis, incorporation of the nucleotide analog 5-bromo-2'-deoxyuridine (BrdU) into newly synthesized DNA was assessed by two-parameter DNA flow cytometry. Cultures were pulse labeled for 1 h with BrdU prior to fixation. The incorporated BrdU was detected with specific anti-BrdU antibodies. As anticipated, MCF7 WT and NSC2 control cultures responding to inhibition of E2 signaling showed a dramatic decrease in BrdU signal intensity (Figure 3-18, rows 1 and 2), whereas similarly treated CycG2 KD clones, showed a less pronounced decrease of incorporated BrdU (rows 3 to 5). As seen before, compared to controls, the G_1-phase arrest response of treated CycG2 KD cell populations is reduced (Figure 3-18).
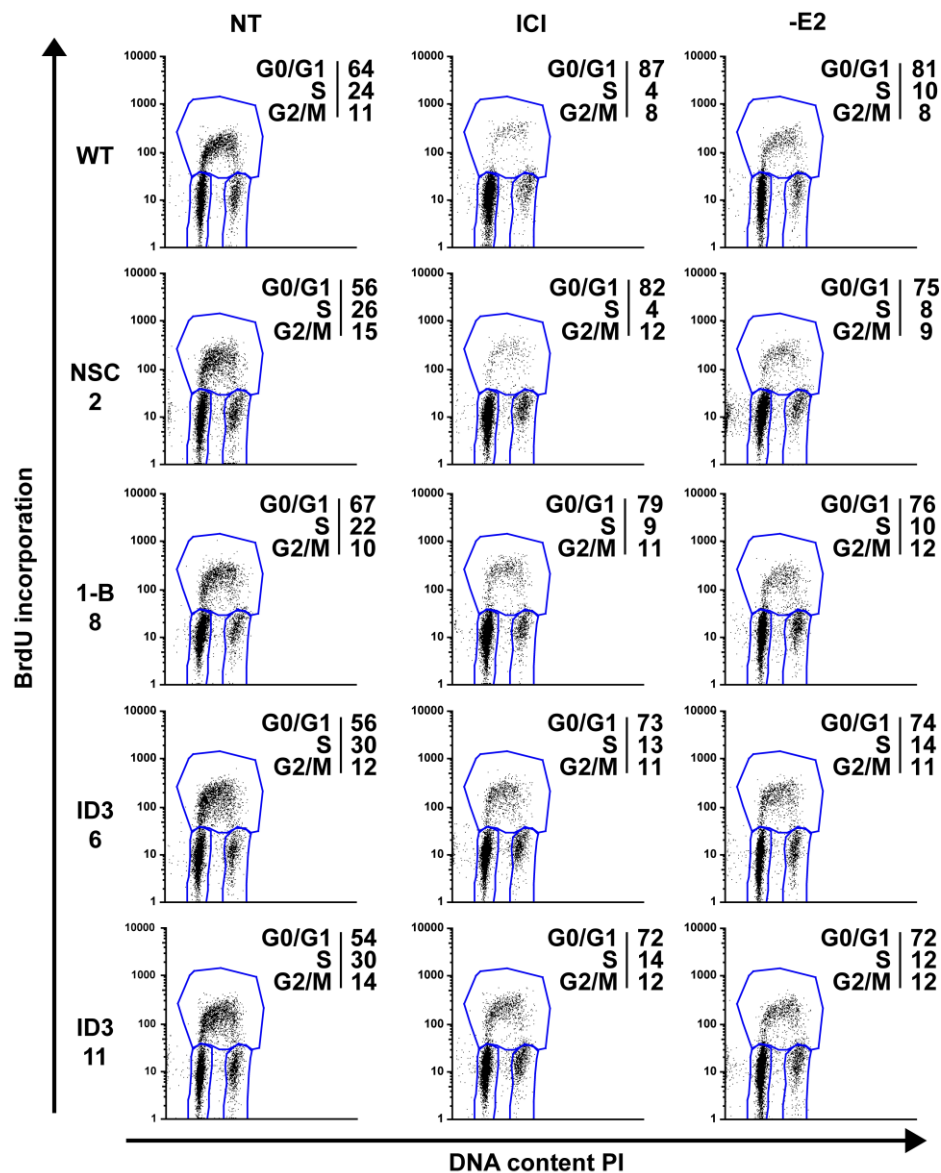
Figure 3-18: Increase of S-phase population is not due to S-phase arrest. BrdU incorporation assay after 48 h ICI treatment (middle) or 4 days E2 depletion (right) of indicated cultures are depicted. Compared to controls (WT, NSC2) CycG2 KD clones (1-B, ID3) demonstrate an increase in DNA synthesis (BrdU incorporation) and a decrease in G_1-phase arrest.

3.2.5 Increased Activation of MAPK Signaling Components in CycG2 KD Clones

Reduced CycG2 mRNA expression correlates with higher recurrence and poor survival probability (Adorno et al., 2009; Hu et al., 2006; van de Vijver et al., 2002). In contrast, higher levels of CycG2 mRNA are present in normally differentiated breast and hormone responsive tumor cells treated with anti-estrogens (Dudek and

Picard, 2008; Frasor et al., 2004). Resistance of ER positive BC tumor cells to E2/ER antagonizing drugs eventually develops in the majority of patients undergoing long-term treatment regimens. The molecular mechanisms behind the development of resistance to these therapies are complex, possibly induced by phosphorylation mediated increases in ER signaling, or through ER-independent pathways, such as increased activation of growth factor signaling (Di Cosimo and Baselga, 2008). To investigate the influence of CycG2 expression levels in the development of resistance to pharmacological inhibition of E2 signaling, immunoblot analysis of the signaling responses following these treatments was carried out.

The phosphorylation ERK-MAPK pathway proteins cRaf, MEK, ERK and Rb was analyzed in MCF7 cell cultures deprived of E2 (left) or treated with ICI (right). MCF7 WT and NSC2 lysates display low basal levels of activating Raf phosphorylation at S338 under control and treatment conditions (Figure 3-19). In contrast to control cell lines, CycG2 KD clones exhibit elevated levels of pRaf S338.
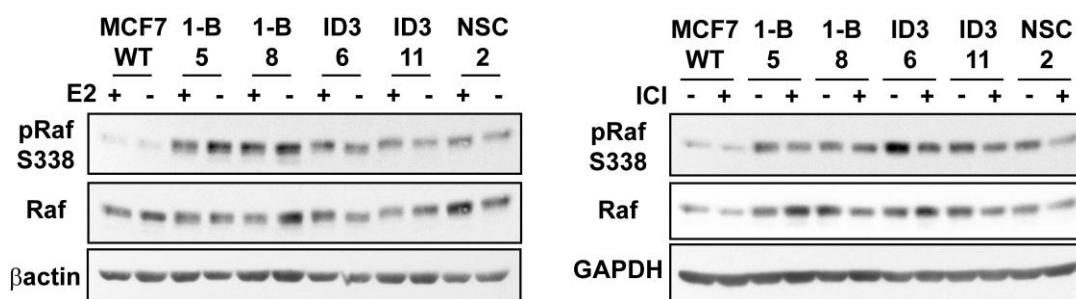
Figure 3-19: CycG2 KD leads to the activation of the pRaf. Immunoblot analysis of indicated proteins in lysates from cultures grown in the presence (+) or absence (-) of E2 (left) or in ICI (right). Phosphorylation status of the activated form of cRaf at Ser338, against total cRaf and loading controls βactin and GAPDH.

Consistent with a low level of cRaf phosphorylation, the downstream components of the MAPK pathway, MEK and ERK, also exhibit little phospho modification in the control cell lines (Figure 3-20). Compared to the WT and NSC2 controls, CycG2 KD clones exhibit not only elevated levels of phosphorylation on Raf, but also of MEK and ERK proteins, under basal conditions and after inhibition of E2 signaling (Figure 3-19 and Figure 3-20).
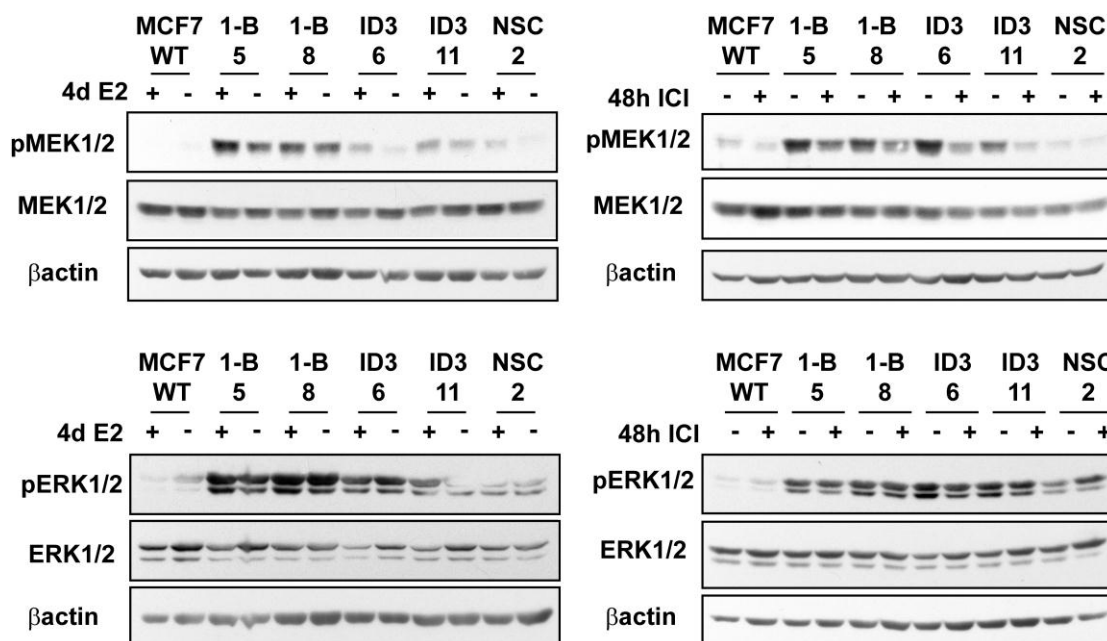
Figure 3-20: Activation of the ERK-MAPK pathway in CycG2 KD clones. Representative immunoblot analysis of indicated proteins in lysates from cultures grown in the presence (+) or absence (-) of E2 (left) or ICI (right). Phosphorylation status of activated forms of proteins of the ERK-MAPK signaling pathway MEK (top) and ERK (bottom) against total protein of MEK and ERK and loading control βactin.

Signal transduction through the MAPK is known to stimulate CycD1 expression and activity of CycD1-CDK4/6 complexes (Lavoie et al., 1996). Activated CycD/CDK complexes phosphorylate Rb proteins, thereby promoting the release of sequestered E2F transcription factors from Rb to allow stimulation of cell cycle-promoting gene transcription (Shaul and Seger, 2007). Consistent with the increased cell proliferation and MAPK cascade activation in CycG2 KD clones, the abundance of CycD1 appears to be increased when compared to WT and NSC2 controls (Figure 3-21). Similarly, the levels of hyperphosphorylated Rb seem to be elevated in a number of CycG2 KD clones, in comparison to the control cell lines (Figure 3-21), as seen in the banding pattern for both S780-phosphorylated Rb and total Rb.
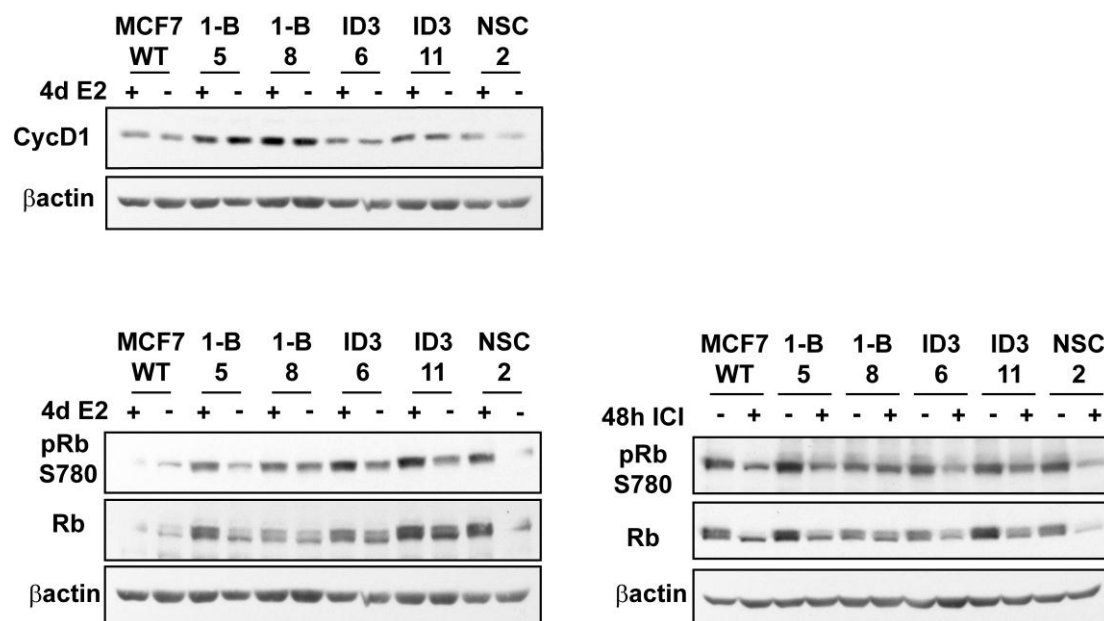
Figure 3-21: CycG2 KD leads to the upregulation of MAPK downstream target CycD1 and phosphorylation of Rb. Representative immunoblot analysis of indicated proteins in lysates from cultures grown in the presence (+) or absence (-) of estrogen (left) or ICI (right). Expression level of downstream protein CycD1 (top) and phosphorylation status of Rb (bottom) compared to loading control βactin.

3.2.6   Co-Purification of CycG2 with CDK10

CDK10 was recently proposed as a critical determinant of BC resistance to E2 signal inhibiting endocrine therapies (Iorns et al., 2008). CDK10 interacts with Ets2 TFs and modulates Ets2 transactivation (Kasten and Giordano, 2001). Downregulation of CDK10 expression results in relief of Ets2 inhibition, leading to elevated cRaf transcription and the upregulation of MAPK signaling (Iorns et al., 2008; Kasten and Giordano, 2001). Little is known about the regulation of CDK10 activity and its putative binding partner. To date, there is no known cyclin partner for CDK10.

To investigate a possible interaction of CycG2 with CDK10, co-immunoprecipitation experiments with ectopic GFP-tagged CycG2 and HA-tagged CDK10 constructs were carried out (Figure 3-22). HA-tagged CDK10 strongly co-purifies with the full length (FL) and the CycG2 1-160 constructs that contains the full cyclin box, but not with CycG2 1-140 construct, that contains only a truncated cyclin box (Figure 3-22, B). Surprisingly, CDK10 also co-purifies with CycG2 142-344 C-terminus. It was previously shown that PP2AB' co-purifies with FL or C-term (142-345) CycG2, but not with the N-terminal regions of CycG2 encompassing the cyclin box (Bennin et al., 2002). Co-expression of CDK10 and myc-tagged PP2A with CycG2 and subsequent co-IP showed that CDK10 and PP2A co-purify with

immunoprecipitated CycG2 (Figure 3-22, B). Reciprocal IPs yielded complementary results, CDK10 and CycG2 co-purify with immunoprecipitated myc-PP2A.
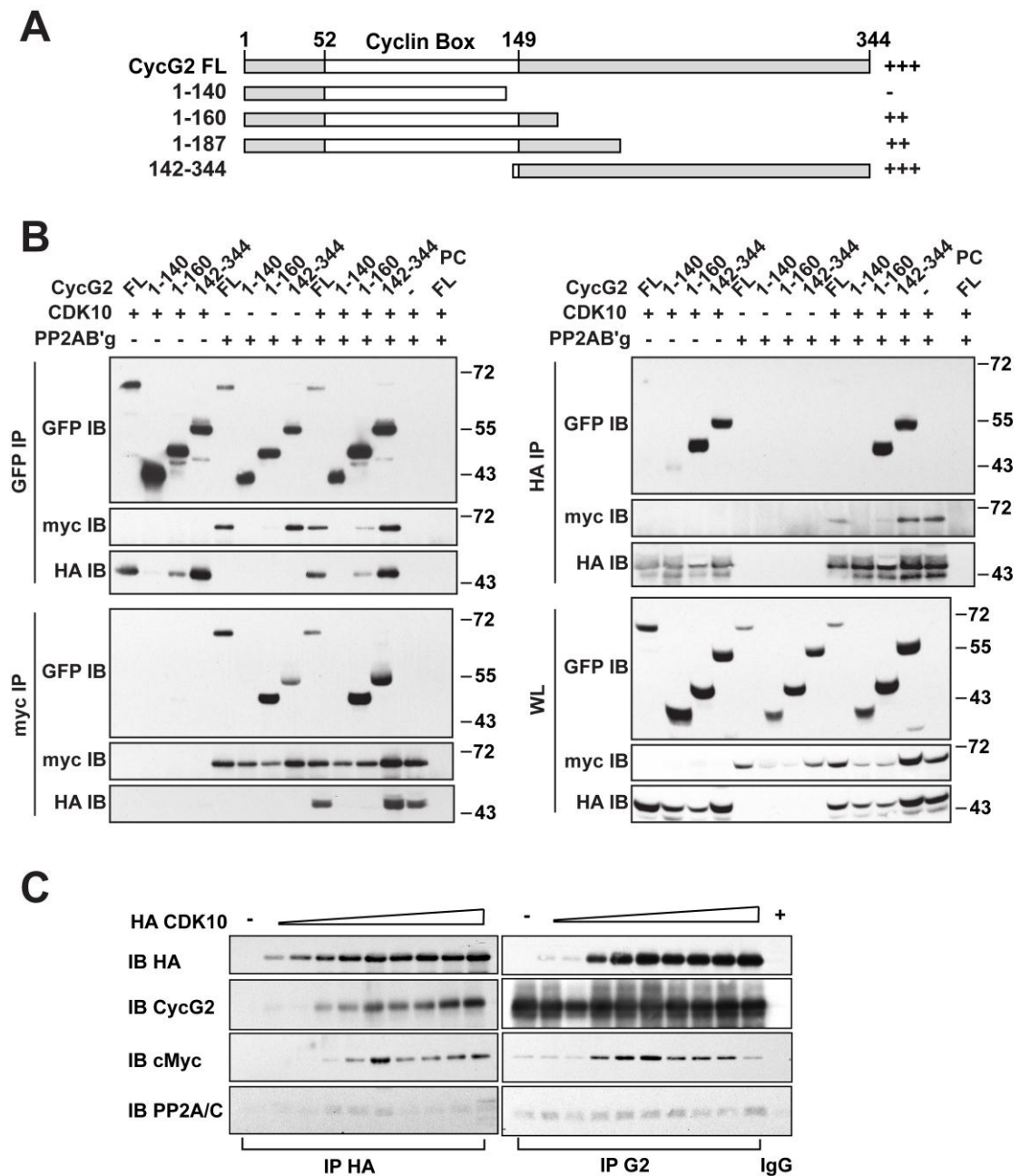
Figure 3-22: CycG2 co-purifies with CDK10 and PP2AB'. A) Schematic of GFP-tagged full length (FL) and truncation CycG2 expression constructs. Indicated to the right is the ability of co-purification of CycG2 with CDK10. **B)** Co-expression of HA-tagged CDK10, myc-tagged PP2AB'g constructs with GFP tagged FL or truncated CycG2 plasmids. CDK10 and PP2A co-purify with the CycG2 C-terminus. In addition CDK10 can co-IP with the entire cyclin-box containing CycG2 construct 1-160 but not with the truncated version 1-140. PP2A constructs only co-purify with FL or C-term (142-345) CycG2. **C)** CDK10 and PP2A bind to different protein regions within CycG2. Co-expression of constant amounts of CycG2 and PP2A with increasing amounts of CDK10 leads to increased CycG2/PP2A complex co-purification. PC indicates sample incubation with non-specific isotype matched antibodies.

Co-expression of constant amounts of CycG2 and PP2A with increasing amounts of CDK10 first promotes increased CycG2/PP2A complex co-purification (Figure 3-22, C). After reaching a maximum, increasing amounts of CDK10 leads to the displacement of PP2A from the immunoprecipitated complexes.

To investigate whether endogenous CDK10 can form complexes with endogenous CycG2, MCF7 cell lysates were used for co-immunoprecipitation experiments (Figure 3-23). Endogenous CycG2 can be detected in CDK10 IPs (Figure 3-23, left) and CDK10 can be detected in CycG2 IPs (Figure 3-23, right). Inhibition of E2 signaling in MCF7 cells via E2 depletion (DM) or inhibitor treatment (ICI and 4OHT) leads to an increase in CycG2-CDK10 co-IP compared to cells grown in regular medium (RM), or E2 supplemented (DM/E2) medium (* indicates specific co-IP signal).
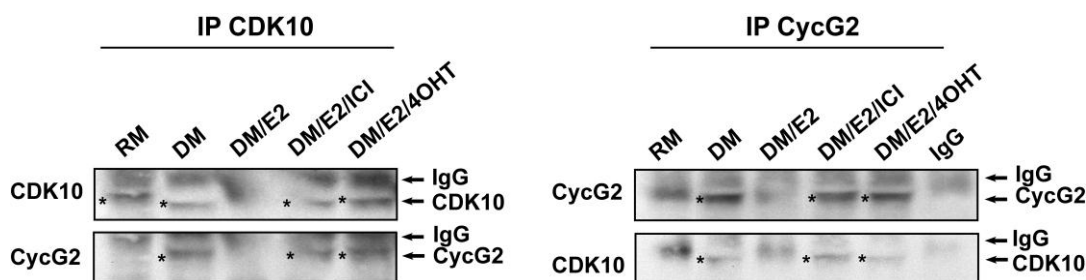
Figure 3-23: CycG2 co-purifies with CDK10 upon inhibition of ER signaling. Western blot analysis of immunoprecipitates (IPs) from MCF7 cell lysates. Cultures were grown for 6 days in regular (RM) or E2 depleted (DM) medium and an additional 3 days in the absence or presence of 10 nM estrogen (E2), 100 nM ICI or 100 nM 4OHT. Proteins were co-IP with CDK10 (left) or CycG2 (right) or control IgG antibodies and blots were probed against indicated antigens (* denotes specific CycG2 or CDK10 band).

To further investigate whether the interaction between CycG2 and CDK10 is reflected by recruitment and colocalization in cells, co-expression studies for confocal immunofluorescence microscopy assays were performed. U2OS and MCF7 cells were transfected with GFP tagged CycG2 and HA tagged CDK10 for 48 h. PFA fixed cells were immunostained with antibodies directed against HA and the microtubule marker α-tubulin, and examined by confocal microscopy (Figure 3-24). Analysis of the captured images using ImageJ 1.45s and JACoP plugin (NIH http://imagej.nih.gov.ij) software revealed that CycG2 co-localizes with CDK10 in co-transfected U2OS and MCF7 cells. The correlation of the intensity distribution between channels (Pearson's coefficient) is r=0.906 for U2OS and r=0.95 for MCF7.
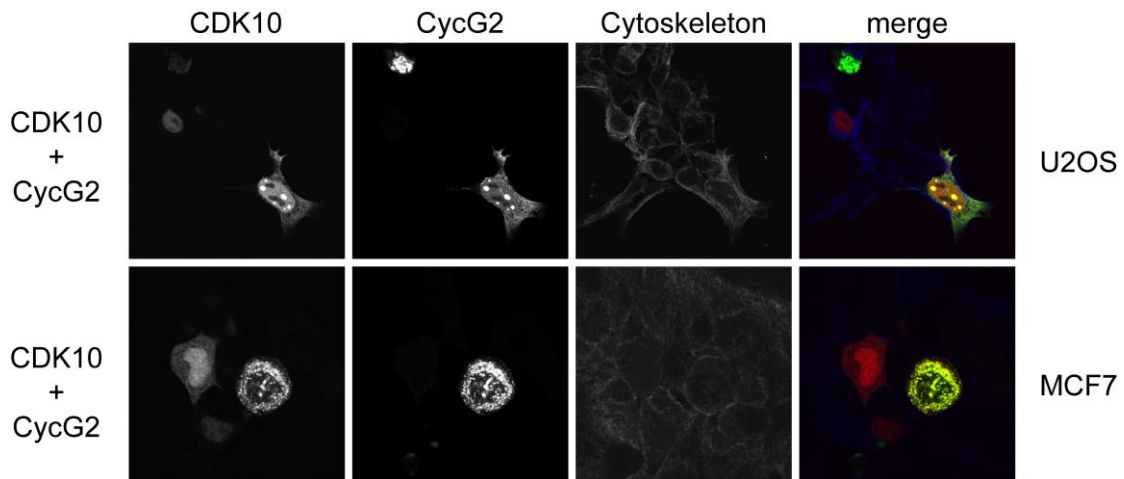
Figure 3-24: CycG2 and CDK10 co-localize. Confocal microscopy images of U2OS (top) and MCF7 (bottom) cells transfected with GFP tagged CycG2 and HA tagged CDK10 constructs for 48 h. PFA fixed cells were stained for HA (CDK10, red) and α-tubulin (cytoskeleton, blue). Immunosignals are shown pseudo-colored in the merged panel (CycG2, green; CDK10, red; Tubulin, blue) and single channel signals are shown in black and white for better contrast.

3.3 Contribution of CycG2 to Growth Arrest Following mTOR Inhibition

It is though that, as BC cells develop resistance to ER targeted therapy, they no longer rely on genomic ER signaling, instead, growth factor receptor signaling pathways are upregulated to stimulate cell growth (Massarweh et al., 2008). Signaling through EGFR, IGFR and HER2 mediates the activation of the PI3K/Akt/mTOR pathway (Zhang et al., 2011). Inhibitors of the downstream kinase mTOR have been successfully used to treat a subset of cancers including lymphoma and BC (Baselga et al., 2009; Witzig et al., 2011). To analyze the contribution of CycG2 expression to the cell cycle inhibitory effects of mTOR signaling blockade, immunoblot and cell cycle analyses were performed.

3.3.1 Rapamycin Induces G_1-Phase Arrest and CycG2 Expression

It was previously shown that treatment of cells with the mTOR inhibitor rapamycin induced CycG2 expression and a G_1-phase cell cycle arrest (Kasukabe et al., 2008; Le et al., 2007; Zhou et al., 2009). Diffuse large B cell lymphomas (DLBCLs) exhibit aberrant regulation of cell-cycle control, apoptosis, differentiation and signal transduction. CycG2 is highly expressed in organs that are enriched for lymphocytes, like spleen, lymph nodes and thymus (Horne et al., 1996). To confirm

published mRNA data, additional experiments in DLBCL cell lines were conducted. In initial experiments, the DLBCL cell lines DHL4, 8 and 16 were treated with rapamycin for 8 and 24 h before analysis of DNA content. These experiments confirmed the rapamycin induced G_1-phase cell cycle arrest in multiple DLBCL cell lines (Figure 3-25).
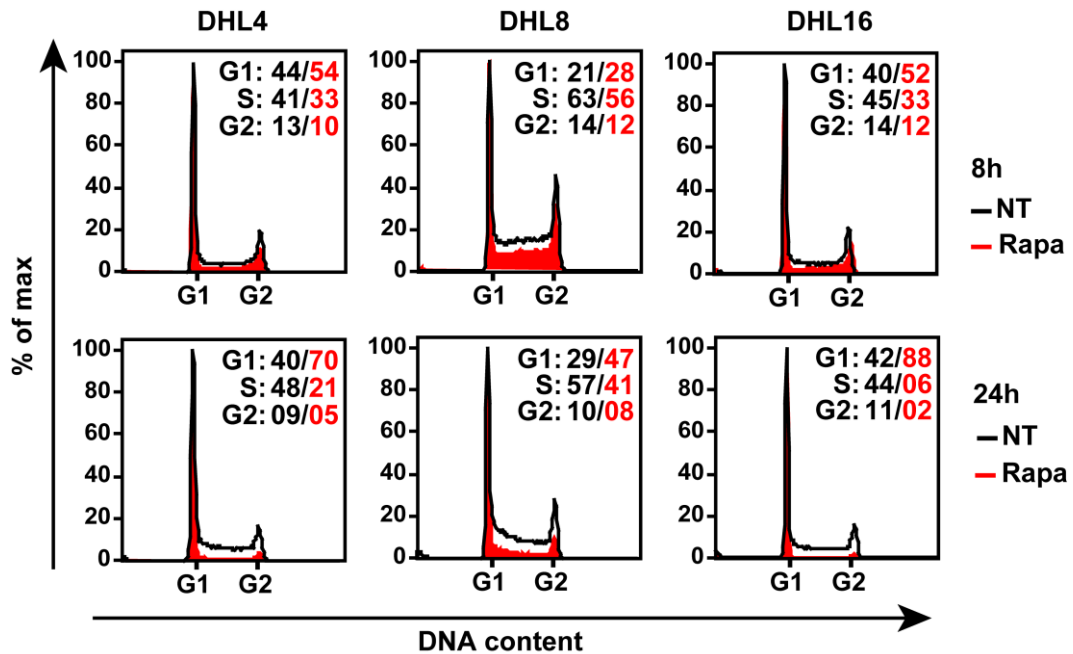
Figure 3-25: Treatment of the B-cell lymphoma lines with rapamycin induces G_1-phase cell cycle arrest. B-cell lymphoma lines SU-DHL4, SU-DHL8 and SU-DHL16 were treated with 10 nM rapamycin for 8 h (top) and 24 h (bottom) before ethanol fixation and cell cycle analysis. Histogram overlays of PI stained DNA of indicated cell lines.

In agreement with the mRNA data, treatment of these cell lines with rapamycin for 9 h induces a 1.6 to 1.7 fold increase in CycG2 protein levels (Figure 3-26).
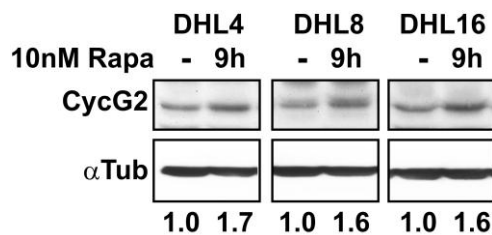
Figure 3-26: Treatment with rapamycin induces CycG2 expression. B-cell lymphoma lines SU-DHL4, SU-DHL8 and SU-DHL16 were treated with 10 nM rapamycin for 9h and protein expression was assed via immunoblotting against CycG2 and α-tubulin as loading control. Fold increase of CycG2 expression is indicated under each lane.

3.3.2 Metformin Induces G_1-Phase Arrest and CycG2 Expression

Metformin is a widely prescribed anti-diabetic drug associated with a reduced risk of cancer. In breast and ovarian cancer cells, metformin stimulates the AMP activated protein kinase (AMPK) leading to the activation of the tuberous sclerosis 2 (TSC2) protein and the consequent downstream inhibition of mTOR signaling (Ben Sahra et al., 2010). Treatment of MCF7 cells with metformin (Met) over a timecourse of 48 h showed the induction G_1-phase cell cycle arrest. Cell cycle distribution also revealed a slight reduction in the number of cells in S- and G_2/M-phase (Figure 3-27). In addition to single parameter analysis of PI stained DNA (Figure 3-27, A), BrdU incorporation assays were performed. Two parameter dot plots of BrdU and PI stained DNA are shown in Figure 3-27, B. Treatment with metformin leads to a 36% reduction of cells with BrdU incorporation (DNA synthesis) in MCF7 WT cells.
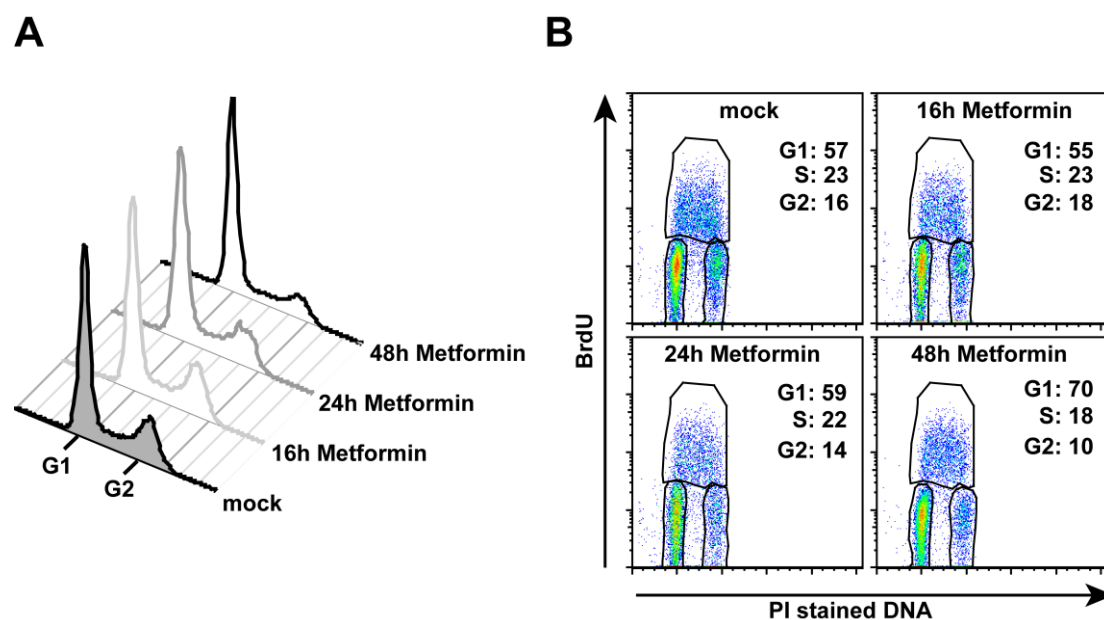
Figure 3-27: mTOR inhibition with metformin leads to reduced BrdU incorporation and G_1-phase cell cycle arrest. A) Offset histogram overlays of PI stained DNA in fixed MCF7 cells treated for indicated time with 1 mM metformin. **B)** Two-dimensional BrdU incorporation assay of PI stained MCF7 cells treated with metformin for indicated periods of time.

Immunoblot analysis of pilot experiments showed that CycG2 protein expression is upregulated up to 2.5 fold following treatment of cell lines derived from normal breast (MCF10a) and breast cancer (MCF7) with metformin (Figure 3-28). Treatment with the mTOR inhibitor rapamycin was used as a positive control for the induction of CycG2 expression.
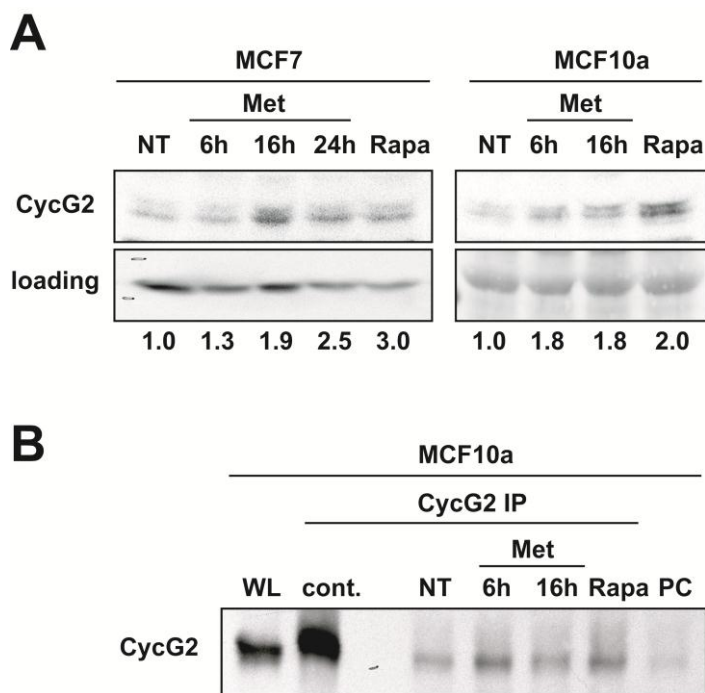
Figure 3-28: Treatment of MCF7 and MCF10a cultures with metformin induces CycG2 expression. Immunoblot analysis of CycG2 expression in normal MCF10a and in the breast cancer cell line MCF7 after treatment with the mTOR inhibitor metformin (Met). CycG2 expression in WL **A)** and IP **B)** samples. Fold increase of CycG2 expression compared to non-treated controls is indicated under each lane. NT controls are set to 1.0.

Initial experiments indicate that the modest metformin induced upregulation of CycG2 expression is abolished in the CycG2 KD clones (Figure 3-29). Immunoblot analysis of metformin treated MCF7 KD and control cell lines shows no changes in CycG2 protein level in KD clones treated with metformin. Simultaneously, CycD1 protein levels appear to be elevated in several of the CycG2 KD clones, whereas its expression is reduced in response to metformin treatment in control and KD samples.
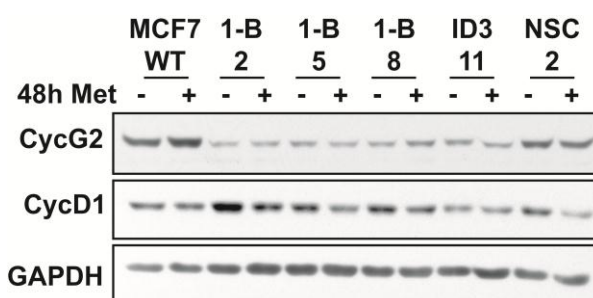
Figure 3-29: Metformin induced upregulation of CycG2 is abolished in CycG2 KD clones. Immunoblot analysis of indicated proteins in MCF7 cells cultured in the presence (+) or absence (-) of 1 mM metformin for 48 h.

To explore the effect that expression of CycG2 has on the metformin-induced cell cycle arrest of MCF7 cells, the CycG2 KD clones and NSC2 control cell cultures were treated for 48 h with metformin and prepared for DNA flow cytometry. Cell cycle analysis of PI stained DNA revealed that the metformin-induced G_1-phase cell cycle arrest response is reduced in CycG2 KD clones (Figure 3-30). In addition to a reduced number of cells in G_1-phase (67% and 63% compared to 77%) of the cell cycle, CycG2 KD clones exhibit higher numbers of cells in S-phase (17 % and 19% compared to 14%) following treatment with metformin, when compared to control NSC2.
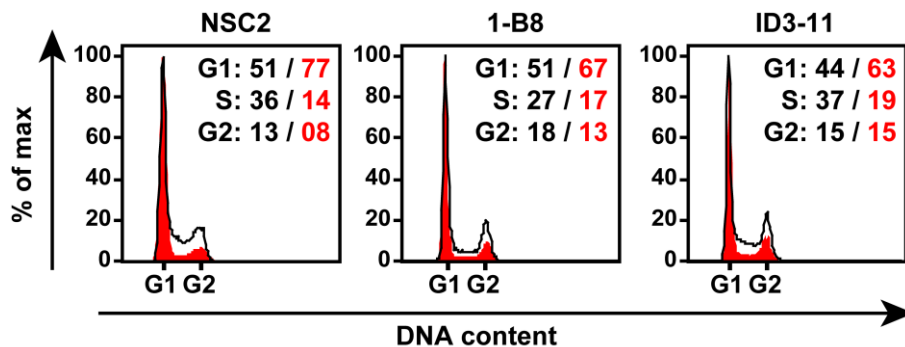
Figure 3-30: CycG2 KD diminishes metformin induced G_1-phase cell cycle arrest. Histogram overlays of PI stained DNA of mock (black line) or metformin treated (red area) NSC2 control and CycG2 KD clones (1-B8, ID3-11). MCF7 cultures were treated for 48 h with 1 mM metformin.

3.4   Contribution of CycG2 to Growth Control in Tuberous Sclerosis

Cells isolated from tuberous sclerosis patients with inactivating mutations in genes encoding the tuberous sclerosis complex (TSC) proteins 1 and 2 exhibit excessive mTOR activity (Orlova and Crino, 2011). The hyperactivation of mTOR signaling, however, eventually triggers a negative feedback loop, disinhibiting FOXO transcriptional activity through phosphorylation of the insulin receptor substrate (IRS) that subsequently deactivates Akt signaling (Harvey et al., 2008; Zoncu et al., 2011). The disease is associated by the growth of benign tumors in multiple organ systems (including skin, kidney, brain, heart and lung) (Crino et al., 2006). Treatment of TSC patients with mTOR inhibitors such as rapamycin is one therapeutic approach that holds considerable promise (Bissler et al., 2008; Ozcan et al., 2008). Recent studies

indicate that loss of TSC function triggers endoplasmic reticulum stress (ERS) and an unfolded protein response (UPR) that promotes hypersensitivity to ERS-inducing pharmacological agents (Ozcan et al., 2008). As CycG2 is a rapamycin and ERS-responsive FOXO TF target, the possibility that CycG2 functions as a cell cycle inhibitory protein, counteracting mTOR-driven growth, was examined.

To test the effects of CycG2 depletion in TSC and normal human fibroblasts the previously described (3.1.6 Testing of shRNA Constructs for CycG2 Knockdown) *CCNG2* targeting and non-silencing control shRNA expression vectors were adapted for lentiviral transduction experiments. The potential contribution of CycG2 to the cell cycle arrest responses of WT and TSC fibroblasts responding to rapamycin and ERS invoking drugs was investigated.

3.4.1   CycG2 Expression in TSC Cells

Baseline *CCNG2* expression in three TSC (2332, 6100 and 6121) relative to the normal (IMR90) human fibroblast cell lines was determined by quantitative real-time (qRT) PCR assays. Analysis showed that basal levels of *CCNG2* transcription were greater in two of the three TSC lines examined, the greatest in TSC 6100 (Figure 3-31).
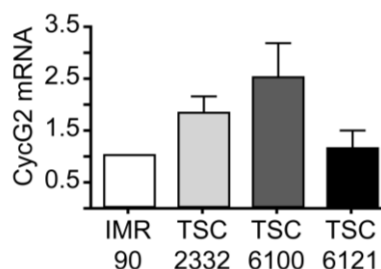
Figure 3-31: Increased basal expression of CycG2 in TSC cells. qRT-PCR analysis of basal *CCNG2* expression in normal human fibroblast cells (IMR90) compared to TSC (2332, 6100 and 6121) cell lines. Note the elevated *CCNG2* transcript level in TSC cell lines 2332 and 6100.

3.4.2   Rapamycin Induces G_1-phase Cell Cycle Arrest in TSC Cells

Treatment of normal (IMR90) and TSC human fibroblast cell lines with rapamycin (Rapa) induced a G_1-phase cell cycle arrest (Figure 3-32). To establish the treatment durations necessary for optimal inhibition of cell cycle progression in the WT and TSC deficient cell lines, timecourse experiments were conducted. Indicated cell lines were treated with 10 nM Rapa for 16, 24 and 32 h and the DNA content was determined by flow cytometry. Compared to mock (NT) treated controls, Rapa

treatment (bold typing or red area) led to the accumulation of cells in G_1-phase and a corresponding reduction in the S- and G_2/M-phase populations of all tested cell lines.

	NT/**16h Rapa**			NT/**24h Rapa**			NT/**32h Rapa**		
	G1	S	G2	G1	S	G2	G1	S	G2
IMR90	69/**78**	16/**13**	13/**6**	69/**83**	16/**10**	13/**8**	69/**86**	16/**6**	13/**6**
TSC 2332	59/**75**	16/**14**	20/**10**	59/**77**	16/**11**	20/**9**	59/**84**	16/**6**	20/**10**
TSC 4520	55/**78**	26/**14**	16/**6**	55/**81**	26/**10**	16/**7**	55/**76**	26/**12**	16/**6**
TSC 6100	56/**60**	28/**28**	11/**7**	56/**71**	28/**17**	11/**7**	56/**71**	28/**18**	11/**5**
TSC 6121	62/**75**	17/**13**	16/**9**	62/**80**	17/**9**	16/**7**	62/**72**	17/**15**	16/**9**
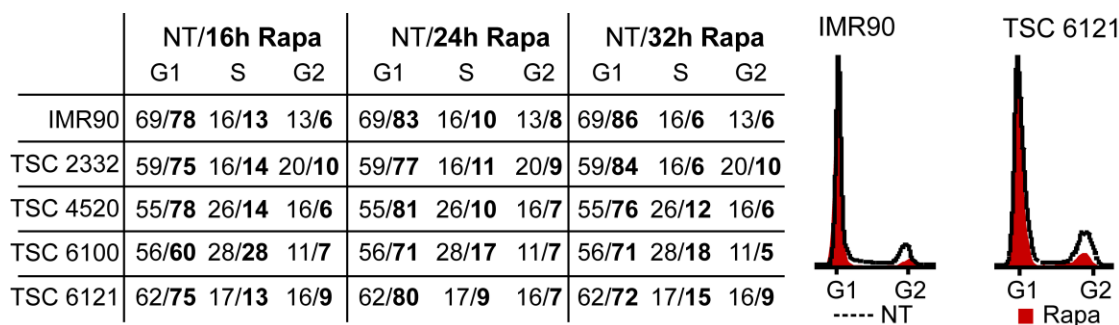
Figure 3-32: Treatment of TSC cultures with the mTOR inhibitor rapamycin induces G_1-phase cell cycle arrest. *Left)* Table of the percentage of cell population in indicated phases of the cell cycle, of vehicle (NT) or Rapa (bold type) treated cell lines. *Right)* Histogram overlays of PI stained DNA in control (IMR90) and TSC cell line 6121, treated with Rapa (red area) or vehicle (black line) for 32 h.

3.4.3 Rapamycin Induces CycG2 Expression

Inhibition of mTOR activation via Rapa treatment induced *CCNG2* expression in all cell lines (Figure 3-33). qRT-PCR analysis showed that Rapa treatment increased *CCNG2* mRNA (Figure 3-33, A) in WT and TSC fibroblast cell lines. The most robust increase (3 to 5 fold) was observed in IMR90 (WT) and TSC 6121 cells. Consistent with the mRNA data, CycG2 protein expression levels in the WT and TSC-deficient fibroblasts increased within 16 to 24h of treatment (Figure 3-33, B). Initial immunoblot analysis of the cells treated with Rapa for 24 h indicated an increased CycG2 expression in two WT human fibroblasts control cell lines GM00637 and IMR90 (Figure 3-33, left). As this analysis of CycG2 levels in extracted lysates from treated and untreated populations of the different WT and TSC deficient lines was to some degree ambiguous, CycG2 was concentrated by immunoprecipitation prior to immunoblot analysis (Figure 3-33, right). Again, treatment with Rapa induced the upregulation of CycG2 expression in both, control and TSC cell lines.

Similar immunoblot analysis of the FOXO regulated CKI, p27, showed that p27 levels are upregulated in Rapa treated samples, but p27 upregulation was not as high in TSC cell lines relative to IMR90 controls. Basal p27 levels appear to be lower in TCS cell lines compared to IMR90 control. Proliferation promoting CycD1 protein levels are elevated in TSC cells compared to controls but are reduced following Rapa treatment (Figure 3-33, C).
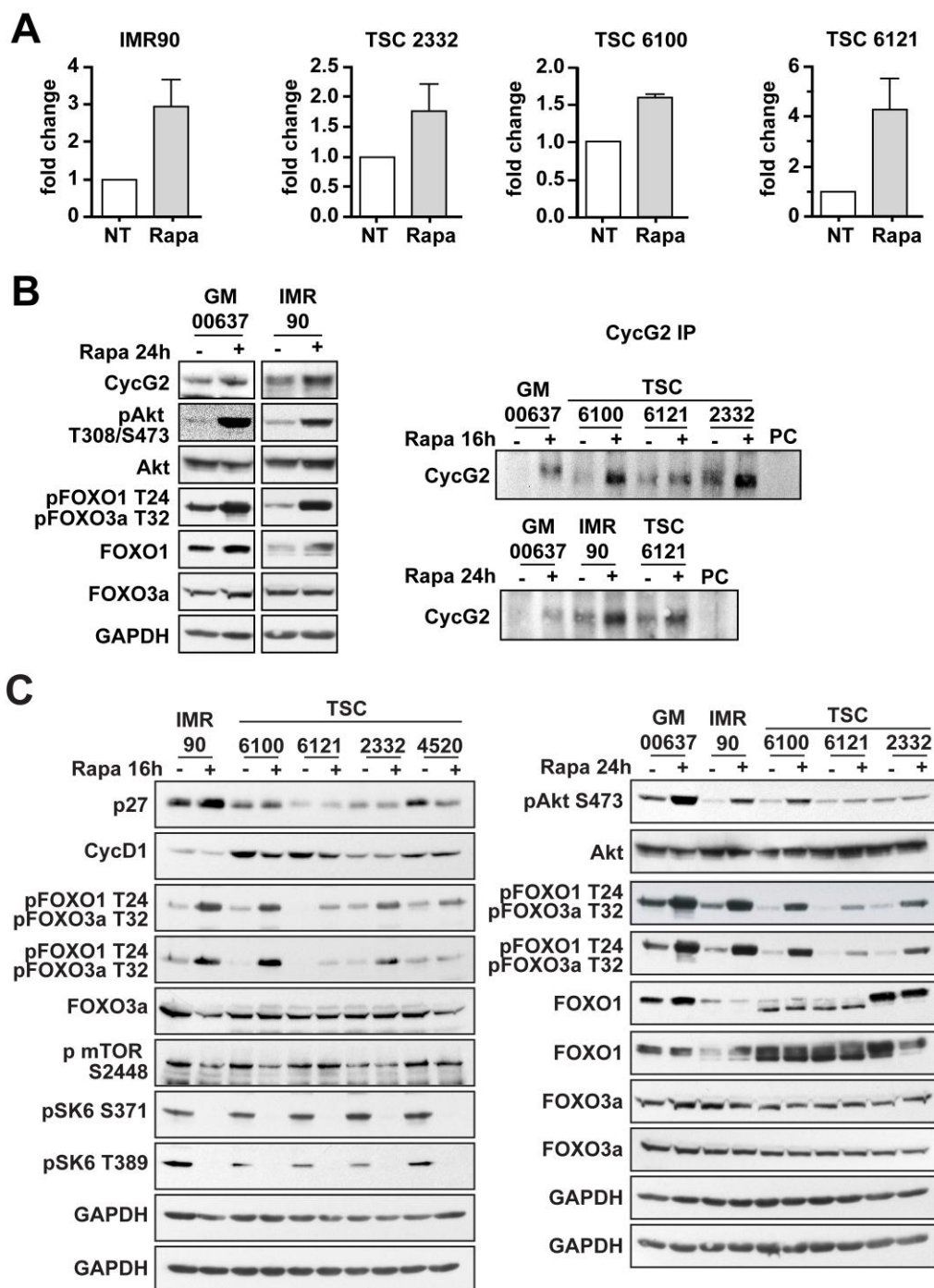
Figure 3-33: Inhibition of mTOR via rapamycin induces CycG2 expression. A) Treatment of indicated cell lines with Rapa increases *CCNG2* transcript levels. qRT-PCR analysis of cultures treated for 24 h with Rapa compared to vehicle (NT) control. **B)** Assessment of change in CycG2 protein expression level after 24 h Rapa treatment in total lysates (left) and immunoprecipitation (right). mTOR inhibition leads to an elevation of CycG2 protein level and phosphorylation of Akt and FOXO proteins in normal human fibroblast cell lines (IMR90 and GM00637). **C)** Immunoblot analysis of specified proteins in indicated cell lines after 16 h (left) and 24 h (right) of Rapa treatment.

Treatment of indicated cell lines with Rapa induced the expression of phospho-activated forms of Akt (pAkt T308/S473) and phospho-inhibited forms of FOXO TFs

(pFOXO1 T24/ pFOXO3a T32) (Figure 3-33 B and C). Phosphorylation of mTOR (p mTOR S2448) and its downstream target S6K (pS6K S371 and pS6K T389) at their activation sites is strongly reduced after Rapa treatment (Figure 3-33 C).

3.4.4 Expression of Stress Response Genes Following mTOR Inhibition

Comparisons of Rapa induced modulation of mRNA expression of selected genes linked to cell cycle arrest (p27, Bim, Chop and CycG1) are shown below (Figure 3-34). The upregulation of p27 and Bim mRNAs was more potent in IMR90 and TSC 6121 cells following Rapa treatment compared to TSC 6100 and 2332. Chop and CycG1 mRNA levels were not appreciably affected by the treatment.
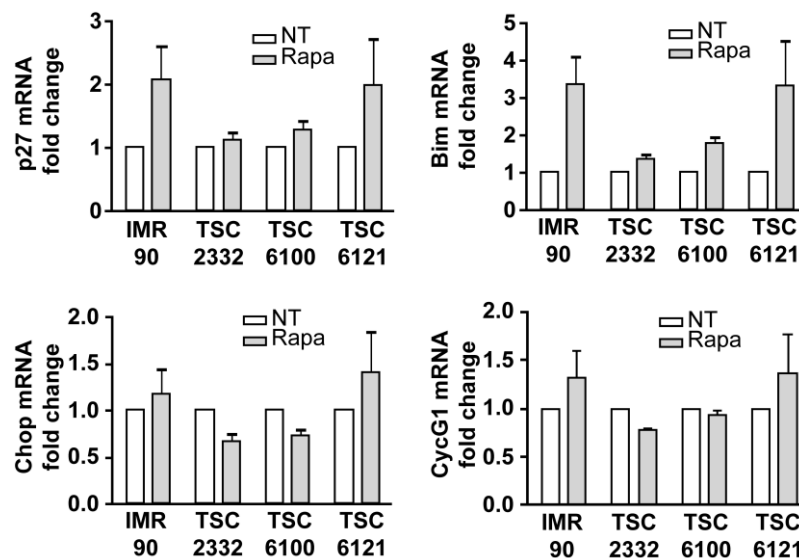
Figure 3-34: Expression of stress response regulated genes following mTOR inhibition. qRT-PCR analysis of the induction of stress response genes for p27, Bim, Chop and CycG1 following mTOR inhibition with rapamycin (Rapa) after 24 h of treatment.

3.4.5 CycG2 KD Diminishes Inhibitory Cell Cycle Effects of Rapamycin

Validated CycG2 shRNAs (see Figure 3-7) were used to assess the contribution of CycG2 upregulation to the cell cycle inhibitory effects of acute blockade of mTOR and induction of ERS signaling. To allow high transduction efficiency in primary human fibroblasts the shRNA expression cassettes were shuttled into a lentiviral expression vector (pVETL.gfp). Co-expression of the GFP marker protein in this expression vector allows the visual identification of transduced cells. We determined that the FIV viroids could transduce both, WT and TSC-deficient primary fibroblast

cultures with the pVETL.gfp-shRNA constructs (>90% efficiency) and blunt basal expression of endogenous CycG2 in infected cell populations (Figure 3-35).
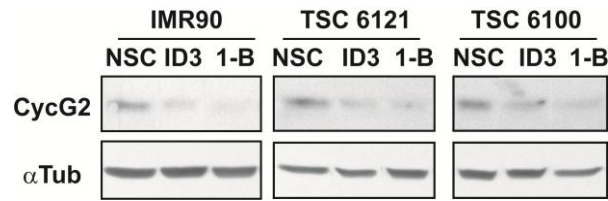
Figure 3-35: FIV transduced primary human fibroblast cell lines with CycG2 shRNA silences CycG2 protein level. TSC 6121 and 6100 fibroblast cell cultures were infected with CCNG2 specific (ID3 and 1-B) shRNAs for 72 h before protein assessment.

To test the consequence of CycG2 KD in cells responding to rapamycin, cultures of the indicated fibroblast cell lines were infected with FIV viroids harboring expression cassettes for control (NSC or NC) or *CCNG2* targeting (1-B or ID3) shRNAs and cultured for 24 h before expansion onto additional dishes. After a further 48 h growth period, cultures were treated with Rapa or vehicle (NT) for an additional 24 h. qRT-PCR analysis (Figure 3-36, A) showed that the increase in *CCNG2* transcript levels following Rapa treatment in NSC controls, was repressed in cultures infected with the shRNAs 1-B and ID3; 1-B had the most potent knockdown.

Immunoblot analysis of CycG2 KD effects on CycD1 expression was performed (Figure 3-36, B). Transduction with CycG2 shRNA viroids resulted in the repression of the basal and Rapa-induced CycG2 protein expression levels in IMR90 cultures (Figure 3-36, left). Importantly, CycD1 protein levels were increased in cultures expressing either of the *CCNG2*-targeting shRNAs (Figure 3-36, right).

To assess the effect of CycG2 KD on Rapa-induced G_1-phase arrest, cell cycle analysis of indicated cultures was performed (Figure 3-36, C). shRNA-mediated depletion of CycG2 blunts the G_1-phase cell cycle arrest response to Rapa in two TSC cell lines and the WT control. Though the effect on the IMR90 WT was quite modest, a clearer effect was seen in the TSC lines 6100 and 6121. Relative to the Rapa treated NSC-expressing control, the 1-B and ID3 transduced cells had a greater percentage of cells in S-phase and decreased percentage of cells in G_1-phase. Even in the untreated cell populations, expression of the *CCNG2*-targeting shRNAs reduced the percentage of cells with a G_1-phase DNA content relative to that found in the NSC shRNA control cells and increased the percentage of cells in S-phase.

A

B

C

	Control shRNA NT/Rapa			shRNA ID3 NT/Rapa			shRNA 1-B NT/Rapa		
	G1	S	G2	G1	S	G2	G1	S	G2
IMR90	67/**86**	19/**4**	12/**8**	61/**88**	21/**5**	13/**7**	61/**85**	23/**5**	12/**7**
TSC 6100	61/**80**	21/**7**	11/**8**	59/**76**	21/**9**	11/**7**	59/**70**	22/**14**	11/**7**
TSC 6121	72/**78**	14/**10**	11/**7**	67/**76**	16/**12**	12/**7**	66/**75**	18/**14**	12/**7**
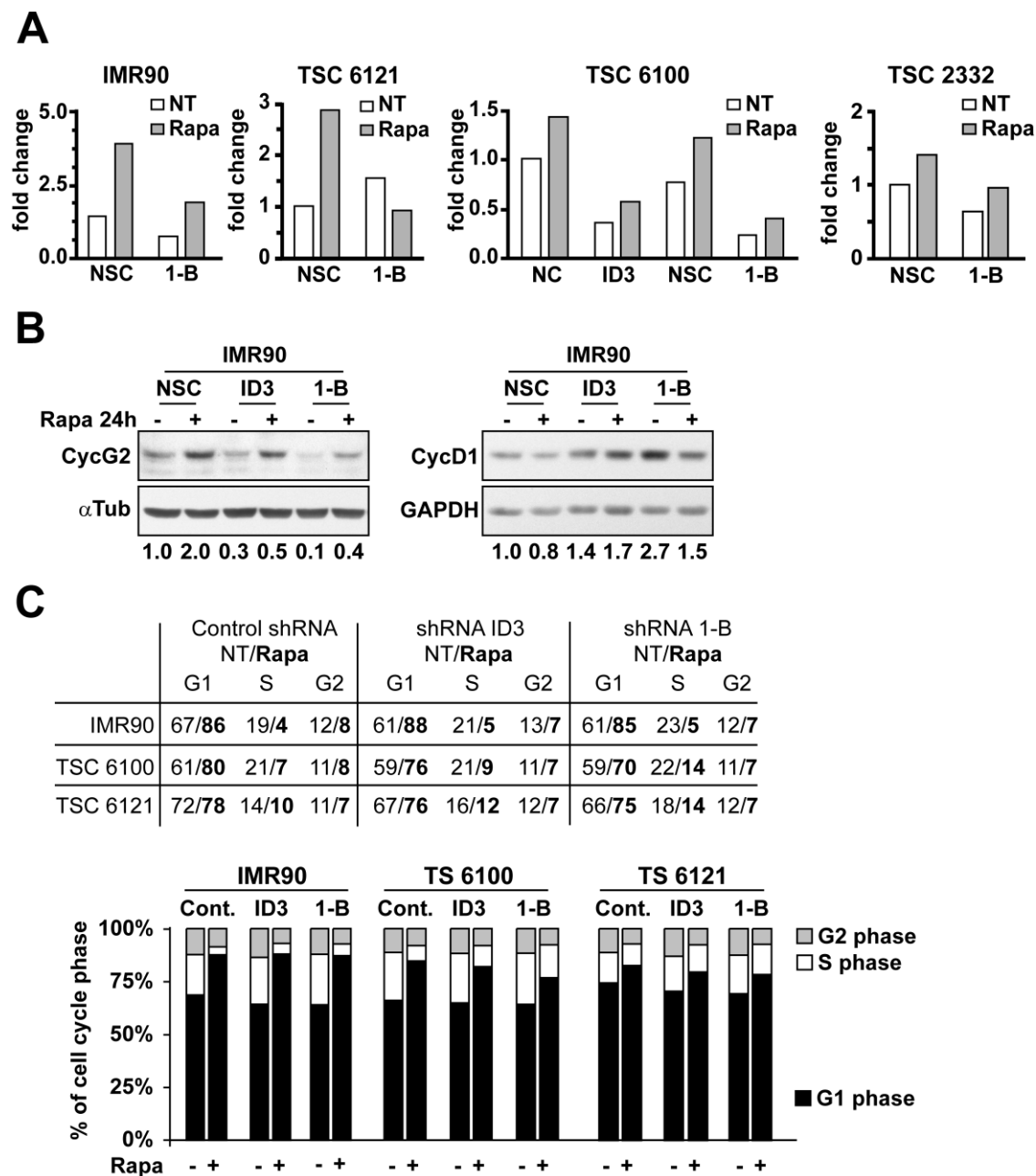
Figure 3-36: KD of CycG2 expression promotes cell cycle progression following mTOR inhibition. A) Analysis of *CCNG2* expression by qRT-PCR of indicated cell lines infected with shRNA constructs for 72 h and treated with Rapa for 24 h. **B)** Reduction of CycG2 protein level in specific shRNA (ID3, 1-B) infected cultures compared to control shRNA (NSC) before and after treatment with Rapa for 24 h. Note the increase in CycD1 expression in CycG2 KD lysates. **C)** Rapa-mediated inhibition of cell cycle is partially blocked by CycG2 knockdown. *Top)* Percentage of cells in different phases of the cell cycle of indicated cultures. *Bottom)* Bar graph of cell cycle phase distribution in indicated cultures.

3.4.6 Induction of ERS Inhibits Cell Proliferation

To establish the effect that ERS has on cell cycle progression of the cell lines used

in this study, treatments with tunicamycin (Tuni) and thapsigargin (Thap) were used

to induce ERS. WT and TSC fibroblasts were treated with for 24 h with 200 and 500 nM of Thap or Tuni (bold typing) and the cell cycle distribution of cells in each culture was determined by DNA flow cytometry (Figure 3-37). Analysis of the DNA content showed that pharmacological induction of ERS induces G_1-phase cell cycle arrest in human fibroblasts. The cell cycle arrest was most potent in the Thap-treated compared to Tuni-treated cultures of both WT and TSC fibroblasts.

	NT/**200nM Thap**			NT/**500nM Thap**			NT/**200nM Tuni**			NT/**500nM Tuni**		
	G1	S	G2	G1	S	G2	G1	S	G2	G1	S	G2
IMR90	69/**86**	18/**8**	10/**6**	69/**88**	18/**6**	10/**6**	69/**84**	18/**7**	10/**7**	69/**89**	18/**5**	10/**5**
TSC 2332	62/**78**	23/**10**	11/**9**	62/**77**	23/**10**	11/**9**	62/**64**	23/**21**	11/**12**	62/**73**	23/**14**	11/**9**
TSC 4520	52/**81**	25/**9**	20/**6**	52/**79**	25/**11**	20/**7**	52/**60**	25/**21**	20/**15**	52/**76**	25/**14**	20/**8**
TSC 6100	65/**70**	22/**17**	9/**7**	65/**80**	22/**10**	9/**8**	65/**66**	22/**21**	9/**13**	65/**73**	22/**14**	9/**11**
TSC 6121	62/**67**	19/**12**	15/**17**	62/**68**	19/**12**	15/**17**	62/**63**	19/**16**	15/**15**	62/**67**	19/**16**	15/**14**

Figure 3-37: Induction of ERS with thapsigargin and tunicamycin induces cell cycle arrest. Treatment of indicated cell lines with the endoplasmic reticulum stress (ERS) evoking agents thapsigargin (Thap) and tunicamycin (Tuni) leads to G_1-phase cell cycle arrest. Shown at the top is the table of the percentage of population in indicated phases of the cell cycle, of vehicle (NT), Thap (bold type) or Tuni (bold type) treated cell lines for 24 h. Cell cycle analysis was performed on ethanol fixed and PI stained cells. *Bottom)* Presentation of histogram overlays of PI stained DNA in control (IMR90) and TSC cell line 2332, treated with 500 nM Thap or Tuni (red area) or vehicle (black line).

3.4.7 ERS Induces CycG2 Expression

Next, the effects of Thap on CycG2 mRNA and protein expression levels were examined (Figure 3-38). Treatment of cultures with 200 nM Thap for 24 h increased *CCNG2* transcript levels between 5 and 12 fold (Figure 3-38, A), substantially more than what was observed for 24 h treatment with 10 nM Rapa. The most prominent increase in the transcript level was observed for WT cells (IMR90) and the TSC lines 6121. Immunoblot analysis of CycG2 protein levels from lysates of treated (+) and

untreated (-) populations of WT and TSC cell lines also showed an increase in the CycG2 protein levels that mirrored what was seen for the upregulation of CycG2 transcripts (Figure 3-38, B). Notably, in contrast to what was seen in fibroblasts treated with rapamycin, expression of the Akt-site phosphorylated forms of FOXO1 and FOXO3a were repressed upon treatment with Thap (Figure 3-33, B and C, Figure 3-38, B).
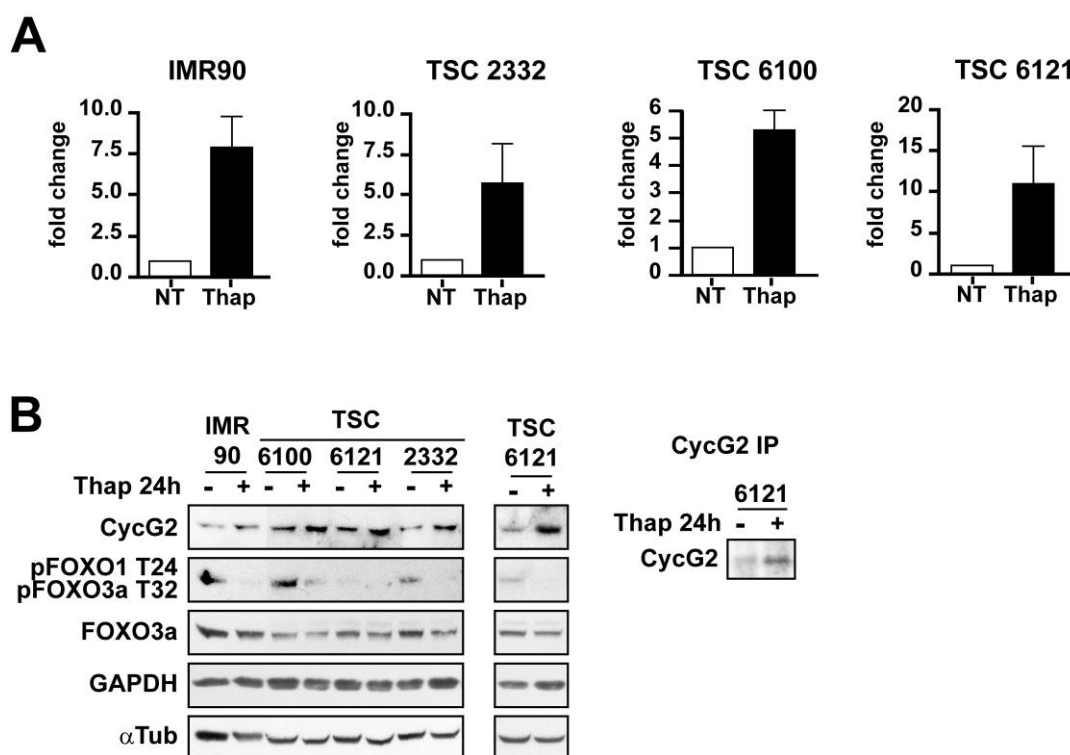
Figure 3-38: CycG2 upregulation after induction of ERS. A-B) Thapsigargin (Thap) induced ERS upregulates CycG2 mRNA and protein level. **A)** qRT-PCR analysis of *CCNG2* expression in vehicle (NT) or 200 nM Thap treated cultures. **B)** Immunoblot analysis of indicated protein after 24 h Thap treatment in total lysates (left) and immunoprecipitates (IP) (right).

3.4.8   Expression of Stress Response Genes Following the Induction of ERS

Comparisons of Thap-induced modulation of mRNA expression levels of selected genes (p27, Bim, Chop and CycG1) that are linked to cell cycle arrest and ERS response are shown below (Figure 3-39). In contrast to Rapa-treatment, 200 nM Thap not only strongly upregulated CycG2 (Figure 3-38) mRNA levels, but also substantially increased Bim and Chop mRNA levels. CycG1 and p27 mRNA was only moderately (up to 2 fold) upregulated, compared to Chop, Bim or CycG2 mRNA.
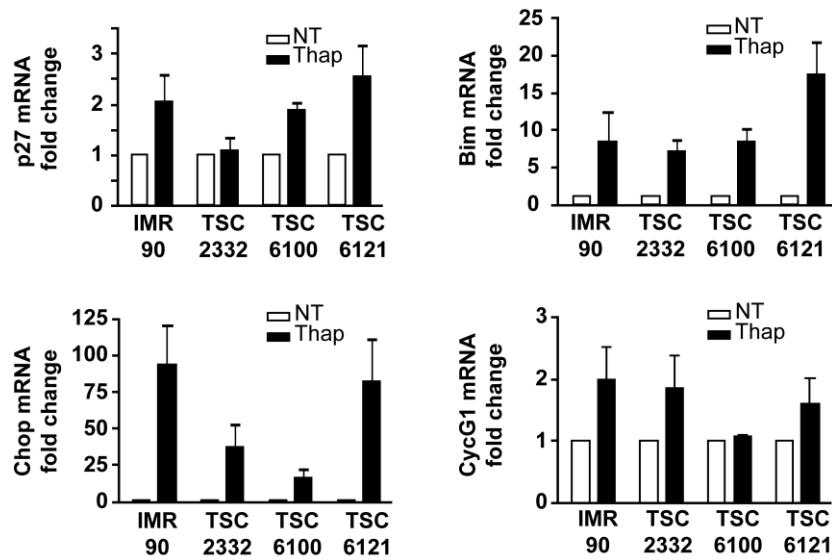
Figure 3-39: Expression of stress response regulated genes following ERS induction. qRT-PCR analysis of the induction of stress response genes, p27, Bim, Chop and CycG1, following induction of ERS by thapsigargin (Thap) after 24 h of treatment.

3.4.9   Reduced Cell Cycle Arrest Induced through ERS in CycG2 KD Clones

The effect of CycG2 KD on mock (NT, -) and Thap (+) treated gene expression and cell cycle progression was assessed to define the CycG2 contribution to the cell cycle inhibitory effects of Thap-induced ERS. Cultures of the indicated cell lines were infected with FIV particles carrying pVETL.gfp plasmids encoding the control (NSC) and *CCNG2*-targeting shRNAs (ID3 and 1-B). After 72 h of infection each culture was treated with 200 nM Thap or vehicle (NT) for an additional 24 h.

Gene expression analysis showed that basal and Thap induced *CCNG2* transcript levels were repressed upon viral mediated KD of *CCNG2* (Figure 3-40, A). In analogous experiments the effect of CycG2 KD on CycD1, p27, phosopho-activated forms of Akt, and the ERS proteins BIP and Chop was assessed (Figure 3-40, B). Immunoblot analysis showed that the induction of the ERS response proteins BIP and Chop were robustly upregulated by Thap treatment and appeared unaffected by transduction with *CCNG2*-targeting shRNAs. Substantial upregulation of p27 was only observed in Thap-treated IMR90 cells and this upregulation was largely maintained irrespective of the transduced shRNA cassette. Expression of the phospho-activated forms of Akt (which acts to repress FOXO activity) was strongly repressed in all Thap-treated cultures, irrespective of the transduced shRNA expression vector. As expected, Thap treatment suppressed CycD1 expression. As seen before,

compared to the NSC control samples, CycG2 KD samples showed an increase in CycD1 protein level (Figure 3-40, B).
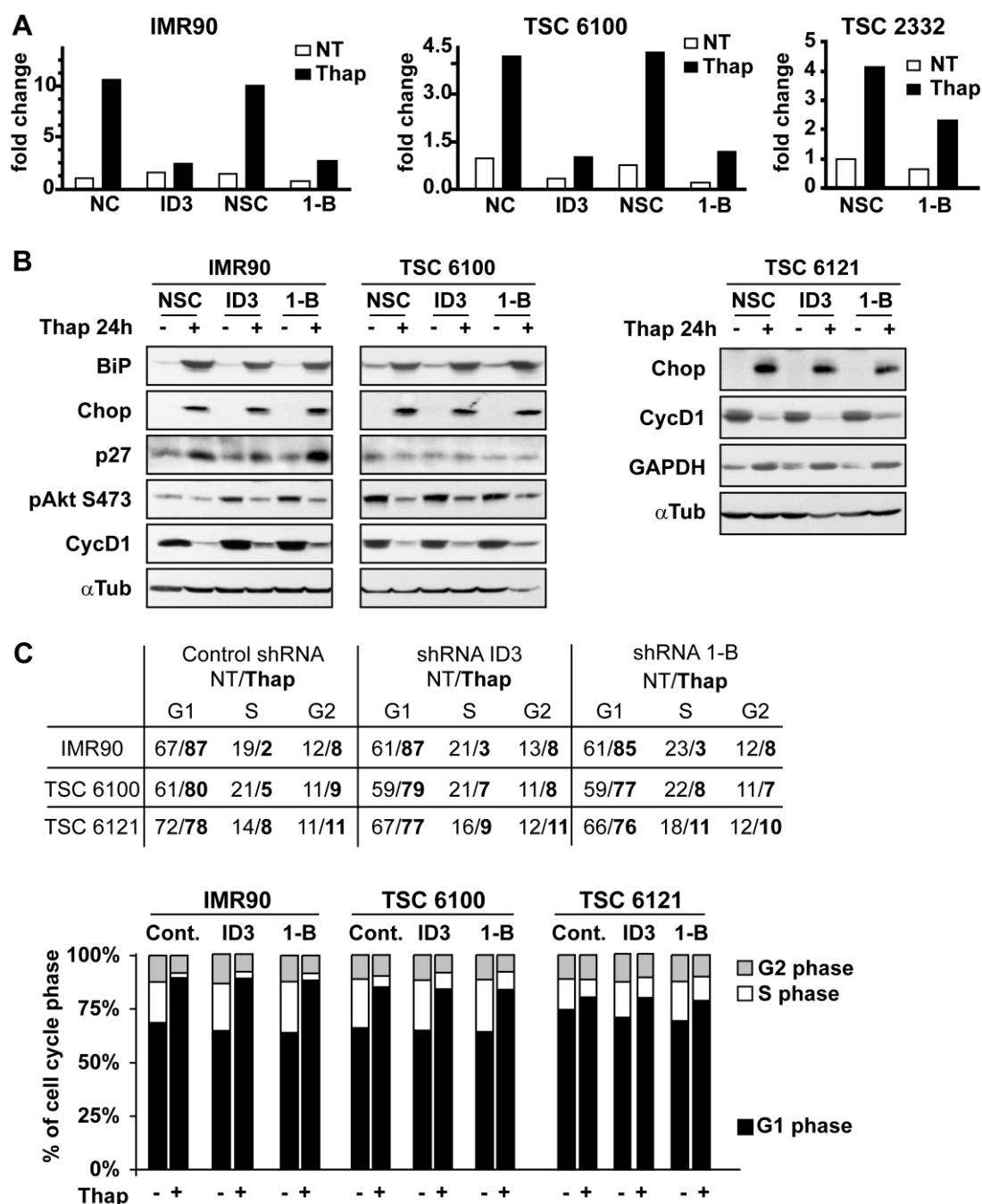
Figure 3-40: Diminished cell cycle inhibitory effects of thapsigargin in CycG2 KD cultures. A) qRT-PCR assay of *CCNG2* expression level in WT and TSC (6100 and 2332) human fibroblasts. Analysis was performed 72 h after transduction with indicated shRNA FIV-viroids and additional 24 h Thap treatment. B) Immunoblot analysis of indicated proteins, after 72 h infection and additional 24 h Thap treatment. C) Cell cycle analysis of indicated cell lines transduced with *CCNG2* (ID3, 1-B) and control (NSC) shRNA expression cassettes for 72 h and an additional 24 h of Thap treatment. *Top)* Table of percentage of cells in different phases of the cell cycle, numbers in bold type indicate values of Thap treated cultures. *Bottom)* Bar graph of cell cycle phase distribution in indicated cell cultures.

Results

Cell cycle analysis of data obtained from a set of similar experiments on FIV transduced cultures in the presence (bold typing) or absence (plain font) of Thap indicated that depletion of CycG2 could modestly blunt the G_1-phase cell cycle arrest response to Thap in some of the tested cell lines, the most potent response was observed in the two TSC cell lines 6100 and 6121 transduced with 1-B constructs (Figure 3-40).

4. Discussion

Cancer is the second most common cause of death (after heart disease) in the US, accounting for one out of four deaths. In women, breast cancer is the most commonly diagnosed cancer type and leads to 29% of all cancer related deaths. Improvement in patient survival is due to advancement in diagnosis and treatment (Siegel et al., 2012). Today's treatment options include surgery, chemotherapy and targeted therapy, all of which are contingent on tumor grade, lymph node status and the expression levels of biomarkers (Howard and Bland, 2012). A low expression of the cell cycle inhibitory protein CycG2 is implicated in poor prognosis and predicts a lower metastasis free survival rate (Adorno et al., 2009). Understanding how CycG2, as a negative regulator of cell cycle progression, contributes to the effects of BC therapeutics may lead to the use of CycG2 expression as a biomarker for therapeutic outcomes and to the development of improved cancer diagnostics and therapies.

4.1 Contribution of CycG2 to DDR Cell Cycle Checkpoint Arrest

DNA double strand break (DSB) inducing chemotherapeutics including topoisomerase II poisons such as doxorubicin (Dox) and etoposite (ETP) are the mainstay of cancer therapy (Jackson and Bartek, 2009; Lord and Ashworth, 2012; Nitiss, 2009). Induction of DSBs activates the DNA damage response (DDR) pathway that mediates the activation of cell cycle checkpoints. Subsequently, induction of cell cycle arrest gives time for DNA repair; if the damage is too severe, apoptosis is induced (Oberle and Blattner, 2010). Cancer cells are very sensitive to DNA damaging agents due to the frequent loss of an efficient G_1/S checkpoint (Kastan et al., 1991; Sherr and McCormick, 2002). A functional G_2/M checkpoint however is usually retained in tumor cells (Kuntz and O'Connell, 2009). Thus a combination of DNA damage induction and simultaneous inhibition of the DNA damage response (DDR) pathway holds promises for the enhancement of current therapeutics (Al-Ejeh et al., 2010).

The observations that CycG2 is upregulated during cell cycle arrest responses to a variety of inhibitory signals (including DNA damage) and induces a G_1-phase cell cycle arrest when ectopically expressed, inspired further study of CycG2's involvement in the DDR (Arachchige Don et al., 2006; Bates et al., 1996; Bennin et

al., 2002; Chen et al., 2006; Horne et al., 1997; Kim et al., 2004; Le et al., 2007; Xu et al., 2008).

In response to DNA DSBs, ATM-dependent T68 phosphorylation of Chk2 triggers a G_1-phase checkpoint arrest (Stracker et al., 2009). Ectopic expression of CycG2 promotes Chk2 dependent G_1-phase cell cycle arrest (Zimmermann et al., 2012, in press) and Chk2 phosphorylation at T68 (Figure 3-2). Previous studies showed that phosphorylation of p53 by activated Chk2 promotes G_1-phase checkpoint arrest (Chehab et al., 2000) indicating that the p53 dependent G_1-phase arrest induced by ectopic CycG2 is likely downstream of T68-activated Chk2. As the CycG2 induced G_1-phase cell cycle arrest did not require ATM function (Figure 3-3), the effects of ectopic CycG2 on Chk2 are likely ATM-independent. Moreover, the phosphorylation of the ATR target Chk1 was not influenced by ectopic CycG2 (Figure 3-2), suggesting that CycG2 overexpression did not activate ATR. A possible explanation for the effects of ectopic CycG2 induced Chk2 phosphorylation in the absence of DNA-damage could be the induction of a defective mitosis. Recent work indicates a DNA-damage independent function of pChk2(T68) during mitosis, to ensure proper spindle assembly and maintain chromosomal stability (Chabalier-Taste et al., 2008; Stolz et al., 2010). The kinases PLK1, TTK/ hMps1 and DNA-PK can each phosphorylate Chk2 on T68 and play DDR-independent roles in regulating mitosis and spindle assembly checkpoints (Chen and Poon, 2008; Lee et al., 2011; Li and Stern, 2005; Tsvetkov et al., 2003; Wei et al., 2005). Ectopic CycG2 expression promotes formation of nocodazole-resistant microtubules and aberrant nuclei (Bennin et al., 2002), therefore, overexpression of CycG2 may trigger a defective mitosis that provokes Chk2 activation through DNA-damage independent pathways. Alternatively, CycG2 may influence PP2A mediated pChk2(T68) dephosphorylation. Phosphorylation of Chk2 on T68 is negatively regulated by B56 isoforms of PP2A (Carlessi et al., 2010; Freeman et al., 2010). As CycG2 can form complexes with PP2A B56- and C-subunits (Bennin et al., 2002; Hofstetter et al., 2012; Rual et al., 2005), it is possible that, in otherwise unperturbed cells, overexpressed CycG2 acts as a PP2A sink preventing Chk2 dephosphorylation by PP2A. In this context it is notable that CycG2, PP2A and Chk2 all associate with centrosomes (Arachchige Don et al., 2006; Bollen et al., 2009; Golan et al., 2010).

Discussion

CCNG2 expression is upregulated as cells undergo cell cycle arrest in response to a variety of growth-inhibitory signals including DNA damage (Bates et al., 1996; Chen et al., 2006; Fang et al., 2007; Gajate et al., 2002; Grolleau et al., 2002; Horne et al., 1997; Le et al., 2007; Martinez-Gac et al., 2004; Murray et al., 2004; Tran et al., 2003; Xu et al., 2008). The increase of endogenous CycG2 expression following the induction of DNA DSB through treatment with Dox and ETP occurs 8 to 12 h before an obvious arrest of cells at the G_2/M boundary (Figure 3-6). This likely reflects that the DDR pathway triggers the upregulation of CycG2 and is not the result of cells accumulation in G_2-phase. The increase in endogenous CycG2 levels followed the activation of ATM signaling by several hours, but coincided with the activation of the late phase DDR protein Chk1 (Figure 3-6), suggesting that CycG2 may play a role in the maintenance of G_2/M checkpoint arrest. Indeed, shRNA mediated CycG2 KD blunts the Dox-induced G_2/M checkpoint arrest (Figure 3-8 and Figure 3-10).

Dox-induced DNA DSBs trigger first the activation of ATM and in the later phase of DNA damage-repair the presence of ssDNA activates ATR (Jackson and Bartek, 2009; Nitiss, 2009). ATR activity is thought to regulate the majority of the late (2-9 h post γ-IR) phase of the checkpoint response to DNA DSBs (Brown and Baltimore, 2003; Shiotani and Zou, 2009a, b). In the absence of ATM both ATR and DNA-PK play dominant roles in promoting G_2/M checkpoint responses to DNA DSBs (Arlander et al., 2008; Tomimatsu et al., 2009). Recently for publication accepted results of Donaldson and Arachchige Don show that Dox-triggered upregulation of CycG2 is neither repressed by the ATM inhibitor KU55933 nor repressed in ATM-deficient fibroblasts, but is blunted by the ATM and ATR inhibitor caffeine (Zimmermann et al., 2012, in press). Thus, DNA DSB-induced stimulation of CycG2 expression is ATM independent. These results, together with the observation that Dox-triggered upregulation of CycG2 is primarily a late phase DDR, suggests that DSB induced CycG2 expression is ATR dependent.

The expression of CycG2's closest homolog CycG1 has been linked to G_2/M checkpoint control, however whether it promotes or inhibits either cell cycle arrest or cell death in response to DNA damage is controversial (Kimura et al., 2001; Kimura and Nojima, 2002; Ohtsuka et al., 2004; Okamoto and Prives, 1999; Seo et al., 2006; Shimizu et al., 1998). CycG1 is a direct transcriptional target of p53, and *CCNG1*

transcript levels are increased in response to DNA damage (Bates et al., 1996; Okamoto and Beach, 1994). Predictably, CycG1 expression was robustly elevated in Dox-treated MCF7 cells and its protein levels were not reduced in CycG2 KD cells (Figure 3-11). The fact that CycG2 depletion leads to a reduced G_2/M-phase arrest despite the rise in CycG1 levels, indicates that CycG1 cannot fully compensate for loss of CycG2 and that these protein homologs are not have redundant function.

Passage from G_2 into M-phase is promoted by activation of CycB1/Cdc2 complexes and their entry into the nucleus. CycB1 protein levels increase as cells enter G_2-phase and decrease as cells proceed through mitosis (Lindqvist et al., 2009). The cell cycle inhibitory kinases Myt1 and Wee1 phosphorylate Cdc2 on T14 and Y15 and thereby restrict CycB1/Cdc2 activity. Dephosphorylation of T14 and Y15 Cdc2 is triggered by Cdc25 phosphatases and leads to the activation of CycB1/Cdc2 complexes (Lindqvist et al., 2009; Stracker et al., 2009). During DDR signaling the dual specificity phosphatases Cdc25B and Cdc25C are themselves subject to inhibitory phosphorylation by Chk1 and Chk2 that promotes Cdc25 degradation (Lindqvist et al., 2009). As predicted, the Dox triggered G_2/M checkpoint arrest led to accumulation of CycB1 and pCdc2(Y15) levels in WT and shRNA control cultures. In addition to their blunted G_2/M checkpoint arrest response (Figure 3-10), CycG2 KD clones also exhibited diminished levels of CycB1 and phospho-inhibited Cdc2 when compared to treated WT and shRNA controls (Figure 3-12). Although Cdc25B expression is not required for G_2/M transition in otherwise unperturbed somatic cell populations, it is essential for resumption of cell cycle progression after DNA damage induced checkpoint arrest (Lindqvist et al., 2009). Even moderately increased Cdc25B expression levels impair proper G_2/M checkpoint control (Aressy et al., 2008; Bansal and Lazo, 2007; Bugler et al., 2006). Compared to mock treated controls, Cdc25B levels are diminished in Dox-treated WT and NSC, but not in CycG2 KD cell cultures (Figure 3-12). These results suggest that the weakened G_2/M checkpoint arrest in CycG2 KD cells is due to a disruption of the regulatory circuit controlling Cdc25B expression. Thus, CycG2 may contribute to G_2/M checkpoint enforcement by limiting the Cdc25B modulated CycB1/Cdc2 activity.

CCNG2 transcripts are upregulated during G_1-phase cell cycle arrest in response to a variety of DDR independent anti-mitogenic signaling cascades (Horne et al.,

1997; Le et al., 2007; Martinez-Gac et al., 2004; Xu et al., 2008). RNAi KD of *CCNG2* has been shown to blunt the G_1-phase arrest response to some of these growth inhibitory signals (Kim et al., 2004; Xu et al., 2008). Given these observations and the effects that ectopic CycG2 expression has on G_1/S phase transition, the diminished G_2/M checkpoint arrest response of CycG2 KD clones to Dox was somewhat surprising. However, other cell cycle regulators have been described (such as p53 and p21) that can influence G_1/S as well as G_2/M checkpoints (Bunz et al., 1998; Cazzalini et al., 2010; Harper et al., 1993; Lee et al., 2009; Waldman et al., 1995). For example, ectopic and endogenous expression of p21 induces G_1-phase checkpoint arrest through binding and inhibition of CDK2 (Lu and Hunter, 2010). Additionally, p21 influences G_2/M transition through binding and inhibition of CycA/Cdc2 and CycB1/Cdc2 complexes (Cazzalini et al., 2010). Although most of the evidence in the literature supports a role for CycG2 in limiting G_1/S-phase transition, there are indications that CycG2 could also participate in G_2/M regulation (Adorno et al., 2009; Shimada et al., 2003; Suenaga et al., 2009; Welcsh et al., 2002). The idea that CycG2 has a regulatory function in G_2/M-phase transition is also supported by the discovery that CycG2 is a substrate of an essential regulator of mitosis, APC, being both ubiquitinated and degraded in mitotic cell extracts enriched with APC-Cdc20 complexes (Merbl and Kirschner, 2009; Mocciaro and Rape, 2012).

4.2 Contribution of CycG2 Expression to Endocrine Therapy Response

Growth of nearly two-thirds of all primary BCs is dependent on estrogen (E2) signaling through ERα (Deroo and Korach, 2006; Fabris et al., 1987). Hence, ER positive BCs are commonly treated with ER antagonists such as the SERM tamoxifen (4OHT) and the SERD fulvestrant (ICI) or aromatase inhibitors (AIs) that prevent E2 production (Di Cosimo and Baselga, 2008). The advantages of these therapeutics are limited by the frequent development of resistance (Lange and Yee, 2011).

Stimulation of E2 dependent BC cell lines with E2 leads to the repression of *CCNG2* expression. CycG2 transcription is negatively regulated by the E2 occupied ER through the recruitment of the N-CoR co-repressor complex and histone deacetylases (HDAC) to *CCNG2* promoter region (Stossi et al., 2006). Consistent

with these findings, results presented in this thesis show CycG2 protein levels are elevated after blockade of E2 signaling through either E2 depletion, or through treatment with ICI and 4OHT. Furthermore, upregulation of CycG2 expression is repressed upon re-stimulation with E2 (Figure 3-14). These results suggest that the growth inhibitory properties of SERMs and SERDs could be mediated, in part, through upregulation of CycG2 expression. In accordance with this idea, MCF7 cells depleted of CycG2 expression via shRNA mediated KD, show, compared to controls, a diminished accumulation of cells in G_1-phase in response to inhibition of E2 signaling (Figure 3-16 and Figure 3-17). These results indicate that elevated CycG2 expression contributes to the treatment induced G_1-phase cell cycle arrest. Additional ICI treatment or E2 depletion experiments showed, that in contrast to MCF7 control cultures, CycG2 KD clones exhibit an increased number of cells with an S-phase content that are actively synthesizing DNA (Figure 3-17 and Figure 3-18). Thus, indicating that upregulation of CycG2 is important to enforce cell cycle arrest responses following inhibition of E2 signaling. Accordingly, loss of CycG2 expression might contribute to the development of tumor cell resistance against therapeutically induced ER inhibition in ER positive BCs. Numerous models of endocrine-resistance show ER-independent stimulation of CycD1 expression through activation of the MAPK pathway downstream of elevated growth factor signaling (Kato, 2001; Lannigan, 2003; Zhang et al., 2002). Active CycD1/CDK complexes phosphorylate Rb, thereby releasing E2F transcription factors that drive the expression of proliferation promoting genes. CycG2 KD clones with diminished arrest responses to E2 signaling inhibition exhibit elevated CycD1 protein levels and increased activation of the components in the MAPK signaling pathway (Figure 3-19, Figure 3-20 and Figure 3-21). These results indicate that the loss of CycG2 expression contributes to the development of tumor cell resistance to inhibition of E2 signaling by increasing MAPK signaling and the subsequent upregulation of CycD1 expression.

A recent report showed that development of resistance of ER positive BC to E2 withdrawal or tamoxifen could be linked to loss of CDK10 expression (Iorns et al., 2008). CDK10 is a CDK homolog and previously shown to play a role in G_2/M transition (Li et al., 1995). CDK10 can bind to and inhibit the activity of Ets2 transcription factors (Kasten and Giordano, 2001). Active Ets2 stimulates Raf1 kinase

expression. Growth factor receptor induction of Ras signaling stimulates Raf1-mediated activation of the MAPK signaling pathway (Iorns et al., 2008; Shaul and Seger, 2007). The resulting increase in CycD1 expression mediates tamoxifen resistance by abolishing the reliance on E2 signaling (Wilcken et al., 1997). Reduced CDK10 expression is associated with reduced time until relapse and poor overall survival (Iorns et al., 2008). Although CDK10 shares the conserved protein sequence, common to other CDKs, which is essential for cyclin binding (Brambilla and Draetta, 1994), its corresponding cyclin has not been identified to date. Ectopic and endogenous CycG2 can form complexes with CDK10 that co-localize in a distinct pattern in the nucleus and cytosol (Figure 3-22, Figure 3-23 and Figure 3-24). Binding of CDK10 to CycG2 seems to be mediated not only through the cyclin box within the CycG2 N-terminus, but also through CycG2's C-term. Additionally, co-IP of endogenous proteins is enhanced after the inhibition of E2-mediated ER signaling and subsequent upregulation of CycG2 (Figure 3-23). Given that both CycG2 KD and CDK10 KD lead to increased MAPK activation, CycG2 effects on cell cycle arrest response toward ER inhibition might be mediated through binding and activation of CDK10. However, it is not clear if CycG2/CDK10 complexes are catalytically active and if kinase activity is necessary for its function. CDK10 mediated inhibition of Ets2 transactivation seems to be independent of CDK10's kinase activity (Kasten and Giordano, 2001). Kinase dead CDK10 is able to suppress Ets2 transactivation, perhaps through blockage of Ets2's association with the basal transcription machinery or other co-activators. In addition, Ets2 activity is positively regulated via phosphorylation (Yang et al., 1996). It is known that CycG2 can form phosphatase active complexes with PP2A (Bennin et al., 2002). Therefore, CycG2/PP2A complexes could, through binding to CDK10, inactivate Ets2 by dephosphorylation.

4.3 Regulation of CycG2 Expression Following mTOR Inhibition

It is believed that ER positive BC tumors develop resistance to ER targeted therapy as a consequence of increased signaling through one or more of the transmembrane growth factor receptors HER2, EGFR and IGFR (Massarweh et al., 2008). Growth factor mediated activation of EGFR, IGFR and HER2 triggers the activation of two key proliferation-promoting pathways, the MAPK and PI3K/mTOR

pathways (Becker et al., 2011; Lange and Yee, 2011; Massarweh et al., 2008; Miller et al., 2011a; Zhang et al., 2011). Increased activation of PI3K signaling is linked to oncogenesis and resistance to cancer therapy (Ogita and Lorusso, 2011). Therapeutics inhibiting the downstream kinase mTOR have been successfully used to treat a subset of cancers, including lymphoma and BC and improved inhibitors are in the stages of clinical development (Baselga et al., 2009; Witzig et al., 2011). CycG2 expression in BC tumor cells is not only inhibited by E2 signaling, but is also negatively regulated by HER2/PI3K/Akt/mTOR pathway (Le et al., 2007; Stossi et al., 2006). Importantly, treatment of BC cell lines with rapamycin (Rapa) is known to upregulate *CCNG2* mRNA expression (Kasukabe et al., 2008; Le et al., 2007). In agreement with these earlier findings, treatment of both MCF7 BC cells and diffuse large B-cell lymphoma cell lines (SU-DHL 4, 8 and 16) induces a potent G_1-phase arrest and upregulation of CycG2 protein expression (Figure 3-25 and Figure 3-26). Moreover recent studies indicate that *CCNG2* transcripts are downregulated following stimulation of IGFR signaling in BC cells (Casa et al., 2011). Thus elevation of HER2 and IGFR signaling through PI3K/Akt/mTOR would be predicted to limit CycG2 associated cell cycle inhibitory activity that restricts tumor growth.

Interestingly, use of the widely prescribed anti-diabetic drug metformin (Met) has recently been linked to reduce cancer incidence in treated patients (Evans et al., 2005). Treatment of BC cells with Met activates the AMP activated protein kinase (AMPK) that negatively regulates mTOR activity via activation of TSC2 and induction of G_1/G_0-phase cell cycle arrest (Ben Sahra et al., 2010). In agreement with this, treatment of the BC cell line MCF7 with Met induces G_1-phase cell cycle arrest characterized through a reduction in DNA synthesis and reduced CycD1 protein levels (Figure 3-27 and Figure 3-28). Simultaneously, CycG2 protein levels are increased in MCF7 cultures and in the normal breast cell line MCF10a treated with Met (Figure 3-28). Blockade of CycG2 induction via shRNA mediated KD results in increased expression of CycD1 protein and in a decreased G_1-phase arrest (Figure 3-28 and Figure 3-29). This indicates CycG2 KD blocks Met induced CycD1 downregulation and thereby promotes cell cycle progression. By extension, these results suggest that CycG2 expression likely contributes to Met-induced cell cycle arrest through signaling pathways that restrict CycD1 expression. It is notable that KD

of CycG2 relieves the repression of both CycD1 expression and cell cycle progression that is imposed by ER antagonists and mTOR inhibitor Met. Co-inhibition of multiple signaling pathways such ER and mTOR signaling has been proposed as an effective treatment regimen for endocrine resistant BCs. Results presented in this work, demonstrate that the elevation of CycG2 levels contributes to the cell cycle inhibitory effects of the discussed BC therapeutics and that its expression could be an important prognostic indicator for treatment choice and outcome.

4.4 Potential Contribution of CycG2 to Growth Control in TSC

Tumor growth in TSC patients is promoted by mutational inactivation of either of the mTOR regulatory proteins, TSC1 or TSC2. Loss or inhibition of TSC1 or 2 leads to mTOR hyperactivation (Crino et al., 2006; Orlova and Crino, 2011). Cell growth in these tumors is thought to be limited by an mTOR-dependent negative feedback mechanism, that inhibits Akt signaling through blockade of the insulin receptor substrate (IRS) signaling downstream of growth factor receptors (Harvey et al., 2008; Zoncu et al., 2011). The inhibition of mTOR activity by Rapa and its derivatives has been proposed as a therapeutic option for TSC patients (Bissler et al., 2008; Ozcan et al., 2008). As noted above, CycG2 expression is upregulated in human BC cell lines in response to Rapa treatment (Kasukabe et al., 2008; Le et al., 2007). The function of CycG2 in growth control in TSC and its contribution to the cell cycle inhibitory effects of Rapa, however, are not clear.

Consistent with previous work (Kasukabe et al., 2008; Le et al., 2007), mTOR inhibition via Rapa treatment robustly increased CycG2 expression levels in both normal (IMR90, GM00637) and TSC-deficient (6100, 6121, 2332) primary human fibroblasts (Figure 3-33). Given that basal *CCNG2* mRNA of non-treated TSC 6100 and 2332 cells were higher (Figure 3-31) it is not surprising that the Rapa-induced upregulation of *CCNG2* transcript levels was greatest in IMR90 and TSC 6121 cultures that showed lower basal *CCNG2* mRNA level. The expression of the FOXO target, p27, appears to be lower in TSC cell lines and Rapa treatment only leads to a modest increase, whereas CycD1 level are elevated in TSC cell lines and strongly reduced following Rapa treatment (Figure 3-33). Importantly, Rapa-induced upregulation of CycG2 in WT cells appeared to be independent of FOXO TF

activation as the increase was concurrent with increase in phospho-activated forms of Akt and phospho-inhibited forms of FOXO1 and FOXO3a (Figure 3-33). The results suggest that long-term Rapa mediated inhibition of mTOR in human fibroblasts abolishes the TORC1 driven negative feedback loop to inhibit Akt activity. Sustained Akt activation then leads to the inhibition of FOXO TFs (Hay, 2011; Huang and Manning, 2009). However, the basal levels of phospho-inhibited FOXO3a/FOXO1 in the TSC deficient cell lines appeared to be lower than in the WT cells, consistent with the idea that, chronic activation of mTORC1 in TSC deficient cells constitutively inhibits Akt signaling and in turn increases FOXO TF transcriptional activity (Harvey et al., 2008; Huang and Manning, 2009). Comparison of Rapa-induced modulation of gene expression shows that CycG2 mRNAs were more potently upregulated compared to *CCNG1* and CKI p27, but similar to the pro-apoptotic FOXO target Bim (Figure 3-34). This suggests that, a FOXO-independent mechanism induces growth inhibition and the upregulation of both, CycG2 and Bim.

The Rapa induced CycG2 upregulation coincides with a G_1-phase cell cycle arrest (Figure 3-32) that was diminished after CycG2 KD in two TSC and in the WT control cell lines (Figure 3-36). Similar experiments show that CycD1 protein levels decrease with Rapa treatment but stayed elevated in CycG2 KD cultures (Figure 3-36). This indicates that loss of CycG2 expression promotes upregulation of CycD1 and thus cell cycle progression. CycG2 expression may contribute to the cell cycle inhibitory response of both WT and TSC cells to mTOR inhibition. Even in the untreated cell populations, expression of the *CCNG2*-targeting shRNAs seemed to reduce the percentage of cells with a G_1-phase DNA content relative to shRNA control cells, consistent with the idea that CycG2 expression delays progression of cells from G_1- into S-phase.

Loss of TSC function results in the induction of endoplasmic reticulum stress (ERS) and activates the unfolded protein response in TSC tumors (Ozcan et al., 2008). To determine whether CycG2 upregulation during ERS modulates cell proliferation, the same molecular and cellular biology methods as for Rapa treatment were used. Induction of ERS response by thapsigargin (Thap) treatment robustly increased both CycG2 mRNA and protein expression in the tested cell lines (Figure 3-38), with the most robust increase seen for treated IMR90 and TSC 6121 fibroblasts, the cell lines

that showed the lowest basal *CCNG2* transcription level (Figure 3-31). CycG2 upregulation by Thap treatment correlated with the induced G_1-phase cell cycle arrest (Figure 3-37). Notably, in contrast to what was seen in fibroblasts treated with Rapa, expression of the phosphorylated forms of FOXO1 and FOXO3a were repressed upon treatment with Thap (Figure 3-38), suggesting that the more dramatic upregulation of CycG2 expression under these ERS-inducing conditions could occur through increased FOXO1/3a transcriptional activation of *CCNG2*. Comparison of Thap-induced modulation of gene expression indicates that CycG2 mRNAs were more potently upregulated than p27 and but similar to the robust increase in Bim mRNA levels. As expected, Thap also substantially increased the transcription of the ERS responsive TF, C/EBP homologous protein (Chop) (Figure 3-39). The expression of CycG1 was again only modestly influenced by ERS induction. This would indicate that CycG2 plays a more central role in regulating cell cycle responses to mTOR inhibition and ERS than either its closest homolog CycG1, or the FOXO TF target protein and CDK inhibitor p27.

To assess the contribution of CycG2 upregulation to the cell cycle inhibitory effects of Thap-induced ERS, CycG2 was depleted in WT and TSC cell lines (Figure 3-35). Immunoblot analysis showed that CycG2 KD had did not blunt Thap-induced upregulation of either Chop or BIP (Figure 3-40). Robust upregulation of p27 protein level was only observed in Thap-treated IMR90 cells (Figure 3-40), and was largely maintained in both CycG2 KD and control cell cultures. This suggests that the Thap-mediated cell cycle arrest in the TSC lines does not require increased expression of p27. It is notable that expression of the phospho-activated forms of Akt (which act to repress FOXO activity) was strongly repressed in all Thap-treated cultures, irrespective of the transduced shRNA expression vector. The data indicated that the increase in CycG2 expression following Rapa-mediated inhibition of mTOR is not FOXO-dependent; whereas, Thap induced ERS appears to reduce active forms of Akt and disinhibition of FOXO TFs. The potent upregulation of CycG2 during Thap stimulation could therefore occur through direct FOXO mediated transcriptional activation of *CCNG2*. Importantly, as seen with CycG2 KD cells treated with ER antagonists and mTOR inhibitors, CycD1 levels increased in Thap-treated cultures expressing the *CCNG2*-targeting shRNAs (Figure 3-40), suggesting that loss of

CycG2 expression promotes upregulation of CycD1 and thus cell cycle progression. Indeed, cell cycle analysis of Thap-treated cultures indicated that CycG2 KD can at least modestly blunt the G_1-phase cell cycle arrest response (Figure 3-40). The data suggest that one mechanism by which CycG2 upregulation might inhibit cell cycle progression is through the reduction of CycD1 expression levels.

These results point to a role for CycG2 in mTOR inhibitor and ERS mediated repression of fibroblast proliferation. Together with the findings outlined in 3.3 and 4.3, these results suggest that CycG2 is a Rapa and Met stimulated ERS response protein that restricts cell cycle progression and could play a role in limiting tumor growth in TSC.

4.5 Future Directions

The results presented in this work show that DNA DSB induced CycG2 expression is not ATM dependent, but suggests the involvement of ATR. Additional information regarding the upstream regulators of CycG2 expression in the DDR may be informative. Through the utilization of specific ATR and DNA-PK inhibitors as well as ATR/DNA-PK siRNA or KO cell lines, the DDR kinase pathway could be further delineated. Also an open question is the precise mechanism by which CycG2 could repress the Cdc25B/Cdc2/CycB1 pathway during DDR to DSBs. Cdc25B is known to be regulated at the transcriptional level and via phosphorylation mediated degradation through the proteasome pathway. Further dissecting the mechanism of CycG2 in these processes would be useful in understanding the involvement of CycG2 in cell cycle control.

Distinct from the DNA damage checkpoint function of CycG2 is its role in restricting the G_1/S transition in response to the inhibition of E2 signaling. We hypothesize that CycG2 acts as a positive regulator of associated CDK10 activity and that loss of CycG2 results in the enhanced ability of Ets2 to promote *RAF1* expression. However, it is yet unclear if CycG2/CDK10 complexes contain kinase activity. Analysis of how CycG2 binding to CDK10 influences its inhibitory properties toward Ets2 would be required to better define the relationship between these two regulators of E2-dependent growth. Site directed mutagenesis of residues in CycG2 that are implicated in cyclin/CDK binding would give further insight into the

binding characteristics of CycG2 to CDK10. Furthermore, the expression of siRNA-resistant CycG2 point mutants, deficient in PP2A or CDK-binding, in CycG2 KD cell lines would be helpful to elucidate the mechanisms behind CycG2-mediated cell cycle inhibitory effects. Analysis of mutant CycG2 properties on associated phosphatase and kinase activity, as well as cell cycle progression would provide a better understanding in the mechanism behind CycG2 actions.

To further confirm the preliminary results of CycG2's involvement in the cell cycle restriction of primary human fibroblasts responding to Rapa and ERS, additional repeat experiments are necessary. Given that the TSC cell lines expressed different levels of basal CycG2 and varied in the degree of their responses to *CCNG2* KD, additional experiments would be particularly informative. The variations exhibited by the different TSC fibroblast lines may originate from their diverse genetic background that is not well characterized. To circumvent this problem TSC2 negative MEFs, isolated from knockout mice, could be obtained to further analyze the role of CycG2 in cell cycle restriction in TSC. As an alternative, laboratory cell lines with a well-characterized genetic background could be utilized through RNAi-mediated stable suppression of TSC expression.

The generation of CycG2 KO mice would provide central information about CycG2 functions in organismal development, cell differentiation and cancer formation.

5. Summary

Cancers develop as the result of uncontrolled proliferation, growth and metastasis of aberrantly differentiated cells. CycG2 is an unconventional cyclin homolog linked to inhibition of cellular proliferation and promotion of cell differentiation. Expression of the CycG2 gene, *CCNG2*, is repressed in variety of human cancers. Reduced *CCNG2* transcript levels are found in more aggressive, poor-prognosis breast cancer (BC) subtypes, compared to normally differentiated breast tissues, and are elevated in tumor cells responding to cancer therapies. This thesis addresses the question of CycG2's contribution to the cell cycle inhibitory responses of tumor cells to chemotherapeutics and growth inhibitory drugs; namely, DNA damaging topoisomerase II poisons, estrogen signaling inhibitors, mTOR signaling inhibitors and drugs that induce endoplasmic reticulum stress (ERS).

Evaluation of previous findings suggested that CycG2 could be a DNA damage response (DDR) protein that participates in DNA damage checkpoint regulation. This thesis further defines the involvement of CycG2 in the DDR signaling pathway. Ectopic expression of CycG2 promotes phosphorylation of the DDR checkpoint kinase Chk2 on an activational target site. Furthermore, induction of DNA double strand breaks (DSBs) through treatment with the chemotherapeutic doxorubicin (Dox) induces CycG2 expression that correlates with the induced cell cycle arrest and the activation of DDR proteins. Transient and stable shRNA mediated knockdown (KD) of CycG2 attenuates the G_2/M checkpoint arrest response of multiple cell lines caused by the Dox-induced DNA damage. Furthermore, KD of CycG2 blunts the DDR-triggered reduction in Cdc25B levels, inhibitory-phosphorylation of Cdc2 and accumulation of CycB1, which are important processes for a potent G_2/M checkpoint arrest. Thus, CycG2 may participate in the enforcement and maintenance of G_2/M checkpoints by limiting the Cdc25B-mediated promotion of CycB1/Cdc2 activity.

The role CycG2 plays in the anti-proliferative responses of BC cells to estrogen (E2)-signaling deprivation was analyzed in a second study. CycG2 expression is elevated in E2-deprived cells, but reduced in E2-stimulated cells. CycG2 KD diminishes the cell cycle arrest response following inhibition of E2 signaling. In addition, these clones showed elevated levels of the growth promoting cyclin, CycD1,

and elevated activation of the growth factor signaling cascade, mitogen activated protein kinase (MAPK), pathway. These results indicate that loss of CycG2 expression may promote the development of BC tumor cell resistance to E2 antagonizing therapeutics by stimulating the activation of the MAPK pathway. Importantly, results presented here show that CycG2 can associate with the cyclin dependent kinase (CDK) 10, which was recently implicated as an upstream repressor of MAPK signaling. Thus suggesting that the resistance of BC cells to the inhibition of E2 signaling that is acquired following CycG2 KD could result from loss of CycG2-mediated stimulation of CDK10 activity.

CycG2 expression is upregulated following inhibition of the growth promoting kinase mTOR and the induction of ERS. KD of CycG2 expression in multiple cell lines induces CycD1 expression and attenuates cell cycle arrest responses to treatments with rapamycin, metformin and thapsigargin. These results suggest that CycG2 expression restricts proliferation of cells responding to mTOR inhibition (rapamycin and metformin) and ERS-induction (thapsigargin). The data further indicate that rapamycin-induced CycG2 expression is not dependent on FOXO TF expression. In contrast, the potent upregulation of CycG2 expression triggered by thapsigargin is likely the consequence of the FOXO TF activity at the *CCNG2* promoter.

6. Zusammenfassung

Die Entwicklung von Krebs ist die Folge von unkontrollierter Zellproliferation, Zellwachstum und Bildung von Metastasen aus abnormal differenzierten Zellen. Das unkonventionelle Cyclin, CycG2, ist wichtig für Zellzykluskontrolle und Förderung von Zelldifferenzierung. Die Expression des Gens für CycG2, *CCNG2*, ist in vielen Krebsarten vermindert. Die Expression von *CCNG2* ist erhöht in chemotherapeutisch behandeltem Brustkrebs (BC), ebenso wie in normalen Brustgewebe. Eine geringe Expression von *CCNG2* wird unter anderem mit einem aggressivem Krankheitsverlauf und schlechteren Heilungschancen assoziiert. Im Rahmen dieser Arbeit wurde die Rolle von CycG2 im durch Chemotherapeutika und wachstumsinhibierende Medikamente ausgelösten Zellzyklusarrest untersucht. Genauer gesagt wurde der Einfluss von CycG2 auf Behandlung mit DNA schädigenden Topoisomerase II Giften, Inhibitoren von wachstumsstimulierendem Östrogen und mTOR Signalvermittlungswegen sowie Medikamenten die Stress des Endoplasmatischen Retikulums (ERS) auslösen, untersucht.

Es wurde gezeigt, dass die Expression von *CCNG2* durch die von DNA Schäden ausgelöste Zellantwort (DDR) induziert wird und wichtig ist für die Regulation von Zellzyklus-checkpoints. Diese Arbeit untersucht die genaue Funktion von CycG2 in der Regulation des DDR Signalweges. Gezielte Überexprimierung von CycG2 führt zu einer Aktivierung von verschieden Komponenten des DDR Signalweges und einem Zellzyklusarrest in der G_1-Phase. Die Behandlung von Zellen mit dem Chemoterapeutikum Doxorubicin (Dox) induziert DNA Doppelstrangbrüche (DSB) und einen Zellzyklusarrest in der G_2-Phase. Damit einher geht ein Anstieg der CycG2 Expression und die Aktivierung des DDR Signalweges. Der zeitliche Ablaufs dieser Vorgänge lässt darauf schließen, dass die Expression von CycG2 in der späten Phase des DDR Signalweges induziert wird. Zudem vermindert ein transienter und stabiler knockdown (KD) von CycG2 den Dox-induzierten G_2/M Checkpointarrest in verschiedenen Zelllinien. Die Ergebnisse verdeutlichen, dass die Expression von CycG2 notwendig ist für die Durchsetzung des DDR induzierten Zellzyklusarrest.

Des Weiteren wurde im Rahmen dieser Arbeit, die Rolle von CycG2 mit Hilfe stabiler CycG2 KD Zelllinien in der endokrinen Brustkrebstherapie untersucht.

Zusammenfassung

Behandlung von BC mit Inhibitoren des Östrogensignalweges führt zu einer Erhöhung der Expression von CycG2 und einem Zellzyklusarrest in der G_1-Phase. Die CycG2 KD Zelllininen zeigen im Vergleich zu normalen Brustkrebszellen nach der Inhibierung des Östrogensignalweges eine verminderte Arrestreaktion und einen erhöhten Expressionslevel des proliferationsstimulierenden Proteins CycD1. Außerdem wurde gezeigt, dass die Aktivität des wachstumsstimulierenden mitogen-activated protein kinase (MAPK) Signalweges in den CycG2 KD Zelllinien erhöht ist. Eine unkontrollierte Aktivierung des MAPK Signalweges steht in Verbindung mit der Entwicklung von Resistenz des BC Tumors gegen Östrogenrezeptor-antagonisten. Zusätzlich wurde mit CDK10 ein neuer Bindungspartener für CycG2 identifiziert. Der Verlust von CDK10 Expression steht in Verbindung mit einer erhöhten Aktivität des MAPK Signalweges. Diese Ergebnisse lassen darauf schließen, dass die Entwicklung von Resistenzen gegen die Inhibierung des Östrogensignalweges in BC Tumoren durch den Verlust von CycG2 Expression gefördert wird, wahrscheinlich durch den Verlust der CycG2 vermittelten CDK10 Aktivität.

In einem weiteren Projekt wurde die Funktion von CycG2 in der Hemmung des Zellzykluses in Folge der Behandlung mit mTOR Inhibitoren (Rapamycin und Metformin) und ERS Auslösern (Thapsigargin) untersucht. Es wurde gezeigt dass die Zellzyklusarrestreaktionen nach der Behandlung mit Rapamycin, Metformin und Thapsigargin in CycG2 KD Zelllinen reduziert sind und sich gleichzeitig die Expression des proliferationsstimulierenden CycD1 erhöht. Diese Ergebnisse zeigen, dass die Expression von CycG2 die Zellproliferation begrenzt und in Folge Zielgerichteter Therapieformen das Tumorwachstum von mehreren Zellarten limitiert.

7. Bibliography

Abe, M.K., Saelzler, M.P., Espinosa, R., 3rd, Kahle, K.T., Hershenson, M.B., Le Beau, M.M., and Rosner, M.R. (2002). ERK8, a new member of the mitogen-activated protein kinase family. J Biol Chem *277*, 16733-16743.

Abraham, D., Podar, K., Pacher, M., Kubicek, M., Welzel, N., Hemmings, B.A., Dilworth, S.M., Mischak, H., Kolch, W., and Baccarini, M. (2000). Raf-1-associated protein phosphatase 2A as a positive regulator of kinase activation. J Biol Chem *275*, 22300-22304.

Adorno, M., Cordenonsi, M., Montagner, M., Dupont, S., Wong, C., Hann, B., Solari, A., Bobisse, S., Rondina, M.B., Guzzardo, V.*, et al.* (2009). A Mutant-p53/Smad complex opposes p63 to empower TGFbeta-induced metastasis. Cell *137*, 87-98.

Ahmed, S., Al-Saigh, S., and Matthews, J. (2012). FOXA1 Is Essential for Aryl Hydrocarbon Receptor-Dependent Regulation of Cyclin G2. Mol Cancer Res *10*, 636-648.

Akli, S., Zheng, P.J., Multani, A.S., Wingate, H.F., Pathak, S., Zhang, N., Tucker, S.L., Chang, S., and Keyomarsi, K. (2004). Tumor-specific low molecular weight forms of cyclin E induce genomic instability and resistance to p21, p27, and antiestrogens in breast cancer. Cancer Res *64*, 3198-3208.

Al-Ejeh, F., Kumar, R., Wiegmans, A., Lakhani, S.R., Brown, M.P., and Khanna, K.K. (2010). Harnessing the complexity of DNA-damage response pathways to improve cancer treatment outcomes. Oncogene *29*, 6085-6098.

Alessi, D.R., Gomez, N., Moorhead, G., Lewis, T., Keyse, S.M., and Cohen, P. (1995). Inactivation of p42 MAP kinase by protein phosphatase 2A and a protein tyrosine phosphatase, but not CL100, in various cell lines. Curr Biol *5*, 283-295.

Alizart, M., Saunus, J., Cummings, M., and Lakhani, S.R. (2012). Molecular classification of breast carcinoma. *18*, 97-103.

Andjelkovic, M., Jakubowicz, T., Cron, P., Ming, X.F., Han, J.W., and Hemmings, B.A. (1996). Activation and phosphorylation of a pleckstrin homology domain containing protein kinase (RAC-PK/PKB) promoted by serum and protein phosphatase inhibitors. Proc Natl Acad Sci U S A *93*, 5699-5704.

Arachchige Don, A.S., Dallapiazza, R.F., Bennin, D.A., Brake, T., Cowan, C.E., and Horne, M.C. (2006). Cyclin G2 is a centrosome-associated nucleocytoplasmic shuttling protein that influences microtubule stability and induces a p53-dependent cell cycle arrest. Exp Cell Res *312*, 4181-4204.

Bibliography

Aressy, B., Bugler, B., Valette, A., Biard, D., and Ducommun, B. (2008). Moderate variations in CDC25B protein levels modulate the response to DNA damaging agents. Cell Cycle *7*, 2234-2240.

Arlander, S.J., Greene, B.T., Innes, C.L., and Paules, R.S. (2008). DNA protein kinase-dependent G2 checkpoint revealed following knockdown of ataxia-telangiectasia mutated in human mammary epithelial cells. Cancer Res *68*, 89-97.

Arpino, G., Wiechmann, L., Osborne, C.K., and Schiff, R. (2008). Crosstalk between the estrogen receptor and the HER tyrosine kinase receptor family: molecular mechanism and clinical implications for endocrine therapy resistance. Endocr Rev *29*, 217-233.

Bae, I., Fan, S., Meng, Q., Rih, J.K., Kim, H.J., Kang, H.J., Xu, J., Goldberg, I.D., Jaiswal, A.K., and Rosen, E.M. (2004). BRCA1 induces antioxidant gene expression and resistance to oxidative stress. Cancer Res *64*, 7893-7909.

Bai, X., Ma, D., Liu, A., Shen, X., Wang, Q.J., Liu, Y., and Jiang, Y. (2007). Rheb activates mTOR by antagonizing its endogenous inhibitor, FKBP38. Science *318*, 977-980.

Bansal, P., and Lazo, J.S. (2007). Induction of Cdc25B regulates cell cycle resumption after genotoxic stress. Cancer Res *67*, 3356-3363.

Bartek, J., Lukas, C., and Lukas, J. (2004). Checking on DNA damage in S phase. Nat Rev Mol Cell Biol *5*, 792-804.

Baselga, J., Semiglazov, V., van Dam, P., Manikhas, A., Bellet, M., Mayordomo, J., Campone, M., Kubista, E., Greil, R., Bianchi, G.*, et al.* (2009). Phase II randomized study of neoadjuvant everolimus plus letrozole compared with placebo plus letrozole in patients with estrogen receptor-positive breast cancer. J Clin Oncol *27*, 2630-2637.

Bates, S., Rowan, S., and Vousden, K.H. (1996). Characterization of human cyclin G1 and G2: DNA damage inducible genes. Oncogene *13*, 1103-1109.

Becker, M.A., Ibrahim, Y.H., Cui, X., Lee, A.V., and Yee, D. (2011). The IGF pathway regulates ERalpha through a S6K1-dependent mechanism in breast cancer cells. Mol Endocrinol *25*, 516-528.

Ben Sahra, I., Le Marchand-Brustel, Y., Tanti, J.F., and Bost, F. (2010). Metformin in cancer therapy: a new perspective for an old antidiabetic drug? Mol Cancer Ther *9*, 1092-1099.

Bennin, D.A., Don, A.S., Brake, T., McKenzie, J.L., Rosenbaum, H., Ortiz, L., DePaoli-Roach, A.A., and Horne, M.C. (2002). Cyclin G2 associates with protein

phosphatase 2A catalytic and regulatory B' subunits in active complexes and induces nuclear aberrations and a G1/S phase cell cycle arrest. J Biol Chem *277*, 27449-27467.

Beroukhim, R., Mermel, C.H., Porter, D., Wei, G., Raychaudhuri, S., Donovan, J., Barretina, J., Boehm, J.S., Dobson, J., Urashima, M.*, et al.* (2010). The landscape of somatic copy-number alteration across human cancers. Nature *463*, 899-905.

Bissler, J.J., McCormack, F.X., Young, L.R., Elwing, J.M., Chuck, G., Leonard, J.M., Schmithorst, V.J., Laor, T., Brody, A.S., Bean, J.*, et al.* (2008). Sirolimus for angiomyolipoma in tuberous sclerosis complex or lymphangioleiomyomatosis. N Engl J Med *358*, 140-151.

Bohgaki, T., Bohgaki, M., and Hakem, R. (2010). DNA double-strand break signaling and human disorders. Genome Integr *1*, 15.

Bollen, M., Gerlich, D.W., and Lesage, B. (2009). Mitotic phosphatases: from entry guards to exit guides. Trends Cell Biol *19*, 531-541.

Brognard, J., Sierecki, E., Gao, T., and Newton, A.C. (2007). PHLPP and a second isoform, PHLPP2, differentially attenuate the amplitude of Akt signaling by regulating distinct Akt isoforms. Mol Cell *25*, 917-931.

Brown, E.J., and Baltimore, D. (2003). Essential and dispensable roles of ATR in cell cycle arrest and genome maintenance. Genes Dev *17*, 615-628.

Brunet, A., Bonni, A., Zigmond, M.J., Lin, M.Z., Juo, P., Hu, L.S., Anderson, M.J., Arden, K.C., Blenis, J., and Greenberg, M.E. (1999). Akt promotes cell survival by phosphorylating and inhibiting a Forkhead transcription factor. Cell *96*, 857-868.

Bugler, B., Quaranta, M., Aressy, B., Brezak, M.C., Prevost, G., and Ducommun, B. (2006). Genotoxic-activated G2-M checkpoint exit is dependent on CDC25B phosphatase expression. Mol Cancer Ther *5*, 1446-1451.

Bunz, F., Dutriaux, A., Lengauer, C., Waldman, T., Zhou, S., Brown, J.P., Sedivy, J.M., Kinzler, K.W., and Vogelstein, B. (1998). Requirement for p53 and p21 to sustain G2 arrest after DNA damage. Science *282*, 1497-1501.

Calleja, V., Alcor, D., Laguerre, M., Park, J., Vojnovic, B., Hemmings, B.A., Downward, J., Parker, P.J., and Larijani, B. (2007). Intramolecular and intermolecular interactions of protein kinase B define its activation in vivo. PLoS Biol *5*, e95.

Carlessi, L., Buscemi, G., Fontanella, E., and Delia, D. A protein phosphatase feedback mechanism regulates the basal phosphorylation of Chk2 kinase in the absence of DNA damage. Biochim Biophys Acta *1803*, 1213-1223.

Bibliography

Carlessi, L., Buscemi, G., Fontanella, E., and Delia, D. (2010). A protein phosphatase feedback mechanism regulates the basal phosphorylation of Chk2 kinase in the absence of DNA damage. Biochim Biophys Acta *1803*, 1213-1223.

Casa, A.J., Potter, A.S., Malik, S., Lazard, Z., Kuiatse, I., Kim, H.T., Tsimelzon, A., Creighton, C.J., Hilsenbeck, S.G., Brown, P.H.*, et al.* (2011). Estrogen and insulin-like growth factor-I (IGF-I) independently down-regulate critical repressors of breast cancer growth. Breast Cancer Res Treat.

Castro, D.S., Martynoga, B., Parras, C., Ramesh, V., Pacary, E., Johnston, C., Drechsel, D., Lebel-Potter, M., Garcia, L.G., Hunt, C.*, et al.* (2011). A novel function of the proneural factor Ascl1 in progenitor proliferation identified by genome-wide characterization of its targets. Genes Dev *25*, 930-945.

Cazzalini, O., Scovassi, A.I., Savio, M., Stivala, L.A., and Prosperi, E. (2010). Multiple roles of the cell cycle inhibitor p21(CDKN1A) in the DNA damage response. Mutat Res *704*, 12-20.

Cellai, C., Balliu, M., Laurenzana, A., Guandalini, L., Matucci, R., Miniati, D., Torre, E., Nebbioso, A., Carafa, V., Altucci, L.*, et al.* (2011). The new low-toxic histone deacetylase inhibitor S-(2) induces apoptosis in various acute myeloid leukemia cells. J Cell Mol Med.

Chabalier-Taste, C., Racca, C., Dozier, C., and Larminat, F. (2008). BRCA1 is regulated by Chk2 in response to spindle damage. Biochim Biophys Acta *1783*, 2223-2233.

Chau, V., Tobias, J.W., Bachmair, A., Marriott, D., Ecker, D.J., Gonda, D.K., and Varshavsky, A. (1989). A multiubiquitin chain is confined to specific lysine in a targeted short-lived protein. Science *243*, 1576-1583.

Chehab, N.H., Malikzay, A., Appel, M., and Halazonetis, T.D. (2000). Chk2/hCds1 functions as a DNA damage checkpoint in G(1) by stabilizing p53. Genes Dev *14*, 278-288.

Chen, J., Yusuf, I., Andersen, H.M., and Fruman, D.A. (2006). FOXO transcription factors cooperate with delta EF1 to activate growth suppressive genes in B lymphocytes. J Immunol *176*, 2711-2721.

Chen, Y., and Poon, R.Y. (2008). The multiple checkpoint functions of CHK1 and CHK2 in maintenance of genome stability. Front Biosci *13*, 5016-5029.

Chowdhury, D., Keogh, M.C., Ishii, H., Peterson, C.L., Buratowski, S., and Lieberman, J. (2005). gamma-H2AX dephosphorylation by protein phosphatase 2A facilitates DNA double-strand break repair. Mol Cell *20*, 801-809.

Bibliography

Chu, I.M., Hengst, L., and Slingerland, J.M. (2008). The Cdk inhibitor p27 in human cancer: prognostic potential and relevance to anticancer therapy. Nat Rev Cancer *8*, 253-267.

Clurman, B.E., Sheaff, R.J., Thress, K., Groudine, M., and Roberts, J.M. (1996). Turnover of cyclin E by the ubiquitin-proteasome pathway is regulated by cdk2 binding and cyclin phosphorylation. Genes Dev *10*, 1979-1990.

Crino, P.B., Nathanson, K.L., and Henske, E.P. (2006). The tuberous sclerosis complex. N Engl J Med *355*, 1345-1356.

Croxtall, J.D., and McKeage, K. (2011). Fulvestrant: a review of its use in the management of hormone receptor-positive metastatic breast cancer in postmenopausal women. Drugs *71*, 363-380.

Dauvois, S., White, R., and Parker, M.G. (1993). The antiestrogen ICI 182780 disrupts estrogen receptor nucleocytoplasmic shuttling. J Cell Sci *106 (Pt 4)*, 1377-1388.

Davidson, B.L., and Harper, S.Q. (2005). Viral delivery of recombinant short hairpin RNAs. Methods Enzymol *392*, 145-173.

DeNardo, D.G., Cuba, V.L., Kim, H., Wu, K., Lee, A.V., and Brown, P.H. (2007). Estrogen receptor DNA binding is not required for estrogen-induced breast cell growth. Mol Cell Endocrinol *277*, 13-25.

Derheimer, F.A., and Kastan, M.B. (2010). Multiple roles of ATM in monitoring and maintaining DNA integrity. FEBS Lett *584*, 3675-3681.

Deroo, B.J., and Korach, K.S. (2006). Estrogen receptors and human disease. J Clin Invest *116*, 561-570.

Dessev, G., Iovcheva-Dessev, C., Bischoff, J.R., Beach, D., and Goldman, R. (1991). A complex containing p34cdc2 and cyclin B phosphorylates the nuclear lamin and disassembles nuclei of clam oocytes in vitro. J Cell Biol *112*, 523-533.

Di Cosimo, S., and Baselga, J. (2008). Targeted therapies in breast cancer: where are we now? Eur J Cancer *44*, 2781-2790.

Dong, X.Y., Chen, C., Sun, X., Guo, P., Vessella, R.L., Wang, R.X., Chung, L.W., Zhou, W., and Dong, J.T. (2006). FOXO1A is a candidate for the 13q14 tumor suppressor gene inhibiting androgen receptor signaling in prostate cancer. Cancer Res *66*, 6998-7006.

Bibliography

Dozier, C., Bonyadi, M., Baricault, L., Tonasso, L., and Darbon, J.M. (2004). Regulation of Chk2 phosphorylation by interaction with protein phosphatase 2A via its B' regulatory subunit. Biol Cell *96*, 509-517.

Dudek, P., and Picard, D. (2008). Genomics of signaling crosstalk of estrogen receptor alpha in breast cancer cells. PLoS ONE *3*, e1859.

Dulic, V., Lees, E., and Reed, S.I. (1992). Association of human cyclin E with a periodic G1-S phase protein kinase. Science *257*, 1958-1961.

Evans, J.M., Donnelly, L.A., Emslie-Smith, A.M., Alessi, D.R., and Morris, A.D. (2005). Metformin and reduced risk of cancer in diabetic patients. BMJ *330*, 1304-1305.

Fabris, G., Marchetti, E., Marzola, A., Bagni, A., Querzoli, P., and Nenci, I. (1987). Pathophysiology of estrogen receptors in mammary tissue by monoclonal antibodies. J Steroid Biochem *27*, 171-176.

Fang, J., Menon, M., Kapelle, W., Bogacheva, O., Bogachev, O., Houde, E., Browne, S., Sathyanarayana, P., and Wojchowski, D.M. (2007). EPO modulation of cell-cycle regulatory genes, and cell division, in primary bone marrow erythroblasts. Blood *110*, 2361-2370.

Frasor, J., Danes, J.M., Komm, B., Chang, K.C., Lyttle, C.R., and Katzenellenbogen, B.S. (2003). Profiling of estrogen up- and down-regulated gene expression in human breast cancer cells: insights into gene networks and pathways underlying estrogenic control of proliferation and cell phenotype. Endocrinology *144*, 4562-4574.

Frasor, J., Stossi, F., Danes, J.M., Komm, B., Lyttle, C.R., and Katzenellenbogen, B.S. (2004). Selective estrogen receptor modulators: discrimination of agonistic versus antagonistic activities by gene expression profiling in breast cancer cells. Cancer Res *64*, 1522-1533.

Freeman, A.K., Dapic, V., and Monteiro, A.N. Negative regulation of CHK2 activity by protein phosphatase 2A is modulated by DNA damage. Cell Cycle *9*, 736-747.

Freeman, A.K., Dapic, V., and Monteiro, A.N. (2010). Negative regulation of CHK2 activity by protein phosphatase 2A is modulated by DNA damage. Cell Cycle *9*, 736-747.

Fu, G., and Peng, C. (2011). Nodal enhances the activity of FoxO3a and its synergistic interaction with Smads to regulate cyclin G2 transcription in ovarian cancer cells. Oncogene *30*, 3953-3966.

Bibliography

Gajate, C., An, F., and Mollinedo, F. (2002). Differential cytostatic and apoptotic effects of ecteinascidin-743 in cancer cells. Transcription-dependent cell cycle arrest and transcription-independent JNK and mitochondrial mediated apoptosis. J Biol Chem *277*, 41580-41589.

Gartel, A.L., and Radhakrishnan, S.K. (2005). Lost in transcription: p21 repression, mechanisms, and consequences. Cancer Res *65*, 3980-3985.

Golan, A., Pick, E., Tsvetkov, L., Nadler, Y., Kluger, H., and Stern, D.F. (2010). Centrosomal Chk2 in DNA damage responses and cell cycle progression. Cell Cycle *9*, 2647-2656.

Grolleau, A., Bowman, J., Pradet-Balade, B., Puravs, E., Hanash, S., Garcia-Sanz, J.A., and Beretta, L. (2002). Global and specific translational control by rapamycin in T cells uncovered by microarrays and proteomics. J Biol Chem *277*, 22175-22184.

Hagting, A., Karlsson, C., Clute, P., Jackman, M., and Pines, J. (1998). MPF localization is controlled by nuclear export. EMBO J *17*, 4127-4138.

Hanahan, D., and Weinberg, Robert A. (2011). Hallmarks of Cancer: The Next Generation. Cell *144*, 646-674.

Harbour, J.W., and Dean, D.C. (2000). The Rb/E2F pathway: expanding roles and emerging paradigms. Genes Dev *14*, 2393-2409.

Harper, J.W., Adami, G.R., Wei, N., Keyomarsi, K., and Elledge, S.J. (1993). The p21 Cdk-interacting protein Cip1 is a potent inhibitor of G1 cyclin-dependent kinases. Cell *75*, 805-816.

Harper, S.Q., Staber, P.D., Beck, C.R., Fineberg, S.K., Stein, C., Ochoa, D., and Davidson, B.L. (2006). Optimization of feline immunodeficiency virus vectors for RNA interference. J Virol *80*, 9371-9380.

Harvey, K.F., Mattila, J., Sofer, A., Bennett, F.C., Ramsey, M.R., Ellisen, L.W., Puig, O., and Hariharan, I.K. (2008). FOXO-regulated transcription restricts overgrowth of Tsc mutant organs. J Cell Biol *180*, 691-696.

Hay, N. (2011). Interplay between FOXO, TOR, and Akt. Biochim Biophys Acta.

Hay, N., and Sonenberg, N. (2004). Upstream and downstream of mTOR. Genes Dev *18*, 1926-1945.

Hill, R., and Lee, P.W. (2010). The DNA-dependent protein kinase (DNA-PK): More than just a case of making ends meet? Cell Cycle *9*, 3460-3469.

Bibliography

Hofstetter, C.P., Burkhardt, J.K., Shin, B.J., Gursel, D.B., Mubita, L., Gorrepati, R., Brennan, C., Holland, E.C., and Boockvar, J.A. (2012). Protein phosphatase 2A mediates dormancy of glioblastoma multiforme-derived tumor stem-like cells during hypoxia. PLoS One *7*, e30059.

Horne, M.C., Donaldson, K.L., Goolsby, G.L., Tran, D., Mulheisen, M., Hell, J.W., and Wahl, A.F. (1997). Cyclin G2 is up-regulated during growth inhibition and B cell antigen receptor-mediated cell cycle arrest. Journal of Biological Chemistry *272*, 12650-12661.

Horne, M.C., Goolsby, G.L., Donaldson, K.L., Tran, D., Neubauer, M., and Wahl, A.F. (1996). Cyclin G1 and cyclin G2 comprise a new family of cyclins with contrasting tissue-specific and cell cycle-regulated expressions. Journal of Biological Chemistry *271*, 6050-6061.

Houldsworth, J., Heath, S.C., Bosl, G.J., Studer, L., and Chaganti, R.S. (2002). Expression profiling of lineage differentiation in pluripotential human embryonal carcinoma cells. Cell Growth Differ *13*, 257-264.

Houtgraaf, J.H., Versmissen, J., and van der Giessen, W.J. (2006). A concise review of DNA damage checkpoints and repair in mammalian cells. Cardiovasc Revasc Med *7*, 165-172.

Howard, J.H., and Bland, K.I. (2012). Current management and treatment strategies for breast cancer. Curr Opin Obstet Gynecol *24*, 44-48.

Hu, Z., Fan, C., Oh, D.S., Marron, J.S., He, X., Qaqish, B.F., Livasy, C., Carey, L.A., Reynolds, E., Dressler, L.*, et al.* (2006). The molecular portraits of breast tumors are conserved across microarray platforms. BMC Genomics *7*, 96.

Huang, J., and Manning, B.D. (2009). A complex interplay between Akt, TSC2 and the two mTOR complexes. Biochem Soc Trans *37*, 217-222.

Huang, X., Gao, L., Wang, S., McManaman, J.L., Thor, A.D., Yang, X., Esteva, F.J., and Liu, B. (2010). Heterotrimerization of the growth factor receptors erbB2, erbB3, and insulin-like growth factor-i receptor in breast cancer cells resistant to herceptin. Cancer Res *70*, 1204-1214.

Inoki, K., Li, Y., Zhu, T., Wu, J., and Guan, K.L. (2002). TSC2 is phosphorylated and inhibited by Akt and suppresses mTOR signalling. Nat Cell Biol *4*, 648-657.

Inoki, K., Zhu, T., and Guan, K.L. (2003). TSC2 mediates cellular energy response to control cell growth and survival. Cell *115*, 577-590.

Bibliography

Iorns, E., Turner, N.C., Elliott, R., Syed, N., Garrone, O., Gasco, M., Tutt, A.N., Crook, T., Lord, C.J., and Ashworth, A. (2008). Identification of CDK10 as an important determinant of resistance to endocrine therapy for breast cancer. Cancer Cell *13*, 91-104.

Ito, T., Tsukumo, S., Suzuki, N., Motohashi, H., Yamamoto, M., Fujii-Kuriyama, Y., Mimura, J., Lin, T.M., Peterson, R.E., Tohyama, C.*, et al.* (2004). A constitutively active arylhydrocarbon receptor induces growth inhibition of jurkat T cells through changes in the expression of genes related to apoptosis and cell cycle arrest. J Biol Chem *279*, 25204-25210.

Ito, Y., Yoshida, H., Uruno, T., Nakano, K., Takamura, Y., Miya, A., Kobayashi, K., Yokozawa, T., Matsuzuka, F., Kuma, K.*, et al.* (2003). Decreased expression of cyclin G2 is significantly linked to the malignant transformation of papillary carcinoma of the thyroid. Anticancer Res *23*, 2335-2338.

Jacinto, E., Facchinetti, V., Liu, D., Soto, N., Wei, S., Jung, S.Y., Huang, Q., Qin, J., and Su, B. (2006). SIN1/MIP1 maintains rictor-mTOR complex integrity and regulates Akt phosphorylation and substrate specificity. Cell *127*, 125-137.

Jackson, S.P., and Bartek, J. (2009). The DNA-damage response in human biology and disease. Nature *461*, 1071-1078.

Janssens, V., and Goris, J. (2001). Protein phosphatase 2A: a highly regulated family of serine/threonine phosphatases implicated in cell growth and signalling. Biochemical Journal *353*, 417-439.

Jayapal, S.R., Lee, K.L., Ji, P., Kaldis, P., Lim, B., and Lodish, H.F. (2010). Down-regulation of Myc is essential for terminal erythroid maturation. J Biol Chem *285*, 40252-40265.

Jazayeri, A., Falck, J., Lukas, C., Bartek, J., Smith, G.C., Lukas, J., and Jackson, S.P. (2006). ATM- and cell cycle-dependent regulation of ATR in response to DNA double-strand breaks. Nat Cell Biol *8*, 37-45.

Jensen, M., Palsgaard, J., Borup, R., de Meyts, P., and Schaffer, L. (2008). Activation of the insulin receptor (IR) by insulin and a synthetic peptide has different effects on gene expression in IR-transfected L6 myoblasts. Biochem J *412*, 435-445.

Jordan, V.C., Gapstur, S., and Morrow, M. (2001). Selective estrogen receptor modulation and reduction in risk of breast cancer, osteoporosis, and coronary heart disease. J Natl Cancer Inst *93*, 1449-1457.

Bibliography

Kastan, M.B., Onyekwere, O., Sidransky, D., Vogelstein, B., and Craig, R.W. (1991). Participation of p53 protein in the cellular response to DNA damage. Cancer Research *51*, 6304-6311.

Kasten, M., and Giordano, A. (2001). Cdk10, a Cdc2-related kinase, associates with the Ets2 transcription factor and modulates its transactivation activity. Oncogene *20*, 1832-1838.

Kasukabe, T., Okabe-Kado, J., and Honma, Y. (2008). Cotylenin A, a new differentiation inducer, and rapamycin cooperatively inhibit growth of cancer cells through induction of cyclin G2. Cancer Sci *99*, 1693-1698.

Kasukabe, T., Okabe-Kado, J., Kato, N., Sassa, T., and Honma, Y. (2005). Effects of combined treatment with rapamycin and cotylenin A, a novel differentiation-inducing agent, on human breast carcinoma MCF-7 cells and xenografts. Breast Cancer Res *7*, R1097-1110.

Kato, S. (2001). Estrogen receptor-mediated cross-talk with growth factor signaling pathways. Breast Cancer *8*, 3-9.

Kim, Y., Shintani, S., Kohno, Y., Zhang, R., and Wong, D.T. (2004). Cyclin G2 dysregulation in human oral cancer. Cancer Res *64*, 8980-8986.

Kimura, S.H., Ikawa, M., Ito, A., Okabe, M., and Nojima, H. (2001). Cyclin G1 is involved in G2/M arrest in response to DNA damage and in growth control after damage recovery. Oncogene *20*, 3290-3300.

Kimura, S.H., and Nojima, H. (2002). Cyclin G1 associates with MDM2 and regulates accumulation and degradation of p53 protein. Genes Cells *7*, 869-880.

King, A.J., Sun, H., Diaz, B., Barnard, D., Miao, W., Bagrodia, S., and Marshall, M.S. (1998). The protein kinase Pak3 positively regulates Raf-1 activity through phosphorylation of serine 338. Nature *396*, 180-183.

Koepp, D.M., Harper, J.W., and Elledge, S.J. (1999). How the cyclin became a cyclin: regulated proteolysis in the cell cycle. Cell *97*, 431-434.

Krude, T., Jackman, M., Pines, J., and Laskey, R.A. (1997). Cyclin/Cdk-dependent initiation of DNA replication in a human cell-free system. Cell *88*, 109-119.

Kuntz, K., and O'Connell, M.J. (2009). The G(2) DNA damage checkpoint: could this ancient regulator be the Achilles heel of cancer? Cancer Biol Ther *8*, 1433-1439.

Bibliography

Kutay, U., and Guttinger, S. (2005). Leucine-rich nuclear-export signals: born to be weak. Trends Cell Biol *15*, 121-124.

Lange, C.A., and Yee, D. (2011). Killing the second messenger: targeting loss of cell cycle control in endocrine-resistant breast cancer. Endocr Relat Cancer *18*, C19-24.

Lannigan, D.A. (2003). Estrogen receptor phosphorylation. Steroids *68*, 1-9.

Lavoie, J.N., L'Allemain, G., Brunet, A., Muller, R., and Pouyssegur, J. (1996). Cyclin D1 expression is regulated positively by the p42/p44MAPK and negatively by the p38/HOGMAPK pathway. J Biol Chem *271*, 20608-20616.

Le, X.-F., Arachchige Don, A.S., Mao, W., Horne, M.C., and Bast, J., R. C. (2007). Roles of human epidermal growth factor receptor 2, c-jun NH2-terminal kinase, phosphoinositide 3-kinase, and p70 S6 kinase pathways in regulation of cyclin G2 expression in human breast cancer cells. Mol Cancer Ther *6*, 2843-2857.

Lee, J., Kim, J.A., Barbier, V., Fotedar, A., and Fotedar, R. (2009). DNA damage triggers p21WAF1-dependent Emi1 down-regulation that maintains G2 arrest. Mol Biol Cell *20*, 1891-1902.

Lee, J.H., and Paull, T.T. (2004). Direct activation of the ATM protein kinase by the Mre11/Rad50/Nbs1 complex. Science *304*, 93-96.

Lee, K.J., Lin, Y.F., Chou, H.Y., Yajima, H., Fattah, K.R., Lee, S.C., and Chen, B.P. (2011). Involvement of DNA-dependent protein kinase in normal cell cycle progression through mitosis. J Biol Chem *286*, 12796-12802.

Lemaire, M., Ducommun, B., and Nebreda, A.R. (2010). UV-induced downregulation of the CDC25B protein in human cells. FEBS Lett *584*, 1199-1204.

Leygue, E., Dotzlaw, H., Watson, P.H., and Murphy, L.C. (1998). Altered estrogen receptor alpha and beta messenger RNA expression during human breast tumorigenesis. Cancer Res *58*, 3197-3201.

Li, J., and Stern, D.F. (2005). Regulation of CHK2 by DNA-dependent protein kinase. J Biol Chem *280*, 12041-12050.

Li, S., MacLachlan, T.K., De Luca, A., Claudio, P.P., Condorelli, G., and Giordano, A. (1995). The cdc-2-related kinase, PISSLRE, is essential for cell growth and acts in G2 phase of the cell cycle. Cancer Res *55*, 3992-3995.

Bibliography

Lindqvist, A., Rodriguez-Bravo, V., and Medema, R.H. (2009). The decision to enter mitosis: feedback and redundancy in the mitotic entry network. J Cell Biol *185*, 193-202.

Lindqvist, A., van Zon, W., Karlsson Rosenthal, C., and Wolthuis, R.M. (2007). Cyclin B1-Cdk1 activation continues after centrosome separation to control mitotic progression. PLoS Biol *5*, e123.

Lord, C.J., and Ashworth, A. (2012). The DNA damage response and cancer therapy. Nature *481*, 287-294.

Lovejoy, C.A., and Cortez, D. (2009). Common mechanisms of PIKK regulation. DNA Repair (Amst) *8*, 1004-1008.

Lu, Z., and Hunter, T. (2010). Ubiquitylation and proteasomal degradation of the p21(Cip1), p27(Kip1) and p57(Kip2) CDK inhibitors. Cell Cycle *9*, 2342-2352.

Manning, B.D., and Cantley, L.C. (2007). AKT/PKB signaling: navigating downstream. Cell *129*, 1261-1274.

Marshall, G.M., Gherardi, S., Xu, N., Neiron, Z., Trahair, T., Scarlett, C.J., Chang, D.K., Liu, P.Y., Jankowski, K., Iraci, N.*, et al.* (2010). Transcriptional upregulation of histone deacetylase 2 promotes Myc-induced oncogenic effects. Oncogene *29*, 5957-5968.

Martin, D.E., and Hall, M.N. (2005). The expanding TOR signaling network. Curr Opin Cell Biol *17*, 158-166.

Martin, M. (2006). Molecular biology of breast cancer. Clin Transl Oncol *8*, 7-14.

Martinez-Gac, L., Marques, M., Garcia, Z., Campanero, M.R., and Carrera, A.C. (2004). Control of Cyclin G2 mRNA Expression by Forkhead Transcription Factors: Novel Mechanism for Cell Cycle Control by Phosphoinositide 3-Kinase and Forkhead. Mol Cell Biol *24*, 2181-2189.

Massarweh, S., Osborne, C.K., Creighton, C.J., Qin, L., Tsimelzon, A., Huang, S., Weiss, H., Rimawi, M., and Schiff, R. (2008). Tamoxifen resistance in breast tumors is driven by growth factor receptor signaling with repression of classic estrogen receptor genomic function. Cancer Res *68*, 826-833.

McCright, B., Rivers, A.M., Audlin, S., and Virshup, D.M. (1996). The B56 family of protein phosphatase 2A (PP2A) regulatory subunits encodes differentiation-induced phosphoproteins that target PP2A to both nucleus and cytoplasm. J Biol Chem *271*, 22081-22089.

Bibliography

McDonnell, D.P., and Wardell, S.E. (2010). The molecular mechanisms underlying the pharmacological actions of ER modulators: implications for new drug discovery in breast cancer. Curr Opin Pharmacol *10*, 620-628.

Merbl, Y., and Kirschner, M.W. (2009). Large-scale detection of ubiquitination substrates using cell extracts and protein microarrays. Proc Natl Acad Sci U S A *106*, 2543-2548.

Miller, T.W., Balko, J.M., and Arteaga, C.L. (2011a). Phosphatidylinositol 3-kinase and antiestrogen resistance in breast cancer. J Clin Oncol *29*, 4452-4461.

Miller, T.W., Balko, J.M., Ghazoui, Z., Dunbier, A., Anderson, H., Dowsett, M., Gonzalez-Angulo, A.M., Mills, G.B., Miller, W.R., Wu, H.*, et al.* (2011b). A gene expression signature from human breast cancer cells with acquired hormone independence identifies MYC as a mediator of antiestrogen resistance. Clin Cancer Res *17*, 2024-2034.

Miyata, H., Doki, Y., Yamamoto, H., Kishi, K., Takemoto, H., Fujiwara, Y., Yasuda, T., Yano, M., Inoue, M., Shiozaki, H.*, et al.* (2001). Overexpression of CDC25B overrides radiation-induced G2-M arrest and results in increased apoptosis in esophageal cancer cells. Cancer Res *61*, 3188-3193.

Mocciaro, A., and Rape, M. (2012). Emerging regulatory mechanisms in ubiquitin-dependent cell cycle control. J Cell Sci *125*, 255-263.

Morgan, D.O. (1997). Cyclin-dependent kinases: engines, clocks, and microprocessors. Annu Rev Cell Dev Biol *13*, 261-291.

Murray, J.I., Whitfield, M.L., Trinklein, N.D., Myers, R.M., Brown, P.O., and Botstein, D. (2004). Diverse and specific gene expression responses to stresses in cultured human cells. Mol Biol Cell.

Myatt, S.S., and Lam, E.W. (2007). The emerging roles of forkhead box (Fox) proteins in cancer. Nat Rev Cancer *7*, 847-859.

Nakayama, K., Nagahama, H., Minamishima, Y.A., Miyake, S., Ishida, N., Hatakeyama, S., Kitagawa, M., Iemura, S., Natsume, T., and Nakayama, K.I. (2004). Skp2-mediated degradation of p27 regulates progression into mitosis. Dev Cell *6*, 661-672.

Nakayama, K.I., and Nakayama, K. (2006). Ubiquitin ligases: cell-cycle control and cancer. Nat Rev Cancer *6*, 369-381.

Nitiss, J.L. (2009). Targeting DNA topoisomerase II in cancer chemotherapy. Nat Rev Cancer *9*, 338-350.

O'Connell, M.J., Walworth, N.C., and Carr, A.M. (2000). The G2-phase DNA-damage checkpoint. Trends Cell Biol *10*, 296-303.

O'Donnell, A.J., Macleod, K.G., Burns, D.J., Smyth, J.F., and Langdon, S.P. (2005). Estrogen receptor-alpha mediates gene expression changes and growth response in ovarian cancer cells exposed to estrogen. Endocr Relat Cancer *12*, 851-866.

O'Farrell, P.H. (2001). Triggering the all-or-nothing switch into mitosis. Trends Cell Biol *11*, 512-519.

Oberle, C., and Blattner, C. (2010). Regulation of the DNA Damage Response to DSBs by Post-Translational Modifications. Curr Genomics *11*, 184-198.

Ogita, S., and Lorusso, P. (2011). Targeting phosphatidylinositol 3 kinase (PI3K)-Akt beyond rapalogs. Target Oncol *6*, 103-117.

Ohren, J.F., Chen, H., Pavlovsky, A., Whitehead, C., Zhang, E., Kuffa, P., Yan, C., McConnell, P., Spessard, C., Banotai, C.*, et al.* (2004). Structures of human MAP kinase kinase 1 (MEK1) and MEK2 describe novel noncompetitive kinase inhibition. Nat Struct Mol Biol *11*, 1192-1197.

Ohtsuka, T., Jensen, M.R., Kim, H.G., Kim, K.T., and Lee, S.W. (2004). The negative role of cyclin G in ATM-dependent p53 activation. Oncogene *23*, 5405-5408.

Okamoto, K., and Beach, D. (1994). Cyclin G is a transcriptional target of the p53 tumor suppressor protein. EMBO Journal *13*, 4816-4822.

Okamoto, K., and Prives, C. (1999). A role of cyclin G in the process of apoptosis. Oncogene *18*, 4606-4615.

Oliver, T.G., Grasfeder, L.L., Carroll, A.L., Kaiser, C., Gillingham, C.L., Lin, S.M., Wickramasinghe, R., Scott, M.P., and Wechsler-Reya, R.J. (2003). Transcriptional profiling of the Sonic hedgehog response: a critical role for N-myc in proliferation of neuronal precursors. Proc Natl Acad Sci U S A *100*, 7331-7336.

Orlova, K.A., and Crino, P.B. (2011). The tuberous sclerosis complex. Ann N Y Acad Sci *1184*, 87-105.

Osborne, C.K., and Schiff, R. (2011). Mechanisms of endocrine resistance in breast cancer. Annu Rev Med *62*, 233-247.

Ozcan, U., Ozcan, L., Yilmaz, E., Duvel, K., Sahin, M., Manning, B.D., and Hotamisligil, G.S. (2008). Loss of the tuberous sclerosis complex tumor suppressors

triggers the unfolded protein response to regulate insulin signaling and apoptosis. Mol Cell *29*, 541-551.

Pateras, I.S., Apostolopoulou, K., Niforou, K., Kotsinas, A., and Gorgoulis, V.G. (2009). p57KIP2: "Kip"ing the cell under control. Mol Cancer Res *7*, 1902-1919.

Pearce, S.T., and Jordan, V.C. (2004). The biological role of estrogen receptors alpha and beta in cancer. Crit Rev Oncol Hematol *50*, 3-22.

Pei, X.H., and Xiong, Y. (2005). Biochemical and cellular mechanisms of mammalian CDK inhibitors: a few unresolved issues. Oncogene *24*, 2787-2795.

Petersen, B.O., Lukas, J., Sorensen, C.S., Bartek, J., and Helin, K. (1999). Phosphorylation of mammalian CDC6 by cyclin A/CDK2 regulates its subcellular localization. EMBO J *18*, 396-410.

Petroski, M.D., and Deshaies, R.J. (2005). Mechanism of lysine 48-linked ubiquitin-chain synthesis by the cullin-RING ubiquitin-ligase complex SCF-Cdc34. Cell *123*, 1107-1120.

Pulido, R., Zuniga, A., and Ullrich, A. (1998). PTP-SL and STEP protein tyrosine phosphatases regulate the activation of the extracellular signal-regulated kinases ERK1 and ERK2 by association through a kinase interaction motif. EMBO J *17*, 7337-7350.

Rainey, M.D., Zachos, G., and Gillespie, D.A. (2006). Analysing the DNA damage and replication checkpoints in DT40 cells. Subcell Biochem *40*, 107-117.

Reinke, V., Bortner, D.M., Amelse, L.L., Lundgren, K., Rosenberg, M.P., Finlay, C.A., and Lozano, G. (1999). Overproduction of MDM2 in vivo disrupts S phase independent of E2F1. Cell Growth Differ *10*, 147-154.

Resing, K.A., Mansour, S.J., Hermann, A.S., Johnson, R.S., Candia, J.M., Fukasawa, K., Vande Woude, G.F., and Ahn, N.G. (1995). Determination of v-Mos-catalyzed phosphorylation sites and autophosphorylation sites on MAP kinase kinase by ESI/MS. Biochemistry *34*, 2610-2620.

Roberts, P.J., and Der, C.J. (2007). Targeting the Raf-MEK-ERK mitogen-activated protein kinase cascade for the treatment of cancer. Oncogene *26*, 3291-3310.

Roskoski, R., Jr. (2012). MEK1/2 dual-specificity protein kinases: structure and regulation. Biochem Biophys Res Commun *417*, 5-10.

Bibliography

Roy, R., Chun, J., and Powell, S.N. (2012). BRCA1 and BRCA2: important differences with common interests. Nat Rev Cancer *12*, 372.

Rual, J.F., Venkatesan, K., Hao, T., Hirozane-Kishikawa, T., Dricot, A., Li, N., Berriz, G.F., Gibbons, F.D., Dreze, M., Ayivi-Guedehoussou, N.*, et al.* (2005). Towards a proteome-scale map of the human protein-protein interaction network. Nature *437*, 1173-1178.

Salih, D.A., and Brunet, A. (2008). FoxO transcription factors in the maintenance of cellular homeostasis during aging. Curr Opin Cell Biol *20*, 126-136.

Satyanarayana, A., and Kaldis, P. (2009). Mammalian cell-cycle regulation: several Cdks, numerous cyclins and diverse compensatory mechanisms. Oncogene *28*, 2925-2939.

Schonn, I., Hennesen, J., and Dartsch, D.C. (2011). Ku70 and Rad51 vary in their importance for the repair of doxorubicin- versus etoposide-induced DNA damage. Apoptosis *16*, 359-369.

Seger, R., Ahn, N.G., Posada, J., Munar, E.S., Jensen, A.M., Cooper, J.A., Cobb, M.H., and Krebs, E.G. (1992). Purification and characterization of mitogen-activated protein kinase activator(s) from epidermal growth factor-stimulated A431 cells. J Biol Chem *267*, 14373-14381.

Seo, H.R., Lee, D.H., Lee, H.J., Baek, M., Bae, S., Soh, J.W., Lee, S.J., Kim, J., and Lee, Y.S. (2006). Cyclin G1 overcomes radiation-induced G2 arrest and increases cell death through transcriptional activation of cyclin B1. Cell Death Differ *13*, 1475-1484.

Sepulveda, D.E., Andrews, B.A., Asenjo, J.A., and Papoutsakis, E.T. (2008). Comparative transcriptional analysis of embryoid body versus two-dimensional differentiation of murine embryonic stem cells. Tissue Eng Part A *14*, 1603-1614.

Shaul, Y.D., and Seger, R. (2007). The MEK/ERK cascade: from signaling specificity to diverse functions. Biochim Biophys Acta *1773*, 1213-1226.

Sherr, C.J., and McCormick, F. (2002). The RB and p53 pathways in cancer. Cancer Cell *2*, 103-112.

Sherr, C.J., and Roberts, J.M. (1999). CDK inhibitors: positive and negative regulators of G1-phase progression. Genes Dev *13*, 1501-1512.

Shimada, M., Nakadai, T., and Tamura, T.A. (2003). TATA-binding protein-like protein (TLP/TRF2/TLF) negatively regulates cell cycle progression and is required for the stress-mediated G(2) checkpoint. Mol Cell Biol *23*, 4107-4120.

Bibliography

Shimizu, A., Nishida, J., Ueoka, Y., Kato, K., Hachiya, T., Kuriaki, Y., and Wake, N. (1998). CyclinG contributes to G2/M arrest of cells in response to DNA damage. Biochem Biophys Res Commun *242*, 529-533.

Shiotani, B., and Zou, L. (2009a). ATR signaling at a glance. J Cell Sci *122*, 301-304.

Shiotani, B., and Zou, L. (2009b). Single-stranded DNA orchestrates an ATM-to-ATR switch at DNA breaks. Mol Cell *33*, 547-558.

Siegel, R., Naishadham, D., and Jemal, A. (2012). Cancer statistics, 2012. CA Cancer J Clin *62*, 10-29.

Society, A.C. (2012). Cancer Facts and Figures 2012.

Song, R.X., Chen, Y., Zhang, Z., Bao, Y., Yue, W., Wang, J.P., Fan, P., and Santen, R.J. (2010). Estrogen utilization of IGF-1-R and EGF-R to signal in breast cancer cells. J Steroid Biochem Mol Biol *118*, 219-230.

Sontag, E., Fedorov, S., Kamibayashi, C., Robbins, D., Cobb, M., and Mumby, M. (1993). The interaction of SV40 small tumor antigen with protein phosphatase 2A stimulates the map kinase pathway and induces cell proliferation. Cell *75*, 887-897.

Stolz, A., Ertych, N., Kienitz, A., Vogel, C., Schneider, V., Fritz, B., Jacob, R., Dittmar, G., Weichert, W., Petersen, I*., et al.* (2010). The CHK2-BRCA1 tumour suppressor pathway ensures chromosomal stability in human somatic cells. Nat Cell Biol *12*, 492-499.

Stossi, F., Likhite, V.S., Katzenellenbogen, J.A., and Katzenellenbogen, B.S. (2006). Estrogen-occupied estrogen receptor represses cyclin G2 gene expression and recruits a repressor complex at the cyclin G2 promoter. J Biol Chem *281*, 16272-16278.

Stossi, F., Madak-Erdogan, Z., and Katzenellenbogen, B.S. (2009). Estrogen receptor alpha represses transcription of early target genes via p300 and CtBP1. Mol Cell Biol *29*, 1749-1759.

Stracker, T.H., Usui, T., and Petrini, J.H. (2009). Taking the time to make important decisions: the checkpoint effector kinases Chk1 and Chk2 and the DNA damage response. DNA Repair (Amst) *8*, 1047-1054.

Suenaga, Y., Ozaki, T., Tanaka, Y., Bu, Y., Kamijo, T., Tokuhisa, T., Nakagawara, A., and Tamura, T.A. (2009). TATA-binding Protein (TBP)-like Protein Is Engaged in Etoposide-induced Apoptosis through Transcriptional Activation of Human TAp63 Gene. J Biol Chem *284*, 35433-35440.

Bibliography

Sun, H., Charles, C.H., Lau, L.F., and Tonks, N.K. (1993). MKP-1 (3CH134), an immediate early gene product, is a dual specificity phosphatase that dephosphorylates MAP kinase in vivo. Cell *75*, 487-493.

Thangavel, C., Dean, J.L., Ertel, A., Knudsen, K.E., Aldaz, C.M., Witkiewicz, A.K., Clarke, R., and Knudsen, E.S. (2011). Therapeutically activating RB: reestablishing cell cycle control in endocrine therapy-resistant breast cancer. Endocr Relat Cancer *18*, 333-345.

Thomas, K.C., Sabnis, A.S., Johansen, M.E., Lanza, D.L., Moos, P.J., Yost, G.S., and Reilly, C.A. (2007). Transient receptor potential vanilloid 1 agonists cause endoplasmic reticulum stress and cell death in human lung cells. J Pharmacol Exp Ther *321*, 830-838.

Tomimatsu, N., Mukherjee, B., and Burma, S. (2009). Distinct roles of ATR and DNA-PKcs in triggering DNA damage responses in ATM-deficient cells. EMBO Rep *10*, 629-635.

Tran, H., Brunet, A., Griffith, E.C., and Greenberg, M.E. (2003). The many forks in FOXO's road. Sci STKE *2003*, RE5.

Truffinet, V., Pinaud, E., Cogne, N., Petit, B., Guglielmi, L., Cogne, M., and Denizot, Y. (2007). The 3' IgH locus control region is sufficient to deregulate a c-myc transgene and promote mature B cell malignancies with a predominant Burkitt-like phenotype. J Immunol *179*, 6033-6042.

Tsvetkov, L., Xu, X., Li, J., and Stern, D.F. (2003). Polo-like kinase 1 and Chk2 interact and co-localize to centrosomes and the midbody. J Biol Chem *278*, 8468-8475.

van de Vijver, M.J., He, Y.D., van't Veer, L.J., Dai, H., Hart, A.A., Voskuil, D.W., Schreiber, G.J., Peterse, J.L., Roberts, C., Marton, M.J.*, et al.* (2002). A gene-expression signature as a predictor of survival in breast cancer. N Engl J Med *347*, 1999-2009.

van den Heuvel, S. (2005). Cell-cycle regulation. WormBook, 1-16.

van Leuken, R., Clijsters, L., and Wolthuis, R. (2008). To cell cycle, swing the APC/C. Biochim Biophys Acta *1786*, 49-59.

Venkitaraman, A.R. (2002). Cancer susceptibility and the functions of BRCA1 and BRCA2. Cell *108*, 171-182.

Viale, G. (2007). Pathological definitions of invasion, metastatic potential and responsiveness to targeted therapies. Breast *16 Suppl 2*, S55-58.

Bibliography

Waldman, T., Kinzler, K.W., and Vogelstein, B. (1995). p21 is necessary for the p53-mediated G1 arrest in human cancer cells. Cancer Res *55*, 5187-5190.

Wan, X., and Helman, L.J. (2007). The Biology Behind mTOR Inhibition in Sarcoma. The Oncologist *12*, 1007-1018.

Wang, Y., Ji, P., Liu, J., Broaddus, R.R., Xue, F., and Zhang, W. (2009). Centrosome-associated regulators of the G(2)/M checkpoint as targets for cancer therapy. Mol Cancer *8*, 8.

Watanabe, N., Arai, H., Nishihara, Y., Taniguchi, M., Hunter, T., and Osada, H. (2004). M-phase kinases induce phospho-dependent ubiquitination of somatic Wee1 by SCFbeta-TrCP. Proc Natl Acad Sci U S A *101*, 4419-4424.

Wei, J.H., Chou, Y.F., Ou, Y.H., Yeh, Y.H., Tyan, S.W., Sun, T.P., Shen, C.Y., and Shieh, S.Y. (2005). TTK/hMps1 participates in the regulation of DNA damage checkpoint response by phosphorylating CHK2 on threonine 68. J Biol Chem *280*, 7748-7757.

Welcsh, P.L., Lee, M.K., Gonzalez-Hernandez, R.M., Black, D.J., Mahadevappa, M., Swisher, E.M., Warrington, J.A., and King, M.C. (2002). BRCA1 transcriptionally regulates genes involved in breast tumorigenesis. Proc Natl Acad Sci U S A *99*, 7560-7565.

Wellbrock, C., Karasarides, M., and Marais, R. (2004). The RAF proteins take centre stage. Nat Rev Mol Cell Biol *5*, 875-885.

Wilcken, N.R., Prall, O.W., Musgrove, E.A., and Sutherland, R.L. (1997). Inducible overexpression of cyclin D1 in breast cancer cells reverses the growth-inhibitory effects of antiestrogens. Clin Cancer Res *3*, 849-854.

Witzig, T.E., Reeder, C.B., LaPlant, B.R., Gupta, M., Johnston, P.B., Micallef, I.N., Porrata, L.F., Ansell, S.M., Colgan, J.P., Jacobsen, E.D.*, et al.* (2011). A phase II trial of the oral mTOR inhibitor everolimus in relapsed aggressive lymphoma. Leukemia *25*, 341-347.

Xu, G., Bernaudo, S., Fu, G., Lee, D.Y., Yang, B.B., and Peng, C. (2008). Cyclin G2 is degraded through the ubiquitin-proteasome pathway and mediates the antiproliferative effect of activin receptor-like kinase 7. Mol Biol Cell *19*, 4968-4979.

Yang, B.S., Hauser, C.A., Henkel, G., Colman, M.S., Van Beveren, C., Stacey, K.J., Hume, D.A., Maki, R.A., and Ostrowski, M.C. (1996). Ras-mediated phosphorylation of a conserved threonine residue enhances the transactivation activities of c-Ets1 and c-Ets2. Mol Cell Biol *16*, 538-547.

Bibliography

Yang, J.Y., Zong, C.S., Xia, W., Yamaguchi, H., Ding, Q., Xie, X., Lang, J.Y., Lai, C.C., Chang, C.J., Huang, W.C.*, et al.* (2008). ERK promotes tumorigenesis by inhibiting FOXO3a via MDM2-mediated degradation. Nat Cell Biol *10*, 138-148.

Zhang, Y., Moerkens, M., Ramaiahgari, S., de Bont, H., Price, L., Meerman, J., and van de Water, B. (2011). Elevated insulin-like growth factor 1 receptor signaling induces anti-estrogen resistance through the MAPK/ERK and PI3K/Akt signaling routes. Breast Cancer Res *13*, R52.

Zhang, Z., Maier, B., Santen, R.J., and Song, R.X. (2002). Membrane association of estrogen receptor alpha mediates estrogen effect on MAPK activation. Biochem Biophys Res Commun *294*, 926-933.

Zhao, L., Samuels, T., Winckler, S., Korgaonkar, C., Tompkins, V., Horne, M.C., and Quelle, D.E. (2003). Cyclin G1 has growth inhibitory activity linked to the ARF-Mdm2-p53 and pRb tumor suppressor pathways. Mol Cancer Res *1*, 195-206.

Zhou, J., Su, P., Wang, L., Chen, J., Zimmermann, M., Genbacev, O., Afonja, O., Horne, M.C., Tanaka, T., Duan, E.*, et al.* (2009). mTOR supports long-term self-renewal and suppresses mesoderm and endoderm activities of human embryonic stem cells. Proc Natl Acad Sci U S A *106*, 7840-7845.

Zimmermann, M., Arachchige Don, A.S., Donaldson, M.S., Dallapiazza, R.F., Cowan, C.E., and Horne, M.C. (2012). Elevated Cyclin G2 expression intersects with DNA damage checkpoint signaling and is required for a potent G2/M checkpoint arrest response to doxorubicin. Journal of Biological Chemistry.

Zoncu, R., Efeyan, A., and Sabatini, D.M. (2011). mTOR: from growth signal integration to cancer, diabetes and ageing. Nat Rev Mol Cell Biol *12*, 21-35.

Zwang, Y., Sas-Chen, A., Drier, Y., Shay, T., Avraham, R., Lauriola, M., Shema, E., Lidor-Nili, E., Jacob-Hirsch, J., Amariglio, N.*, et al.* (2011). Two phases of mitogenic signaling unveil roles for p53 and EGR1 in elimination of inconsistent growth signals. Mol Cell *42*, 524-535.

Abbreviations

4OHT	tamoxifen	ICI	fulvestrant
AMPK	AMP activated protein kinase	IGFR	insulin-like growth factor
APC/C	anaphase promoting complex /cyclosome	IP	immunoprecipitation
		IRS	insulin receptor substrate
ATM	ataxia telangiectasia mutated	KD	knockdown
ATR	ATM and Rad3 related	MAPK	mitogen activated protein kinase
BC	breast cancer	MEK	MAPK/ERK kinase
CDK	cyclin dependent kinase	MeOH	methanol
CKI	CDK inhibitor	MRN	Mre11-Rad50-Nbs1
Cyc	cyclin	mTOR	mammalian target of rapamycin
DDR	DNA damage response	NBS1	Nijmegen breakage syndrome1
Dox	doxorubicin	NHEJ	non-homologous end-joining
DSB	double strand break	PCR	polymerase chain reaction
E2	estrogen/estradiol	PI3K	phosphatidylinositol 3-kinase
EGFR	epidermal growth factor receptor	PIKK	PI3K related kinase
		PIP$_3$	phosphatidylinositol 3,4,5-trisphosphate
ER	estrogen receptor		
ERE	estrogen responsive element	PP2A	protein phosphatase 2A
ERK	extracellular signal regulated kinase	qRT-PCR	quantitative real time PCR
		Rapa	rapamycin
ERS	endoplasmic reticulum stress	Rheb	Ras homologue expressed in brain
EtOH	ethanol		
ETP	etoposide	S6K	S6 kinase
FACS	fluorescence activated cell sorting	SCF	Skp1/Cul1/F-box protein
		SERD	selective estrogen receptor downregulators
FBS	fetal bovine serum		
FRE	FOXO response element	SERM	selective estrogen receptor modulators
FOXO	forkhead box O		
GAPDH	glyceraldehyde-3-phosphate dehydrogenase	TF	transcription factor
		Thap	thapsigargin
GFP	green fluorescent protein	TSC	tuberous sclerosis complex
HDAC	histone deacetylase	UPR	unfolded protein response
HER2	human epidermal growth factor receptor 2	UPS	ubiquitin proteasome system

8. Acknowledgements

First and foremost, I would like to express my deepest gratitude to Dr. Mary Horne for giving me the opportunity to complete my PhD here in the US. This dissertation would not have been possible without her constant support and guidance. I also very much appreciate the trust she has placed in me over the past years.

I would like to thank Dr. Gabriele Fischer von Mollard for reviewing this unconventional thesis and her support during this very interesting time. Her willingness to support an external PhD made this project possible.

In addition I would like to thank Dr. Johannes Hell for the support I received during my time in Iowa and Davis.

I also want to thank the Faculty of Chemistry in Bielefeld and the Departments of Pharmacology in Iowa and Davis.

Special thanks go to my co-workers, Michaela, Nicole and Eric, who helped me with all the little and big things, in the lab and everywhere else. In particular I want to thank Michaela for all the hard work and long ours she invested in my project. I really enjoyed spending time with you guys (in the lab and outside).

I also thank the members from Hell for their open arms, helpful discussions and introduction into the special characteristics of Midwestern lifestyle. Thank you very much Duane, Rob, Jason, Amy, Uche, Cheston, Hui, Cigdem, Lucas, Tom, I had a great time. I hope we will meet again.

Thank you Ivar, you know why. Ohne dich wäre ich nie auf die Idee gekommen Deutschland zu verlassen und mich in ein so großes Abenteuer zu stürzen. Danke dass du so bist wie du bist.

Nicht zuletzt möchte ich meiner Familie danken. Auch wenn ich euch nicht sehr oft sehen konnte, habe ich doch jeden Sonntag auf Neuigkeiten gewartet. Die vielen kleinen und großen "Kehrpakete" haben mir so manchen Abschnitt versüßt und das Weitermachen erleichtert.

Erklärung

Die vorliegende Arbeit wurde unter der wissenschaftlichen Anleitung von Prof. Dr. Mary Horne an der Fakultät für Pharmacology der Universität von Iowa, Iowa City, USA und der Fakultät für Pharmacology der Universität von Kalifornien, Davis, USA angefertigt.

Hiermit versichere ich, dass ich die vorliegende Dissertation ohne fremde Hilfe selbständig verfasst und nur die angegebenen Quellen und Hilfsmittel benutzt habe. Wörtlich oder dem Sinn nach aus Werken entnommene Stellen sind unter Angabe der Quellen kenntlich gemacht. Ich habe bisher an keiner anderen Fakultät oder Hochschule einen Antrag auf Zulassung zur Promotion eingereicht und die vorliegende Dissertation weder in der gegenwärtigen noch in einer anderen Fassung vorgelegt.

Maike Zimmermann

Curriculum Vitae

Maike Zimmermann

Education

PhD (Dr. rer. nat.) Biochemistry, University of California, Davis, USA and University of Bielefeld, Germany, 2012, Dissertation: Contribution of cyclin G2 to the cell cycle inhibitory effects of cancer therapeutics, Advisor: Prof. Dr. Mary Horne

Diplom Biochemistry, University of Bielefeld, Department of Chemistry and Department of Biology, Bielefeld, Germany, 2007, Thesis: Characterization of the hybrid histidine kinase Slr1759 of the cyanobacterium Synechocystis sp. PCC 6803, Advisor: Prof. Dr. Dorothee Staiger

Research Experience

09/09-present Visiting Scholar/Assistant Specialist, The University of California, Davis, School of Medicine, Department of Pharmacology, Davis, California, USA (Dr. Mary Horne lab)

11/07-08/09 Visiting Scholar/Research Assistant III, The University of Iowa College of Medicine, Department of Pharmacology, Iowa City, Iowa, USA (Dr. Mary Horne lab)

05/05-06/05 Advance practical training, University of Bielefeld, Department of Chemistry, Bielefeld, Germany (Dr. Frey lab)

10/01-04/07 Studies of Biochemistry, University of Bielefeld, Department of Chemistry, Bielefeld, Germany

Teaching Experience

10/06-12/06 Preparation and mentoring of undergraduate students during the Basic biology practical course I, University of Bielefeld, Department of Biology, Bielefeld, Germany

10/05-12/05 Preparation and mentoring of undergraduate students during the Immunology practical course, University of Bielefeld, Department of Chemistry, Bielefeld, Germany

Honors and Awards

07/25/11-07/29/11 Trainee scholarship for the Flow Cytometry Intensive Course sponsored by Tree Star

Appendix

Publications

1. Michel, K.P., Schroder, A.K., Zimmermann, M., Brandt, S., Pistorius, E.K., Frankenberg-Dinkel, N., and Staiger, D. (2009). The hybrid histidine kinase Slr1759 of the cyanobacterium Synechocystis sp. PCC 6803 contains FAD at its PAS domain. Archives of microbiology *191*, 553-559.

2. Zhou, J., Su, P., Wang, L., Chen, J., Zimmermann, M., Genbacev, O., Afonja, O., Horne, M.C., Tanaka, T., Duan, E.*, et al.* (2009). mTOR supports long-term self-renewal and suppresses mesoderm and endoderm activities of human embryonic stem cells. Proceedings of the National Academy of Sciences of the United States of America *106*, 7840-7845.

3. Xu, H., Ginsburg, K.S., Hall, D.D., Zimmermann, M., Stein, I.S., Zhang, M., Tandan, S., Hill, J.A., Horne, M.C., Bers, D.*, et al.* (2010). Targeting of protein phosphatases PP2A and PP2B to the C-terminus of the L-type calcium channel Ca v1.2. In Biochemistry, pp. 10298-10307.

4. Zimmermann, M., Arachchige Don, A.S., Donaldson, M.S., Dallapiazza, R.F., Cowan, C.E., and Horne, M.C. (2012). Elevated Cyclin G2 expression intersects with DNA damage checkpoint signaling and is required for a potent G2/M checkpoint arrest response to doxorubicin. Journal of Biological Chemistry.

Abstracts

1. Arachchige Don, A.S., Zimmermann, M., Cowan, C., Dallapiazza, R., Duven, J., Wong, M. and *Horne, M.C. Cyclin G2 intersects with the ATM-Chk2 dsDNA-damage response pathway and contributes to doxorubicin-induced G2/M checkpoint arrest. Midwest Breast Cancer Research Symposium, Iowa City, 2009.

2. Arachchige Don, A.S., *Zimmermann, M., Cowan, C., Le, X.F., Mou, E. and Horne, M.C. Modulation of cyclin G2 expression and localization in tumor cells responding to inhibitors of the PI3K/AKT/mTOR pathway. Midwest Breast Cancer Research Symposium, Iowa City, 2009.

3. *Zimmermann, M., Arachchige Don, A.S., Cowan, C., Mou, E. and Horne, M.C. Binding partners and post-translational regulation of the unconventional, estrogen repressed-cell cycle inhibitor, cyclin G2. Midwest Breast Cancer Research Symposium, Iowa City, 2009.

4. *Zimmermann, M., Cowen, C. and Horne, M.C. The FOXO regulated cell cycle inhibitor Cyclin G2 is upregulated by mTOR inhibitor Rapamycin and opposed by the Skp2 associated ubiquitin Ligase. American Society for Cell Biology meeting, San Diego, 2009.

5. Zimmermann, M., Arachchige Don, A.S., Mou, E., and *Horne, M.C. Modulation of expression and localization of cyclin G2, an estrogen- and HER2 repressed cell cycle inhibitor. American Society for Cell Biology, San Diego, 2009.

6. Arachchige Don, A.S., *Zimmermann, M., Dallapiazza, R., Donaldson, M., Cowan, C., and Horne, M.C. Cyclin G2 intersects with the ATM-Chk2 dsDNA-damage response pathway and contributes to doxorubicin-induced G2/M checkpoint

arrest. University of California, Davis, Annual Cancer Center Research Symposium, 2010.

7. Zimmermann, M., Arachchige Don, A.S., Donaldson, M, Cowan, C, and *Horne, M.C. Cyclin G2 is an Important Determinant for Endocrine Therapy Resistance in Breast Cancers. University of California, Davis, Annual Cancer Center Research Symposium, 2010.

Presenting person marked with asterisk